DESIGN AND DEVELOPMENT OF A MODULAR DYNAMIC TEST SYSTEM FOR RESILIENT MECHANICAL COMPONENTS AND VISCOELASTIC MATERIALS

A THESIS SUBMITTED TO
THE GRADUATE SCHOOL OF NATURAL AND APPLIED SCIENCES
OF
MIDDLE EAST TECHNICAL UNIVERSITY

BY

ERKİN BARIŞ BİLGİ

IN PARTIAL FULFILLMENT OF THE REQUIREMENTS
FOR
THE DEGREE OF MASTER OF SCIENCE
IN
MECHANICAL ENGINEERING

FEBRUARY 2016

Approval of the thesis:

DESIGN AND DEVELOPMENT OF A MODULAR DYNAMIC TEST SYSTEM FOR RESILIENT MECHANICAL COMPONENTS AND VISCOELASTIC MATERIALS

submitted by **ERKİN BARIŞ BİLGİ** in partial fulfillment of the requirements for the degree of **Master of Science in Mechanical Engineering Department, Middle East Technical University** by,

Prof. Dr. M. Gülbin Dural Ünver
Dean, Graduate School of **Natural and Applied Sciences** _________________

Prof. Dr. Tuna Balkan
Head of Department, **Mechanical Engineering** _________________

Asst. Prof. Dr. Gökhan O. Özgen
Supervisor, **Mechanical Engineering Dept., METU** _________________

Examining Committee Members:

Prof. Dr. Mehmet Çalışkan
Mechanical Engineering Dept., METU _________________

Asst. Prof. Dr. Gökhan O. Özgen
Mechanical Engineering Dept., METU _________________

Assoc. Prof. Dr. Ender Ciğeroğlu
Mechanical Engineering Dept., METU _________________

Asst. Prof. Dr. Ali Emre Turgut
Mechanical Engineering Dept., METU _________________

Asst. Prof. Dr. Kutluk Bilge Arıkan
Mechatronics Engineering Dept., Atılım Universtiy _________________

Date: ______________________

I hereby declare that all information in this document has been obtained and presented in accordance with academic rules and ethical conduct. I also declare that, as required by these rules and conduct, I have fully cited and referenced all material and results that are not original to this work.

Name, Last Name : Erkin Barış Bilgi

Signature :

ABSTRACT

DESIGN AND DEVELOPMENT OF A MODULAR DYNAMIC TEST SYSTEM FOR RESILIENT MECHANICAL COMPONENTS AND VISCOELASTIC MATERIALS

Bilgi, Erkin Barış

M.S., Department of Mechanical Engineering

Supervisor: Asst. Prof. Gökhan O. Özgen

February 2016, 128 pages

Vibration is a critical phenomenon because unwanted vibration causes energy wasting, noise, premature failure etc. For this reason, control and isolation of vibration has importance. Viscoelastic materials such as plastics, rubbers etc., which show both viscous and elastic behaviors under the effect of stress, are used in many different vibration control and isolation applications. In addition to viscoelastic materials, resilient mechanical components such as springs, vibration mounts etc. are also important for vibration control and isolation applications. Dynamic properties such as fatigue life, dynamic stiffness, damping properties of these materials and components play important roles to design an effective damping instrument or vibration isolator. On the other hand, dynamic properties are dependent on the frequency and/or temperature. As a result, there is a need for a dynamic test system which characterizes the dynamic properties with respect to the frequency and/or temperature. There are commercially available package test systems, which include both hardware and software components in one product, to determine the dynamic properties of corresponding materials and components. However, these test systems are expensive. The aim of this thesis is to design and develop a custom modular dynamic test system to characterize dynamic properties of viscoelastic materials and resilient mechanical components in 0-100 Hz frequency range with 3 kN maximum force at low and high temperatures. For this purpose, an original mechanical design is prepared for a modular dynamic test system considering the requirements, specifications and constraints.

Keywords: Viscoelastic Materials, Resilient Mechanical Components, Dynamic Properties, Dynamic Stiffness, Complex Modulus, Vibration Testing

ÖZ

ESNEK MEKANİK PARÇALAR VE VİSKOELASTİK MALZEMELER İÇİN MODÜLER BİR DİNAMİK TEST SİSTEMİ TASARIMI VE GELİŞTİRİLMESİ

Bilgi, Erkin Barış

Yüksek Lisans, Makina Mühendisliği Bölümü

Tez Yöneticisi: Yrd. Doç. Dr. Gökhan O. Özgen

Şubat 2016, 128 sayfa

Titreşim önemli bir olgudur çünkü istenmeyen titreşim enerji kaybı, gürültü, zamanından önce bozulma ve benzeri sonuçlara neden olur. Bu nedenle titreşim kontrolü ve izolasyonu önem arz etmektedir. Plastik, kauçuk ve benzeri viskoelastic malzemeler birçok çeşit titreşim kontrolü ve izolasyonu uygulamalarında kullanılmaktadır. Viskoelastik malzemelere ek olarak yay, titreşim takozu ve benzeri elastik mekanik parçalar da titreşim kontrolü ve izolasyonu uygulamaları için önemlidir. Yorulma ömrü, dinamik direngenlik, sönümleme özellikleri gibi bu malzemelere ve parçalara ait dinamik özellikler efektif bir sönümleme aracı veya titreşim izolatörü tasarımında önemli rol oynamaktadır. Bununla birlikte dinamik özellikler frekansa ve/veya sıcaklığa bağlıdır. Sonuç olarak dinamik özelliklerin frekansa ve/veya sıcaklığa bağlı olarak karakterize edilmesini sağlayacak dinamik bir test sistemine ihtiyaç duyulmaktadır. Piyasada hem yazılımsal hem de donanımsal parçaları tek bir üründe toplayan paket halinde test sistemleri bulunmaktadır. Fakat bu paket test sistemleri pahalıdır. Bu tez çalışmasının amacı viskoelastik malzemelerin ve esnek mekanik parçaların dinamik özelliklerinin 0-100 Hz frekans aralığında 3 kN maksimum kuvvet altında düşük ve yüksek sıcaklık değerlerinde karakterizasyonunun yapılmasına olanak sağlayacak özel modüler bir test sisteminin tasarlanması ve

geliştirilmesidir. Bu amaçla modüler test sisteminin mevcut gereksinimler, istenen özellikler ve kısıtlamalar doğrultusunda orjinal bir mekanik tasarımı hazırlanmıştır.

Anahtar Kelimeler: Viskoelastik malzemeler, Esnek mekanik parçalar, Dinamik özellikler, Dinamik Direngenlik, Karmaşık Modülü, Titreşim Testi

ACKNOWLEDGEMENTS

First of all, I would like to express my deepest gratitude to my supervisor Asst. Prof. Dr. Gökhan O. Özgen for his guidance, advice, supervision and invaluable support in the achievement of this thesis.

This thesis was financially supported by KOSGEB-Small and Medium Enterprises Development Organization as part of the R&D innovation project titled “Esnek Mekanik Parçalar ve Viskoelastik Malzemeler İçin Modüler Bir Dinamik Test Sistemi Geliştirilmesi”. I would like to thank KOSGEB for their comprehensive support.

Also, I would like to thank TÜBİTAK BİDEB for their financial support during my graduate education via 2228 scholarship program.

Once and for all, I would like to dedicate this thesis to my parents for their endless faith and support.

TABLE OF CONTENTS

LIST OF TABLES

TABLES

LIST OF FIGURES

FIGURES

CHAPTER 1

1. INTRODUCTION

Mechanical vibrations are one of the major problems of mechanical systems which are subjected to the dynamic loading. These unwanted vibrations may cause energy wasting in the mechanical system, premature failure of the mechanical system due to fatigue and an uncomfortable environment due to structure-borne noise. As a result, the unwanted mechanical vibrations should be reduced through various vibration control and isolation applications.

Viscoelastic materials (plastic, rubber etc.) and resilient mechanical components (spring, vibration mount etc.) are widely used in vibration control and isolation applications. Effective usage of these materials and components can be achieved only if detailed information about the dynamic properties of these materials are available. It should be noted that these dynamic properties are dependent on the temperature and/or frequency. For this reason, special test systems are needed to characterize the dynamic properties of these materials and components as functions of temperature and/or frequency. Such test systems are available in the market which are used for this purpose. However, these test systems are too expensive to buy and use. According to these motivations, the aim of this thesis work is to design and develop a custom modular dynamic test system to characterize dynamic properties of viscoelastic materials and elastic mechanical components. There are some requirements of this test system. Measurement frequency range is chosen as 0-100 Hz, maximum dynamic loading is chosen as 3 kN and tests are conducted both low and high temperature values. These requirements must be met through the use appropriate off-the-shelf hardware and original designs during conceptual and detailed design stages. These are also kind of limitations especially frequency range for the test system design stages. This thesis work mainly consists of design efforts to reach the appropriate test setup design. Data acquisition and testing stages are not part of this thesis. The output of this thesis work is a test setup that all components of it are manufactured, assembled and ready for testing.

At the beginning of the test system design and development workings, a necessary literature survey is done which covers the standard test methods, research about the main test setup components, similar test systems in the market and some previous studies. During the literature survey session about the standard test methods, three main test methods can be reached. These are “direct” method, “indirect” method and “driving-point” method. Between these test methods, “direct” method is chosen to be used for in this thesis work. This method is used to measure the vibrations, which are occurred because of the dynamic excitation of the test specimen, on the input side through blocking the output forces. Corresponding design efforts for the test set-up are conducted according to this method. The main parts of this thesis work are conceptual and detailed design stages. At the conceptual design stage, design problem is divided into subdivisions. Main components of the test system are handled one by one as a subdivision. The conceptual design of the subdivisions (components) are conducted separately. However, these components are in relation to each other. As a result, the dimensions and locations of these components effect each other. This phenomenon is handled during the detailed design stage. During detailed design stage, the dimensions and locations of the test system components are determined through the analyses, discussions and manufacturer firm communications about the designs. The final designs of the main components for the manufacturing stage are prepared. Design stages consist of T-slot table design, test set-up, which includes actuator, preload mechanism, test specimen-actuator connection interface and brackets, design, lifting system design for the temperature chamber. At the final stage, all designed components are gathered to construct whole test set-up in computer environment and virtual tests are conducted using finite element analysis in order to validate the designed test system. It is also planned to manufacture the designed components and assemble them to construct test set-up for real world application.

This thesis composed of five chapters and introduction is the first chapter. Second chapter handles the literature survey stage as a summary. Conceptual and detailed design stages are handled in the third and fourth chapter respectively. In the fifth chapter, test simulations of the final model of test setup are handled. In the sixth and final chapter, the conclusion part of the thesis is presented. In this part, finished and unfinished workings until this point and the future work plans are summarized.

CHAPTER 2

2. LITERATURE SURVEY

In the literature, various methods are used to determine the frequency dependent material properties of viscoelastic materials. “Vibrating beam” method is the most common method to fulfill this purpose [1-2]. However, another common method, which is “direct dynamic stiffness” method, is decided to use for this thesis workings instead of “vibrating beam” method [3-4]. According to direct method, a uniaxial tensile or shear material specimen is loaded using a harmonic force and transmitted force and displacements are measured from the connection points of this specimen.

During the literature survey section of this thesis, firstly, related standards, which cover the determination of dynamic mechanical properties of viscoelastic materials and resilient mechanical elements, are investigated. Through this investigation, useful information about test methods and conceptual design alternatives for the test set-up are gathered. Secondly, main test set-up components like T-slot table, brackets, lifting system for the temperature chamber etc. are researched. This research about individual components is used in the design stage of this thesis as a source for design ideas. Finally, previous studies about this kind of test system and similar test systems in the market are reviewed briefly. Reviewing the previous studies is guided and inspired the design efforts of this thesis work.

2.1. INVESTIGATION OF RELATED STANDARDS

In the literature, there are some standards, which cover standard test methods in details, related to the test system to be designed in this thesis work. These standards are published by International Organization of Standardization (ISO) and American Society of Testing and Materials (ASTM). These standards are discussed in the following sub-sections.

From these standards, useful information about specimen dimensions, test procedure, conceptual and detailed design of specimen connection interface can be obtained. After the investigation of these standards, the following useful information about test set-up are obtained:

- Rigid assembly of test specimen connection interface (testing interface)
- Actuation and sensor components
- Theoretical relation between dynamic stiffness of specimen and modulus and loss factor of material for the appropriate specimen dimensions
- Calculation of dynamic stiffness of test specimen through force and displacement measurements from appropriate locations
- Common types of test methods
- Test Procedure

2.1.1. ISO 10846

The general title of this standard is “Acoustics and vibration - Laboratory measurement of vibro-acoustic transfer properties of resilient elements” [5-7]. The following parts of this standard are investigated for this thesis:

- Part 2: Direct method for determination of the dynamic stiffness of resilient supports for translatory motion [5]

- Part 3: Indirect method for determination of the dynamic stiffness of resilient supports for translatory motion [6]

- Part 5: Driving point method for determination of the low-frequency transfer stiffness of resilient supports for translatory motion [7]

ISO 10846-2 specifies a direct method for measuring the dynamic transfer stiffness function of linear resilient supports. Replacing the support by a tension compression or shear specimen, this method can also be adapted to measure the complex modulus of a viscoelastic solid. The direct method concerns the laboratory measurement of vibrations on the input side and blocking output forces. The direct method covers the frequency range from 1 Hz up to a frequency f_{UL}, which is usually determined by the test rig [5].

ISO 10846-2 standard suggests the test setup given in Fig.1 for the vibration in axial direction.

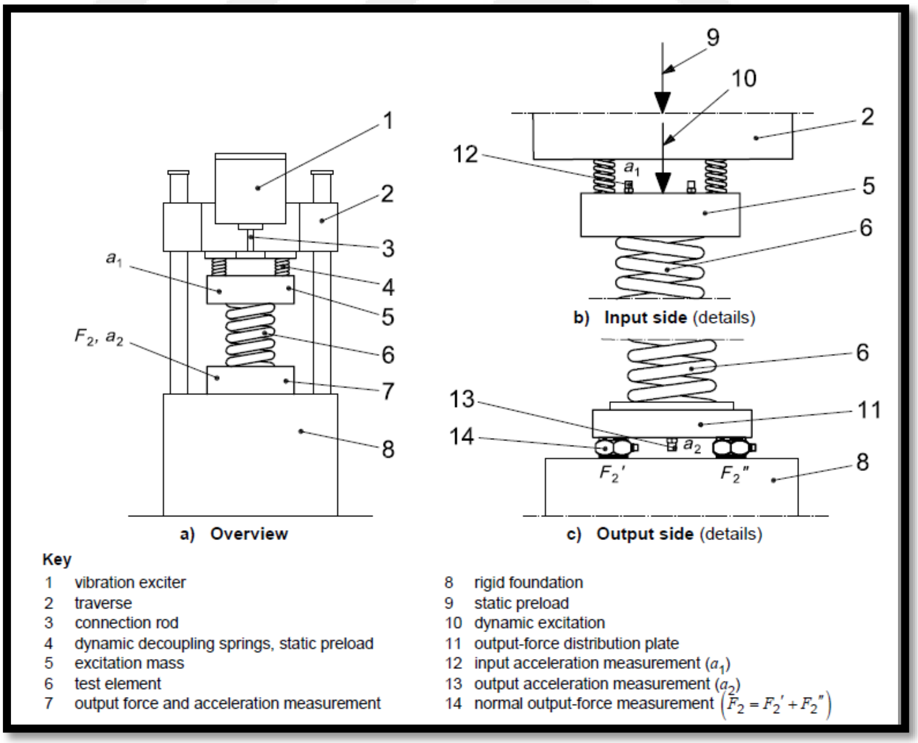

Figure 1. Suggested Test Setup in ISO 10846-2 for Direct Method under Axial Loading [5]

ISO 10846-3 specifies an indirect method for measuring the dynamic transfer stiffness function of linear resilient supports. Replacing the support by a tension compression or shear specimen, this method can also be adapted to measure the complex modulus of a viscoelastic solid. The indirect method concerns the laboratory measurements of vibration transmissibility. The indirect method covers the frequency range from f_2 to f_3. The values of f_2 and f_3 are determined by the test setup and the isolator under test. Typical values are; 20 Hz $\leq f_2 \leq$ 50 Hz and 2 kHz $\leq f_3 \leq$ 5 kHz [6].

ISO 10846-3 standard suggests the test setup given in Fig.2 for the vibration in axial direction.

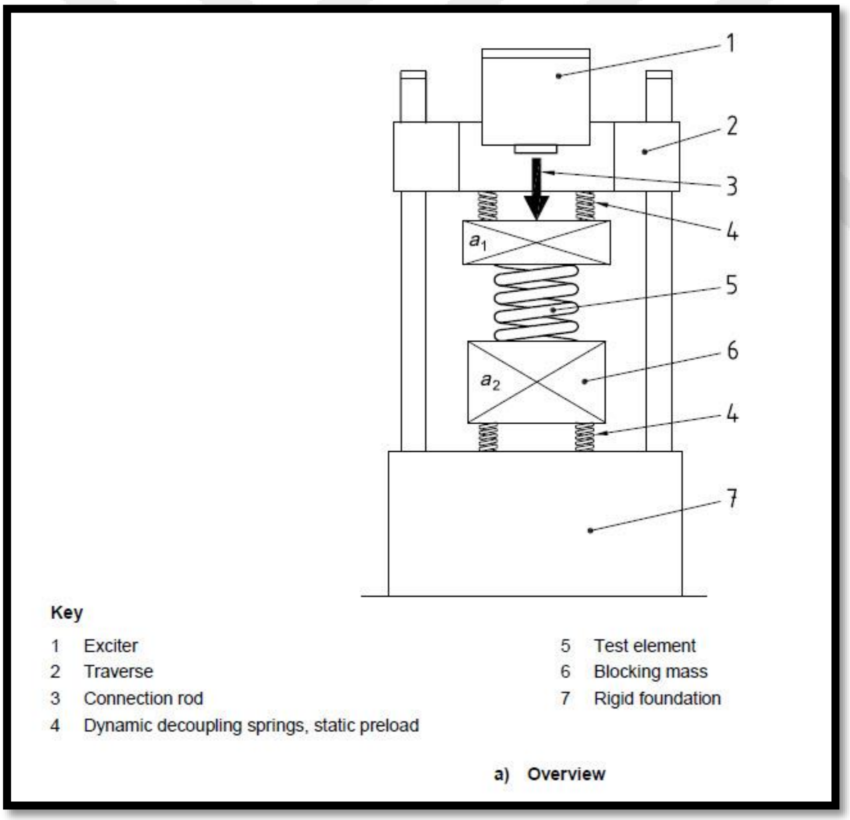

Figure 2. Suggested Test Setup in ISO 10846-3 for Indirect Method under Axial Loading [6]

ISO 10846-5 specifies a driving point method for measuring the low-frequency dynamic transfer stiffness function of linear resilient supports. Replacing the support by a tension compression or shear specimen, this method can also be adapted to measure the complex modulus of a viscoelastic solid. The driving point method concerns the laboratory measurement of vibrations and forces on the input side with the output side blocked. This method covers the frequency range from 1 Hz to the upper limiting frequency f_{UL} which is typically 50 Hz ≤ f_{UL} ≤ 200 Hz [7].

ISO 10846-5 standard suggests the test setup given in Fig.3 for the vibration in axial direction.

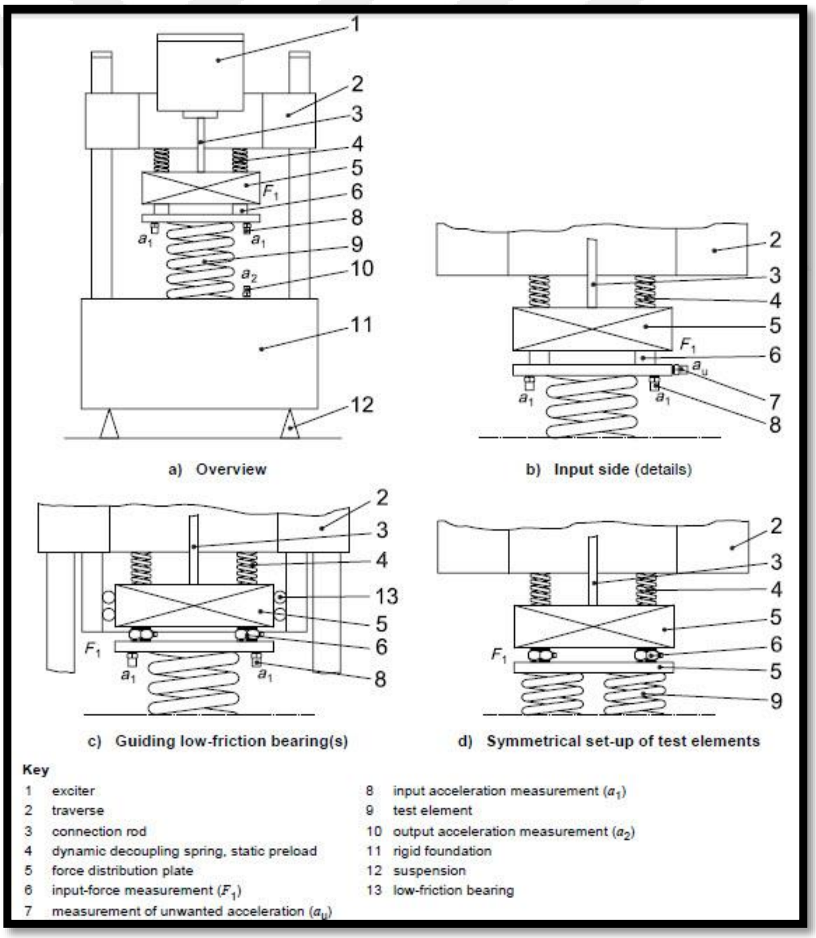

Figure 3. Suggested Test Setup in ISO 10846-5 for Driving Point Method under Axial Loading [7]

2.1.2. ISO 18437

The general title of ISO 18437 is “Mechanical vibration and shock - Characterization of the dynamic mechanical properties of viscoelastic materials” [8]. The following part of this standard is investigated for this thesis:

- Part 4: Dynamic stiffness method [8]

ISO 18437-4 specifies a direct method for measuring the complex dynamic moduli of elasticity for polymeric materials over a wide frequency and temperature range. Measurements are performed by the dynamic stiffness method, which uses electric signals from sensors attached to a test piece [8].

2.1.3. ISO 6721

The general title of this standard is “Plastics - Determination of dynamic mechanical properties” [9-10]. The following parts of this standard are investigated for this thesis:

- Part 4: Tensile vibration — Non-resonance method [9]
- Part 6: Shear vibration — Non-resonance method [10]

ISO 6721-4 is a non-resonance method which can be used to determine the tensile complex modulus of polymers. Typical frequency range for this method is 0.01-100 Hz. Suitable measurement range of this method for dynamic storage moduli is 0.01-5 GPa and for loss factors is greater than 0.1. This method can be used to study the variation of dynamic properties with temperature and frequency through most of the glass-rubber relaxation region. Master plots can be derived from this study which display dynamic properties over an extended frequency range at different temperatures [9].

ISO 6721-6 is a non-resonance method which can be used to determine the shear complex modulus of polymers. Typical frequency range for this method is 0.01-100 Hz. Suitable measurement range of this method for dynamic storage moduli is 0.l-50

MPa and for loss factors is greater than 0.1. This method can be used for the same purpose as part 4 of this standard [10].

2.1.4. ASTM D 4065-06

The title of this standard is “Standard practice for plastics: Dynamic mechanical properties: Determination and report procedures”. This standard includes a practice which is used to determine dynamic mechanical properties of plastics under the effect of various oscillatory deformations. At this practice, free vibration and resonant or non-resonant forced vibration techniques are used with instruments like dynamic mechanical or thermomechanical analyzers [11].

2.1.5. ASTM D 5992-96

The title of this standard is “Standard guide for dynamic testing of vulcanized rubber and rubber-like materials using vibratory method”. This standard includes a guide for dynamic testing of vulcanizing rubber and rubber-like materials and products. At this guide, different vibratory methods like free resonant vibration and forced resonant or non-resonant vibration are described which are used to determine dynamic properties [12].

2.2. Research on Test System Components

At the scope of this thesis, a modular dynamic test system is planned to be designed and validated. The testing methodology is guided by the information available in the standards presented in the previous section. The physical components which will constitute the test system are also important for the design effort. These components can be identified as:

- Brackets which are used to fix the testing interface components (actuator, force transducer etc.),
- T-slot table which is used for the mounting of all test set-up component except temperature chamber,
- Temperature chamber which used for the temperature controlled tests,

- Lifting system which is used to move and position the temperature chamber in test set-up.

From these components, brackets, T-slot table and lifting system will be original designs. Temperature chamber is available from the previous projects and there is no need to design or buy any new temperature chamber. There are some other components like data acquisition components but they are not considered part of this thesis. The literature research about the components which are planned to be designed and validated, is handled in this section.

2.2.1. BRACKETS

Actually, this component is part of the test set-up because it is used to fix the test set-up components (like actuator, force transducer, preload mechanism etc.) to the T-slot base table. At least two brackets are planned to use for the test set-up. One of them is used to fix the actuator to the T-slot base table and the other one is used at opposite side of this bracket to fix the preload mechanism, force transducer and right test specimen connection block. If necessary, additional one or two brackets can be used to fix the components. To learn what kind of brackets are used at this type of test systems, literature research is conducted. At the end of the research, it can be seen that one bracket type is frequently used with minor changes on its shape in similar systems.

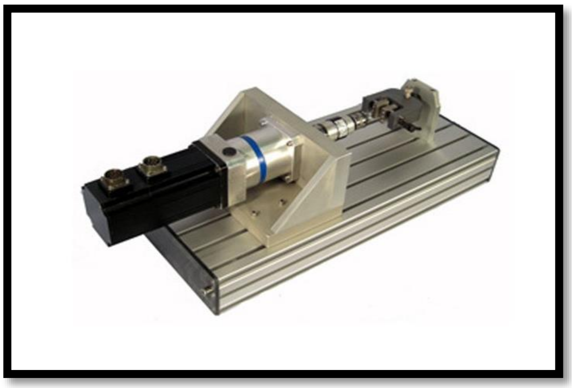

Figure 4. 160 T7 Torsional Electromechanical Universal Test Machine of TestResources Inc. [13]

The set-up which is given in Fig.4 belongs to torsional electromechanical universal test machine of TestResources Inc. 160 family. This test machine is designed for static and simple cyclic tests [13]. The left hand side bracket is appropriate to fix the actuator in thesis test set-up. Different bracket is used on the opposing side for this set-up. Another similar set-up is given in Fig.5 which is electrodynamic test machine belongs to TestResources Inc. 560 family. This test machine is capable of static, dynamic and fatigue testing applications [14]. At this set-up, opposite brackets are nearly similar. Similar brackets with some changes can be used in test set-up of this thesis work.

Figure 5. 560 LTh Electrodynamic Test Machine of TestResources Inc. [14]

2.2.2. T-SLOT TABLE

T-slot table is an important component for the test set-up because all components except temperature chamber and its lifting system are placed and fixed on it. Instead of any table, T-slot table is planned to use because T-slots provide modularity and flexibility in actuator-specimen orientation enabling test configuration for offset testing and different specimen sizes. Internet research is conducted about general T-slot standards and T-slot table dimensions. During this research, DIN 650 standard which is the most commonly used T-slot standard is found (see Fig.7) [16]. In addition, some reference T-slot table dimensions are found. One of this reference is Japanese brand, Ohnishi Measuring. Fig.8 is taken from this reference [17].

Figure 6. Sample T-slot Table with Carcass [15]

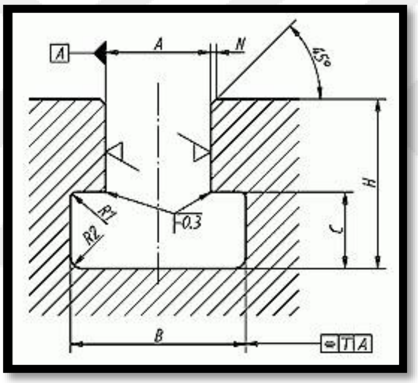

* Tolerance H8 for tenon and clamping slots, H12 for clamping slots
** p.d. = permissible deviation

A*	B	B p.d.**	C	C p.d.**	H max.	H min.	N max.	R1 max.	R2 max.	T
6	11	+1.5	5	+1	13	11	1	0.6	1	0.5
8	14.5	+1.5	7	+1	18	15	1	0.6	1	0.5
10	16	+2	7	+1	21	17	1	0.6	1	0.5
12	19	+2	8	+1	25	20	1	0.6	1	0.5
14	23	+2	9	+2	28	23	1.6	0.6	1.6	0.5
18	30	+2	12	+2	36	30	1.6	1	1.6	0.5
22	37	+3	16	+2	45	38	1.6	1	2.5	0.5
28	46	+4	20	+2	56	48	1.6	1	2.5	0.5
36	56	+4	25	+3	71	61	2.5	1	2.5	1
42	68	+4	32	+3	85	74	2.5	1.6	4	1

6.3 (= 1.6 for tolerance H8 or = 3.2 for tolerance H12)

all dimensions in mm

Figure 7. DIN 650 T-Slot Standards [16]

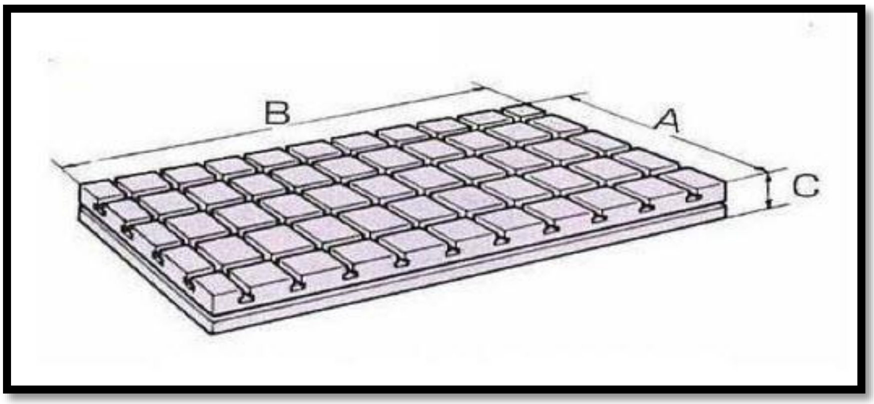

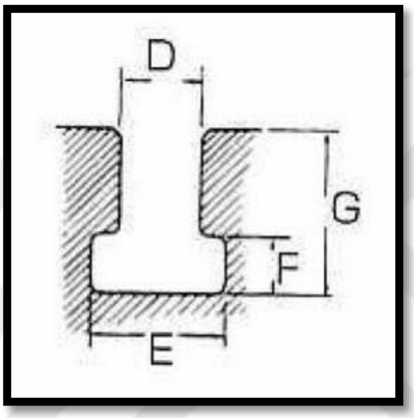

Accuracy & dimensions OSM-315B

No.	Diretion A		Direction B		A	B	C	D	E	F	G	Finish	Weight (kg)
	Number of T-slots	T-slot pitch	Number of T-slots	T-slot pitch									
1	6	100	3	80	300	650	70	18	30	13	30	Grinding the upper and lower surfaces	Approx. 77
2	7	100	4	80	350	800	75						122
3	8	100	5	80	410	900	75						156
4	7	150	5	80	410	1100	80						218
5	8	100	5	80	450	900	75						178
6	8	125	5	80	450	1100	80						238
7	8	125	5	100	500	1000	80						239
8	7	150	5	100	500	1100	80						273
9	8	150	5	100	550	1200	80						323
10	8	150	5	100	550	1300	80						356
11	8	150	5	125	600	1200	80						357
12	9	150	5	125	600	1400	90						486
13	8	200	5	125	650	1650	90						627

Figure 8. Ohnishi Measuring T-Slot Table Specifications [17]

2.2.3. LIFTING SYSTEM FOR THE TEMPERATURE CHAMBER

At this thesis work, a lifting system is planned to be designed to move and position temperature chamber for providing modularity to the test system. Firstly, internet research is conducted about the sigma profiles as structural members for the system and linear motion systems. During this research, many different domestic and foreign companies like Minitec, Da Vinci Mühendislik, Doğuş Kalıp etc. web sites with relevant design information and inspiration are found. Some useful information are gathered from these web sites.

Due to lifting system will be designed to carry heavy load (more than 100 kg), the profiles and linear motion systems must be chosen according to this requirement. In addition, linear motion system which will be used for vertical directional movement of temperature chamber must carry high moments caused by heavy loads. After the research, some sigma profiles (see Fig.9) and linear motion systems (see Fig.10) are found as suitable [18-20]. Some available CAD drawings of sigma profiles and linear motion systems (see Fig.11) are downloaded from the web sites for using at design stage of lifting system [21].

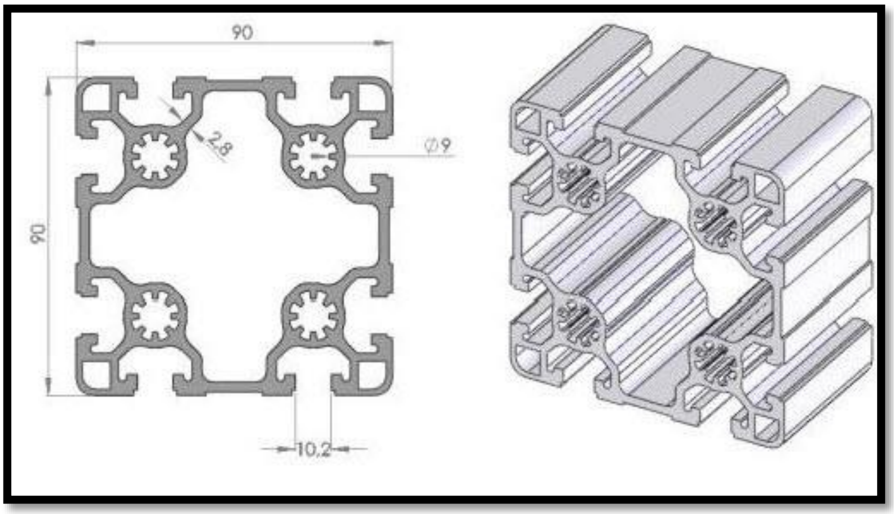

Figure 9. 90×90 Sigma Profile [18]

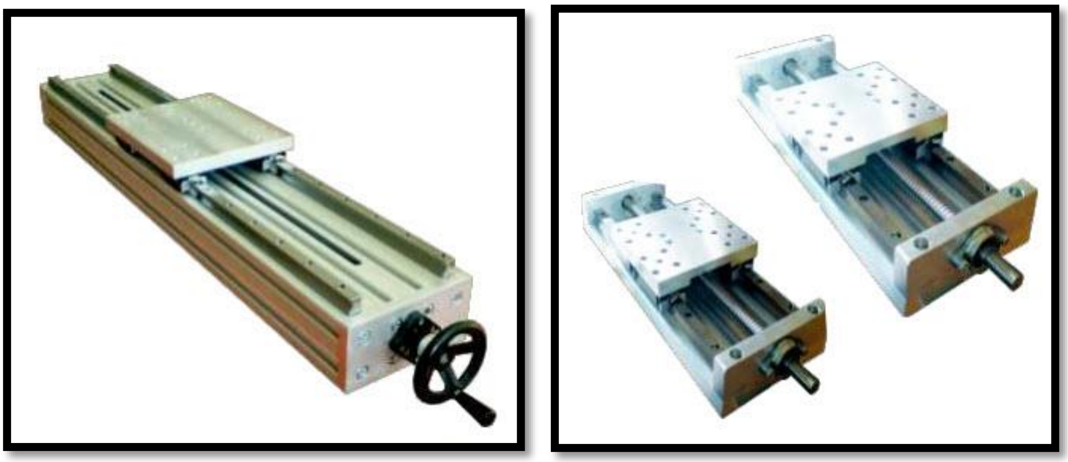

Figure 10. Linear Motion Systems [19-20]

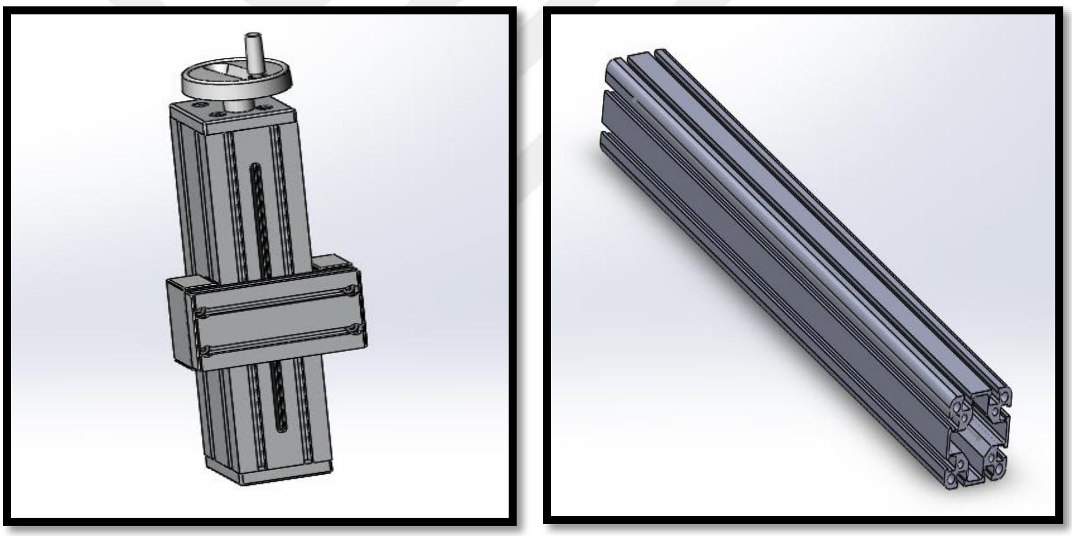

Figure 11. CAD Models of Linear Motion System and 90×90 Sigma Profile [21]

2.3. Previous Studies on Similar Test Systems

At this part of literature survey, previous studies on similar test systems with this thesis work are reviewed briefly. There are companies that produce similar test systems in the market especially MTS and Instron. Elastomer test system of MTS and fatigue test system of Instron are given as an example in Fig.12 [22-23] Because of these test systems are expensive and there are only a few domestic manufacturers alternative, to design this kind of test system is reasonable. For this purpose, some similar test system design and development projects are made before this thesis at mechanical engineering department of METU. Some of these projects are made under the supervision of my thesis advisor Gökhan O. Özgen [24-26]. As an example, Fig.13 and Fig.14 belongs to SAN-TEZ project [26]. For this reason, there are considerable know-how about these test systems. These know-how are used in this thesis as a reference.

Figure 12. Similar Test Systems of MTS (left) and Instron (Right) [22-23]

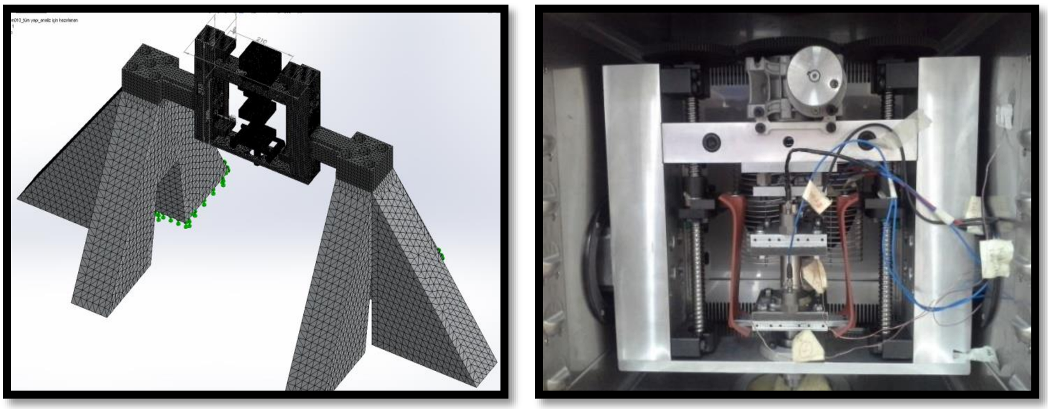

(a) **(b)**

Figure 13. (a) Solid Model (b) Real World Application of Test Specimen Connection Interface [26]

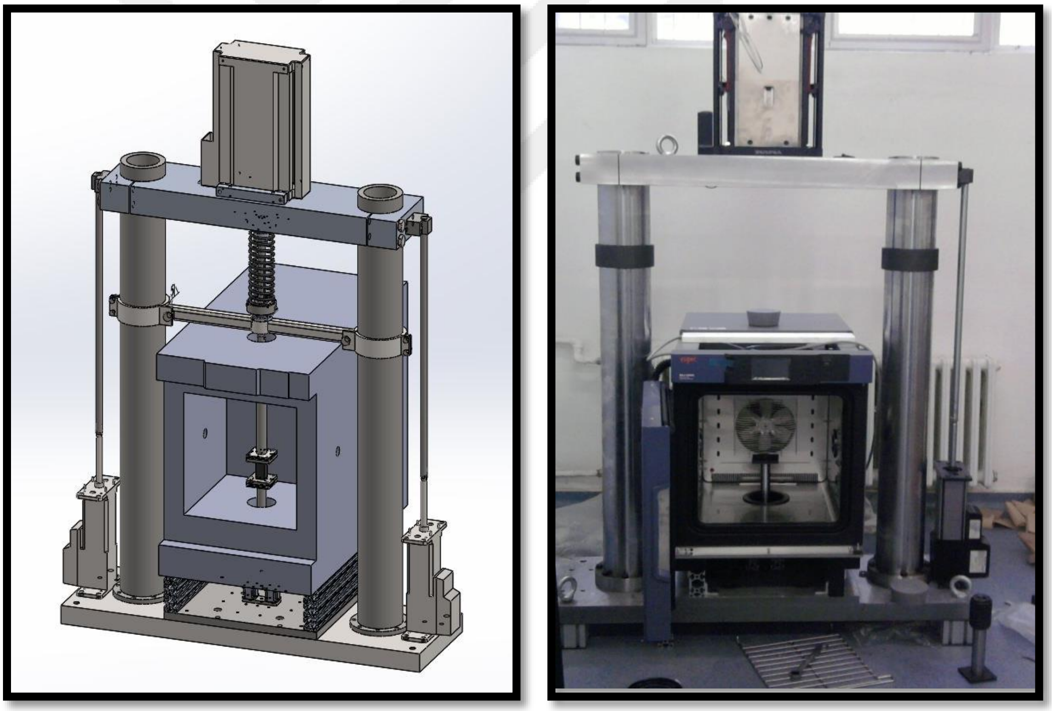

(a) **(b)**

Figure 14. (a) Solid Model (b) Real World Application of Test System [26]

CHAPTER 3

3. CONCEPTUAL DESIGN

During the conceptual design stage of this thesis, first design specifications, requirements and limitations are considered. According to the requirements of the test system, this test system should work (i.e. should be able to measure the dynamic stiffness of a resilient element) in a frequency range of 0-100 Hz applying a harmonic forcing at constant frequency with a maximum dynamic amplitude of 3 kN and perform the tests at low and high temperature values for isothermal conditions. Test system components should be designed and chosen to meet these requirements. For the temperature control of the test specimen, ESPEC model SU 261 temperature chamber which is available from a previous research project is used. To provide necessary dynamic loading, APS 400 long stroke exciter is chosen which is also available from a previous research project. The rest of the test system components are designed and manufactured considering 0-100 Hz operating frequency range of test system. To avoid adverse effects of the structural resonances of the test system supporting structure, lowest structural resonance frequency of whole system (test system with the actuator and the specimen) must be higher than 100 Hz. This requirement is checked at detailed design stage through finite element analysis. In addition to the requirements, modularity and originality are the important specifications of this test system. On the other hand, there are some limitations like budget, weight, transportation of the manufactured components etc.

The components which are original designs work are T-slot table, lifting system for the temperature chamber and test set-up components (preload mechanism, test specimen connection blocks, brackets etc.). The dimensions and positions of these components are affected from each other. For this reason, design efforts are advanced in parallel to each other.

3.1. CONCEPTUAL DESIGN OF TEST SET-UP

Test set-up is consisted of an actuator, test specimen, preload mechanism, test specimen connection blocks, actuator-test specimen connection components and brackets. All of these components are designed originally except the actuator, test specimen, linear stage and gear box used in the preload mechanism. Design efforts of test set-up is mainly concentrated on preload mechanism and its connection with other components (like test specimen connection blocks and preload mechanism side main bracket). Design of preload mechanism is one of the most challenging part of this thesis work. During the conceptual design period of test set-up; actuator is selected and bracket alternatives are prepared for the selected actuator, remaining components (preload mechanism, preload mechanism side main bracket, connection components between test specimen blocks and preload mechanism and main bracket) of test set-up are handled together because these components are strictly related to each other. Generic solid model is prepared for test set-up at the end of the conceptual design period.

3.1.1. CONCEPTUAL DESIGN OF ACTUATOR BRACKET

After the literature research about brackets, it is seen that one type of bracket is mostly used at this kind of set-up. In addition, some different bracket alternatives are determined. In early stage of conceptual design, there are three actuator options. Two of the three, APS 400 long stroke exciter and Tritex T2M090 linear actuator, are available from previous research projects but the other one H2W brand dual voice coil linear actuator is not. Later, APS 400 is chosen as the actuator for the test system between these options. Main reason for this selection is availability of this actuator. There is one more available actuator which is Tritex T2M090 but this actuator has low bandwidth and displacement resolution issues. As a result, APS 400 is found as suitable which is given in Fig.15 [27]. This actuator is about 73 kg. Bracket alternatives are prepared considering this weight. Two separate brackets or one large bracket are used in design efforts. Five bracket alternatives are prepared for this actuator in conceptual design period which are given in Fig.16 through Fig.20.

Figure 15. APS 400 Long Stroke Exciter [27]

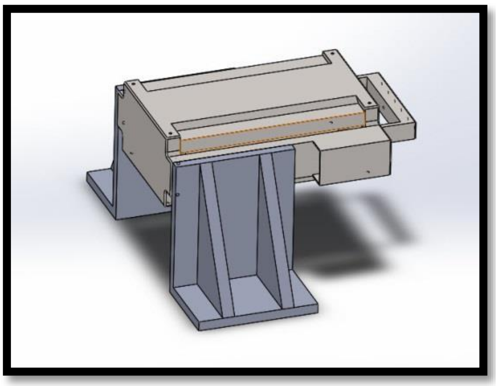

Figure 16. APS 400 First Bracket Alternative

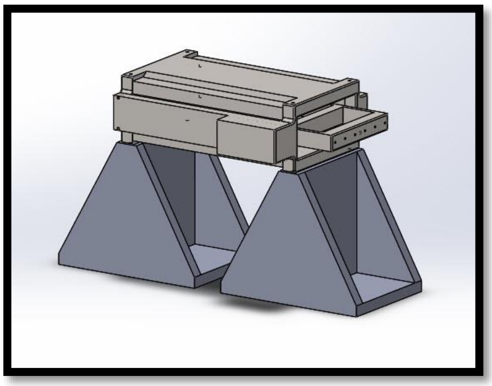

Figure 17. APS 400 Second Bracket Alternative

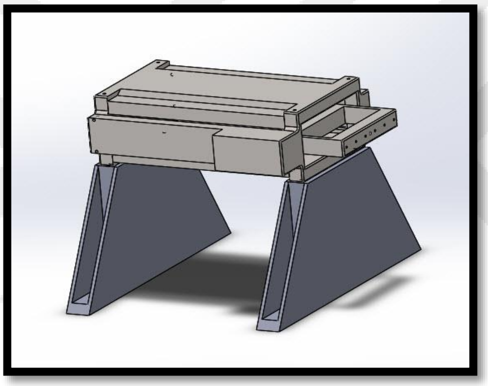

Figure 18. APS 400 Third Bracket Alternative

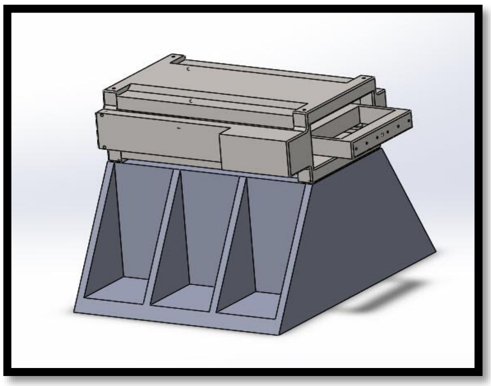

Figure 19. APS 400 Fourth Bracket Alternative

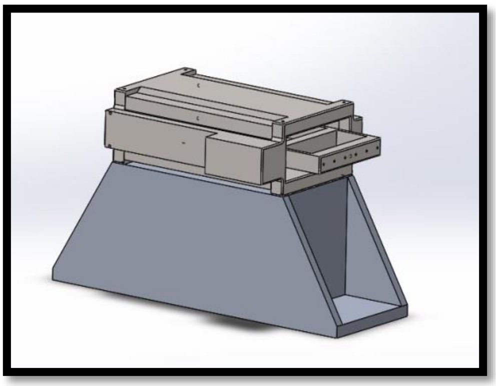

Figure 20. APS 400 Fifth Bracket Alternative

3.1.2. CONCEPTUAL DESIGN OF REMAINING TEST SET-UP COMPONENTS

The remaining test set-up components are preload mechanism, preload mechanism side main bracket, test specimen connection blocks and necessary connection components between them. Force transducer, test specimen and some preload mechanism components (linear stage and reducer) are also part of these remaining components but they are not designed but off-the-shelf products will be used.

Preload mechanism is an important part of test set-up. It is used in test systems for a process where the crosshead moves to load the specimen to a specified value before a test starts. Data is not captured during the preload segment.

Some internet research are conducted about preload mechanism before the conceptual design period but this research is not provided useful information. For this reason, some previous studies are investigated as a result of my supervisor's suggestion [26].

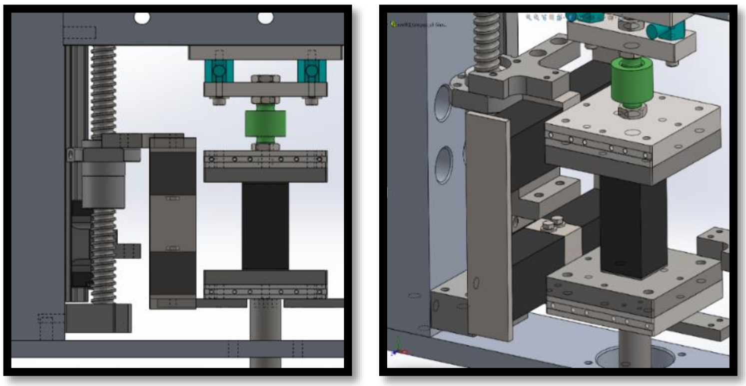

Figure 21. Previous Studies about Preload Mechanism [26]

Fig.21 shows part of the preload mechanism as a solid model from one of the previous study [26]. For the conceptual design period of preload mechanism for this thesis, these kind of figures are investigated to get some useful hints.

After the internet research and investigation of previous studies, some ideas about preload mechanism are occurred. These ideas are visualized through hand drawings for saving time. Some brainstorming sessions are also performed during the conceptual design period. Preload mechanism can be inside or outside the cabin. Main decision is made about this issue. Some alternative hand drawings and also some solid models are prepared about this subject. As a result, it is decided to position the preload mechanism outside the cabin because of the side holes of cabin are so small.

After the location of preload mechanism is decided, design efforts are concentrated on the outside alternatives. Some discussions are performed about the alternatives through hand drawings. At the end, a suitable design is prepared for the preload mechanism. Because of remaining components of test set-up are strictly related with preload mechanism, these components are also added to the conceptual design of preload mechanism. Conceptual model given in Fig.22 is the result of conceptual design effort of the preload mechanism. This model is prepared without actuator, actuator bracket and some preload mechanism components (linear stage and reducer).

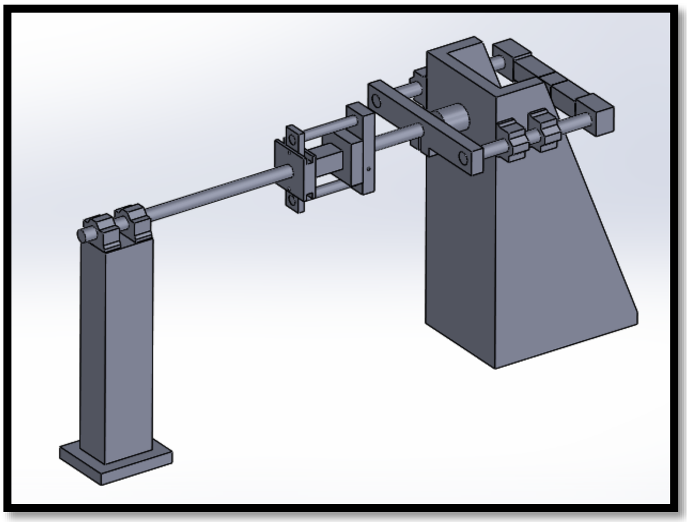

Figure 22. Generic Conceptual Design of Test Set-Up

3.2. CONCEPTUAL DESIGN OF T-SLOT TABLE

T-slot table is one of main components of this thesis test system. T-slot table provides modularity through its T-slots. Other components are positioned on T-slot table and fixed along the T-slots. At early stage of conceptual design, it is planned to lift T-slot table from the ground. Thus, lifting system of the temperature chamber can enter under the T-slot table. However, according to the development on the lifting system design, the need for lifting of T-slot table is removed. As a result, it is planned to place T-slot table on the ground and any design efforts about the bottom of the T-slot table is not spent.

After literature research about the T-slot table, necessary information are gathered. Using these information generic T-slot table design is prepared as a conceptual design (see Fig.23).

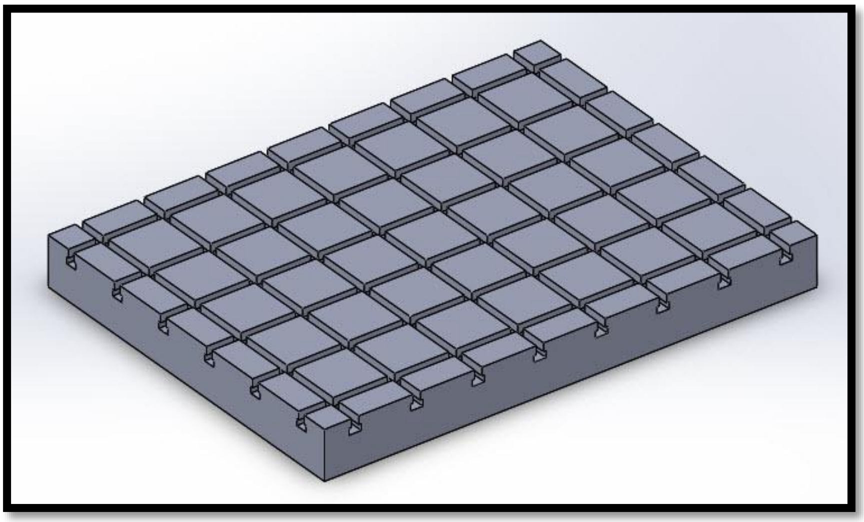

Figure 23. Generic Conceptual Design of T-slot Table

3.3. CONCEPTUAL DESIGN OF LIFTING SYSTEM FOR THE TEMPERATURE CHAMBER

Temperature chamber is the important component of the test system. Specimens can be tested at different temperatures within a certain range inside the temperature chamber. On the other hand, sometimes there is no need to control temperature during tests. In addition, the temperature chamber which is used at this test system can also be used other test applications. For this reason, temperature chamber must be moved and positioned with a certain accuracy depending on the circumstances by the aid of another component which provides modularity to the test system. As a result, a lifting system is decided to be originally designed to meet this need.

At early stage of this design work, the material of liftign system frame was selected as sigma (aluminum) profile. Market research was done on the sigma profiles and the related applications through internet. Some useful CAD drawings are downloaded for using in the design stage. Then, first generic design is prepared for the lifting system with temperature chamber on it which is given in Fig.24. According to this design, the lifting operation of the temperature chamber is fulfilled by two separate linear motion systems with arms attached on their sliders but this usage is practically not feasible. As a result, two options are occurred that can be used instead of two separate linear motion systems. It can be seen from Fig.25, one of them uses one linear motion system and the other one is used two connected linear motion systems.

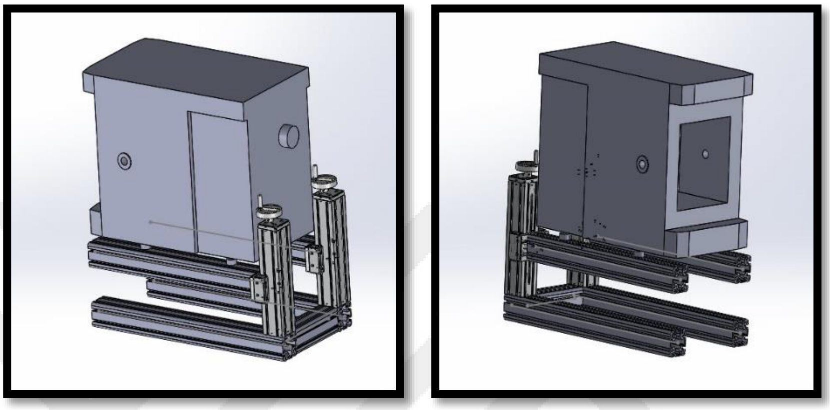

Figure 24. First Generic Conceptual Design of Lifting System with Temperature Chamber

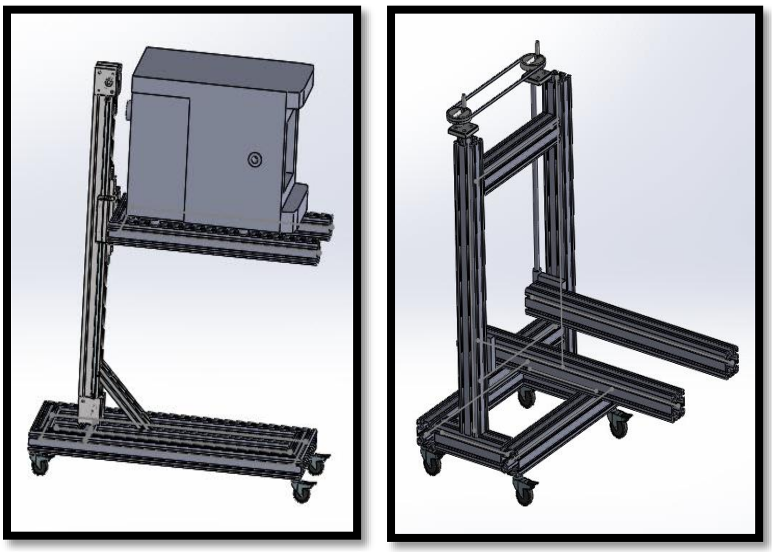

(a) **(b)**

Figure 25. Lifting System with (a) One Linear Stage (b) Two Connected Linear Stages

After some progression is made, a manufacturer firm is found for the lifting system to get ideas about the design and manufacturing through internet research. During the discussion with this firm, some important points are identified. Another progress is made through this way and the design of the lifting system is evolved. One linear motion system option is eliminated. Design efforts are concentrated on two connected linear motion system option. At this point, one of the product of the firm which is similar to lifting system is investigated. As a result, the linear motion system of this product is found as suitable for lifting system. For this reason, the selection and design of linear motion system for the lifting system is left to this firm.

After some discussions about the design of lifting system, two different design alternatives given in Fig.26 are prepared without linear motion system. One of them is suitable to enter under the T-slot table and the other one is suitable to comprise the T-slot table. Final conceptual design is selected between these alternatives (see Fig.27). Lifting system will be used for different applications as well. For this reason, second alternative which is comprised the T-slot table is found more suitable than the first one. As a result, the second alternative is selected as the final conceptual design and some modifications are made on it.

Figure 26. Final Two Conceptual Design Alternatives of Lifting System

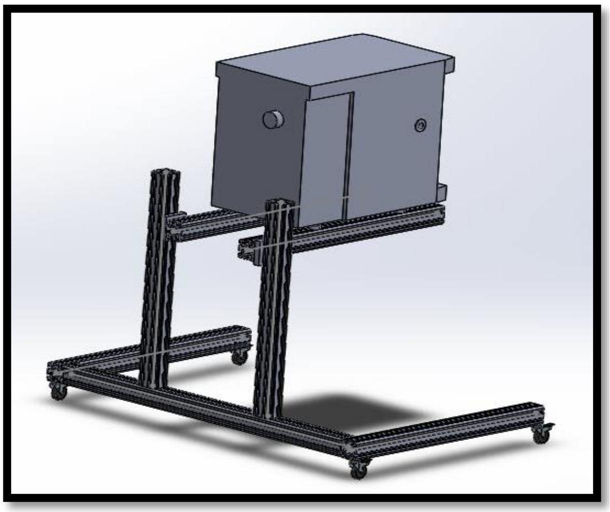

Figure 27. Final Conceptual Design of Lifting System with Temperature Chamber

CHAPTER 4

4. DETAILED DESIGN

This part of the thesis covers the detailed design efforts on the test system components. The details of the components such as dimensions, positions and so on are determined through analyses, references, and discussions. Conceptual designs of these components are used as a starting point for the detailed design stage. For this test system, almost all components are related to each other which means details of one component are affected by details of another component. As a result, detailed design processes of this test system components are advanced in parallel to each other.

Detailed design of test set-up, T-slot table and lifting system for temperature chamber are handled one by one during this chapter and the final detailed design of whole test system is visualized at the end.

4.1. DETAILED DESIGN OF TEST SET-UP

At the end of conceptual design period of test set-up, actuator bracket alternatives are prepared as solid models and generic solid model is prepared for the remaining components of test set-up. At this stage, some analyses are conducted on these solid models to determine the appropriate dimensions and positions of the test set-up components according to the test system specifications and limitations like 0-100 Hz operating frequency range, maximum 1 kN preload and maximum 3 kN force.

4.1.1. DETAILED DESIGN OF ACTUATOR BRACKET

At conceptual design period, some bracket alternatives are prepared for APS 400 actuator. These alternatives are referenced for the appropriate bracket selection of APS 400. During the detailed design stage, additional two bracket alternatives are prepared (see Fig.28) according to minimize the mass and footprint (covered area on T-slot table) of bracket.

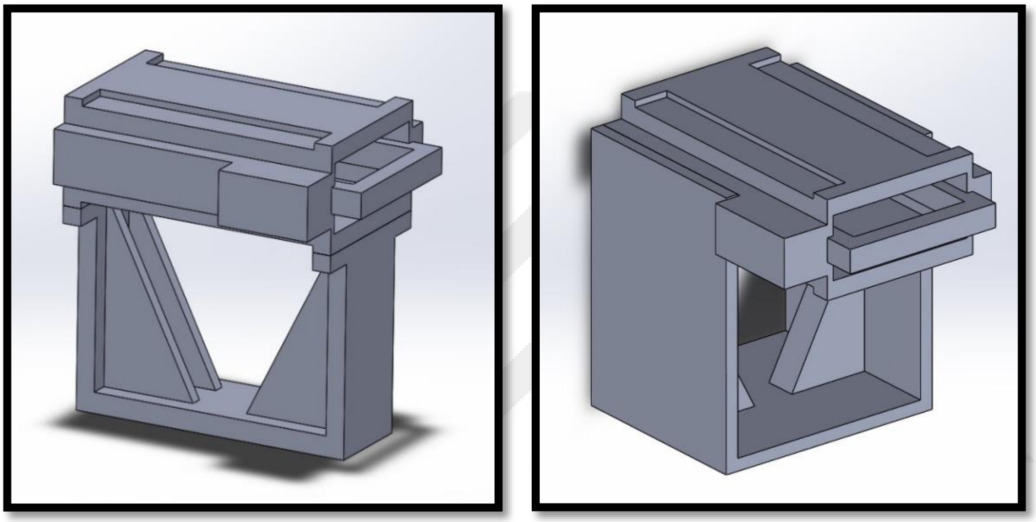

Figure 28. Final Two Bracket Alternatives for APS 400 Actuator

Thus, seven bracket alternatives are prepared for APS 400 actuator. Because of the final two alternatives consider the final state of test set-up, the selection is made between these two instead of the previous alternatives. Modal analyses for specific dimensions are conducted on both these final two alternatives. According to the modal analyses (checking if the first structural resonant frequency of the bracket actuator assembly is higher than 100 Hz), both alternatives are suitable for the test setup. However, left hand side bracket alternative in Fig.28 is selected for the actuator because this bracket is found as compatible with the designs of other test set-up components.

The dimensions of the selected bracket are given in Fig.29. These dimensions are determined according to the other test system components (especially actuator).

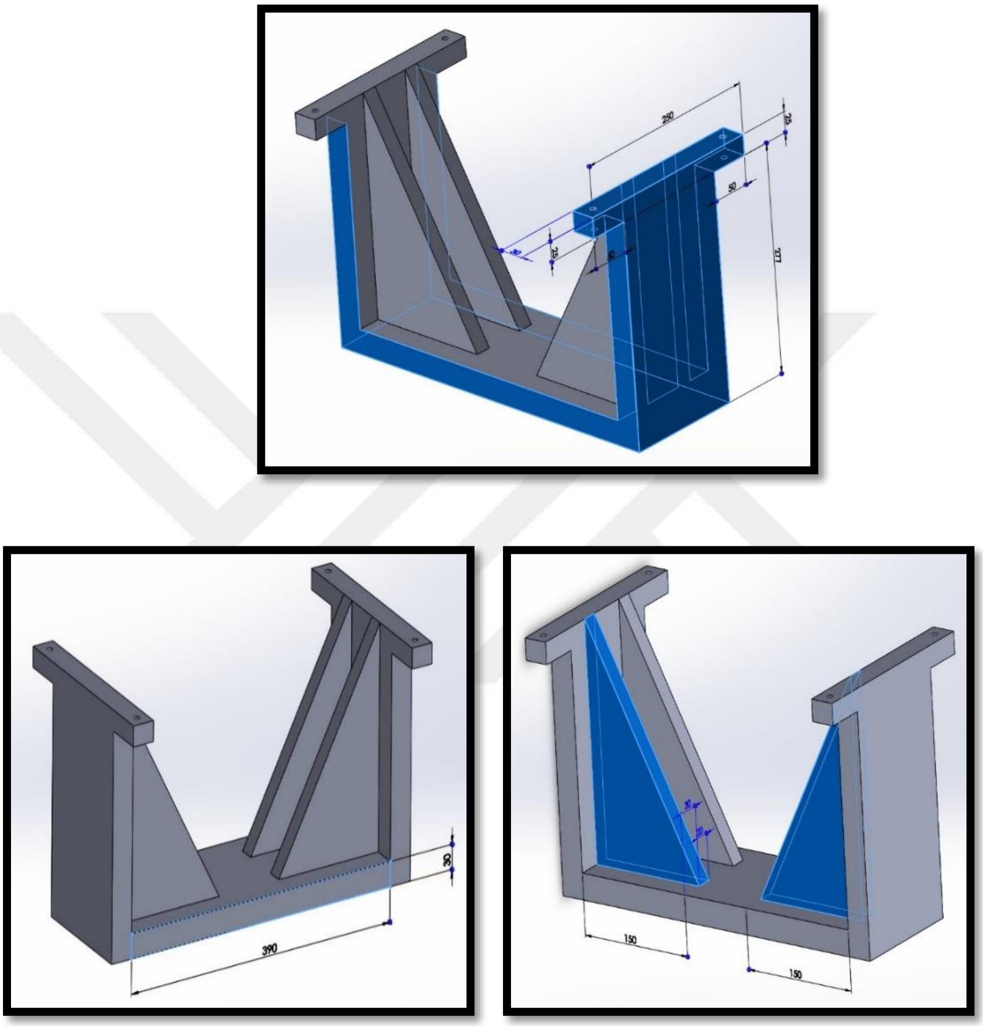

Figure 29. Dimensions of Selected Actuator Bracket

Modal analysis is conducted on selected actuator-bracket assembly with these dimensions of bracket. No further dimension or geometry modification is made because the results of the modal analysis for the initial conditions are found as sufficient large. During modal analysis, special material properties are defined for the actuator to provide both weight and rigidity of APS 400 actuator. On the other hand, structural steel is used for the bracket of actuator. Model is fixed from sidebottom surface of the bracket. Element size for mesh is determined by doing a convergence study. In Fig.30, modal analysis of actuator-bracket assembly is shown. The results of this modal analysis are given in Table 1. It can be seen from the results presented in Table 1 that the first mode of the modal analysis for the actuator-bracket assembly is about 0 Hz. This mode includes the rigid body motion of actuator's armature. For this reason, this mode is disregarded. The important mode for this study is second mode which is 244.12 Hz and much higher than the critical frequency value of the test system (target upper frequency of test system which is 100 Hz).

Thus, detailed design of actuator bracket is completed for now. If it is necessary, some modifications can be made later according to demands of the test set-up. After detailed design of remaining test set-up components are completed, all components will be combined and further analyses will be conducted on this combined model.

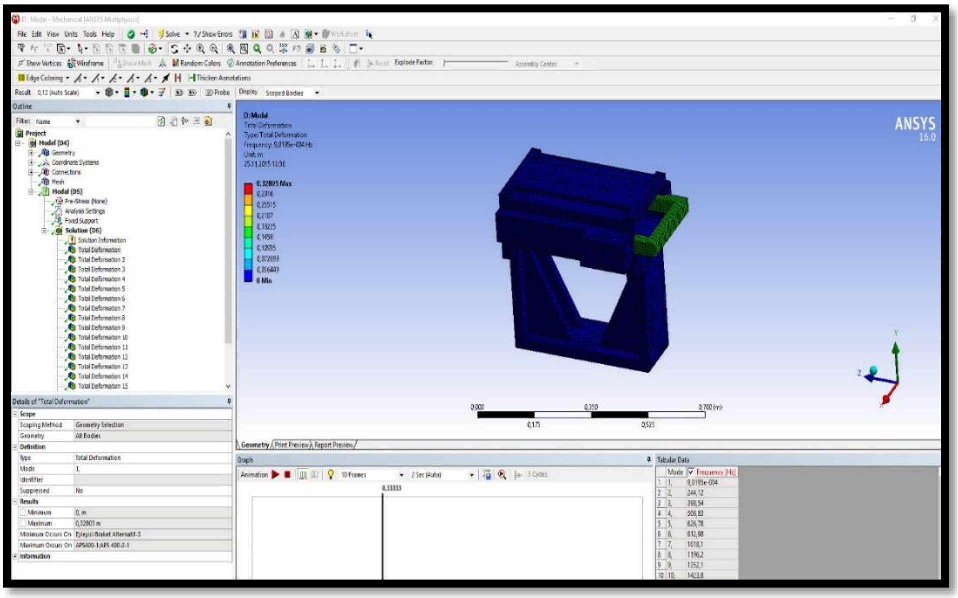

Figure 30. Modal Analysis of Selected APS 400 Actuator-Bracket Assembly

Table 1. Results of Modal Analysis on APS Actuator-Bracket Assembly

	1.Mode	2.Mode	3.Mode	4.Mode	5.Mode
Frequency (Hz)	≈ 0	244.12	398.54	506.83	626.78

4.1.2. Detailed Design of Remaining Test Set-up Components

At the end of the conceptual design period of remaining test set-up components, a generic solid model is prepared. At the beginning of detailed design period, initial dimensions of components are used. Solid model is prepared with using these dimensions for test set-up without actuator-bracket assembly which is given in Fig.31. Modal analyses are conducted on this solid model starting with determined initial dimensions and positions. Some modifications on the components are made during the modal analyses as design iterations.

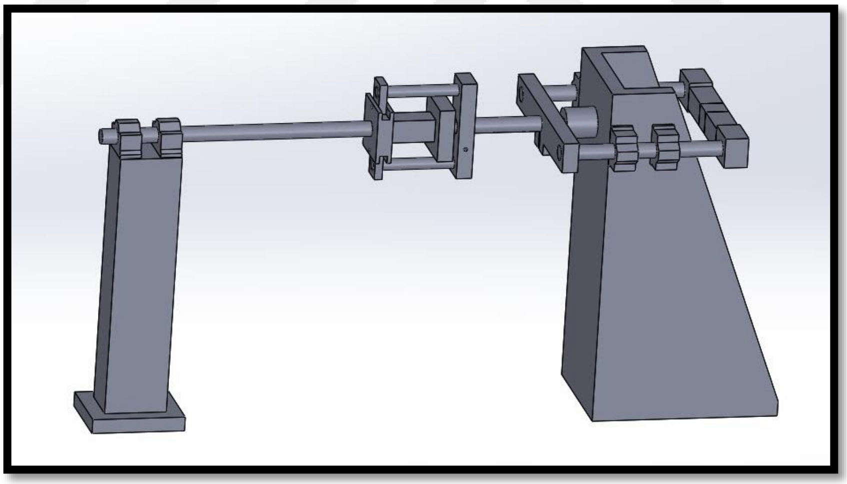

Figure 31. Solid Model of Test Set-Up without Actuator-Bracket Assembly

Before going into design iterations, a convergence analysis is performed to determine the optimum element size for the mesh used in the finite element model of the test system. After some trials, 9 mm element size is selected as the starting point for convergence method because an error message is taken from the analysis above this value. The lower limit for the element size is selected as 4 mm because analyses are taken too much time which is not reasonable for iterations below this value. As a result, analyses are conducted between 4 and 9 mm element sizes with 1 mm decrement.

The results of the modal analyses with respect to the convergence method are given in Table 2. According to the results, there is not much change in lowest structural modal frequencies for different element sizes. The necessary time to analyze a model with lower element size is more than with higher element size. For this reason, an efficient element size should be chosen between these values for the further analyses. Therefore, 8 mm element size is selected for the mesh of finite element model to be used in design iterations.

Table 2. Element Size vs. Modal Frequencies

	1.	**2.**	**3.**	**5.**	**10.**	**15.**	**25.**
9 mm	25,95	146,6	147,3	228,4	266,5	289,4	512,8
8 mm	25,99	146	147	227,2	269,5	289,5	513,7
7 mm	26,00	146,1	146,9	227,5	268,6	289,6	512,7
6 mm	26,02	142,5	144,4	227,9	267,9	289,6	512,7
5 mm	26,05	145,2	146,3	227,6	265,7	289,7	512,6
4 mm	26,07	145	146,5	228	267,2	289,9	512,9

4.1.2.1. Design Iterations Based on Modal Analysis Results

Two different models are selected as the starting points of modal analysis based design iterations because of their different mode shape characteristics. These models are named as Model 0 and Model 1. Model 0 is the first prepared model for test set-up components at the end of the conceptual design stage. To identify the components, each component of Model 0 is numbered like in Fig.32. Model 1 is slightly different version of Model 0 which is given in Fig.33. Two extra linear bearings are used at this model for bearing of connection shafts inside the cabin. Model 1 is accepted as one of two design alternatives because it has different modal behaviours.

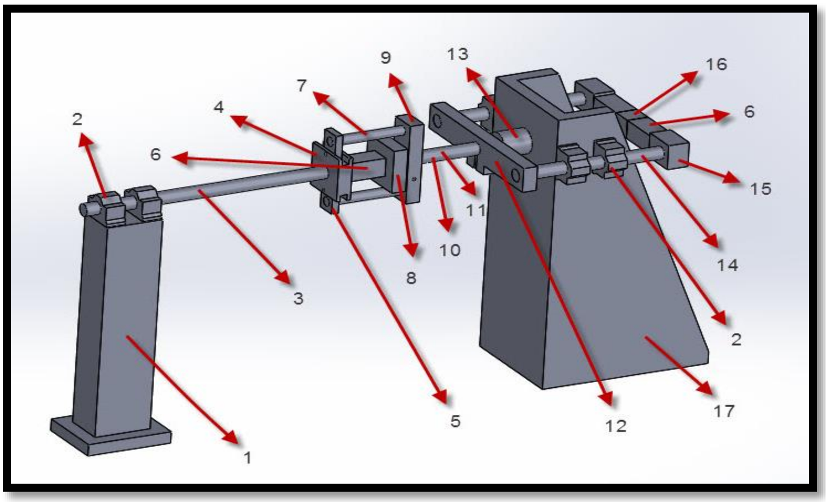

Figure 32. Solid Model of Model 0

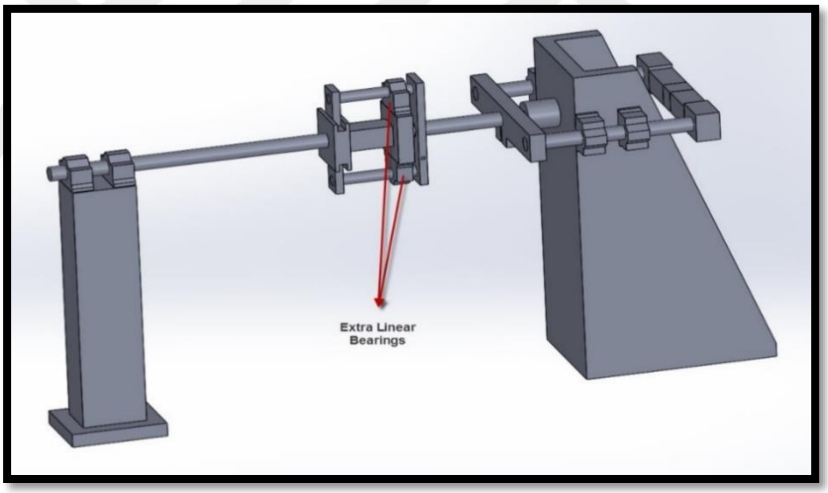

Figure 33. Solid Model of Model 1

Information of all components of Model 0 and Model 1 (extra linear bearings are numbered as 18) are given in Table 3. Three types of materials are used during the analyses. The properties of these materials are given in Table 4.

Table 3. Information of Model 0 Components

Index	Component Name	Material
1	Linear Bearings Support	Structural Steel
2	Linear Bearings	Structural Steel
3	Actuator Side Main Shaft	Structural Steel
4	Specimen Connection Block (Left)	Aluminum
5	Connection Components Inside the Cabin	Aluminum
6	Elastomer Components	Elastomer Material
7	Connection Shafts Inside the Cabin	Structural Steel
8	Specimen Connection Block (Right)	Aluminum
9	Distribution Component Inside the Cabin	Aluminum
10	Counter Side Main Shaft	Structural Steel
11	Hollow Shaft	Structural Steel
12	Distribution Component Outside the	Aluminum
13	Force Transducer	Aluminum
14	Connection Shafts Outside the Cabin	Structural Steel
15	Connection Components Outside the	Aluminum
16	Linear Stage Connection Component	Aluminum
17	Counter Side Bracket	Structural Steel
18	Extra Linear Bearings	Structural Steel

Table 4. Material Properties for Iterations on Modal Analyses

	Density (kg/m^3)	Young Modulus (Pa)	Poisson's Ratio
Structural Steel	7850	2e11	0.3
Aluminum	2700	70e9	0.33
Elastomer Material	1200	5e6	0.499

As part of design iterations, material or dimension modifications are made on the components. Each iteration has different modifications and modal analyses are conducted to the model for each iteration. Ten design iterations (initial design set included) are conducted on Model 0. Each iteration is handled one by one with its details in Tables 5 through Table 14. The results of modal analyses according to the iterations on Model 0 is given in Table 15. Then, mode shapes, which are related to the modes given in Table 15 are presented in Fig.34 through Fig.38.

Table 5. Design Iteration 0 (Initial Design Set) for Model 0

Index	Component Name	Material	Modification	Modification Description
1	Linear Bearings Support	Structural Steel	Non	
2	Linear Bearings	Structural Steel	Non	
3	Actuator Side Main Shaft	Structural Steel	Non	
4	Specimen Connection Block (Left)	Aluminum	Non	
5	Connection Components Inside the Cabin	Aluminum	Non	
6	Elastic Components	Elastic Material	Non	
7	Connection Shafts Inside the Cabin	Structural Steel	Non	
8	Specimen Connection Block (Right)	Aluminum	Non	
9	Distribution Component Inside the Cabin	Aluminum	Non	
10	Counter Side Main Shaft	Structural Steel	Non	
11	Hollow Shaft	Structural Steel	Non	
12	Distribution Component Outside the Cabin	Aluminum	Non	
13	Force Transducer	Aluminum	Non	
14	Connection Shafts Outside the Cabin	Structural Steel	Non	
15	Connection Components Outside the Cabin	Aluminum	Non	
16	Linear Stage Connection Component	Aluminum	Non	
17	Counter Side Bracket	Structural Steel	Non	

Table 6. Design Iteration 1 for Model 0

Index	Component Name	Material	Modification	Modification Description
1	Linear Bearings Support	Structural Steel	Non	
2	Linear Bearings	Structural Steel	Non	
3	Actuator Side Main Shaft	Structural Steel	Yes	This shaft is converted into 15 mm dia. hollow shaft
4	Specimen Connection Block (Left)	Aluminum	Non	
5	Connection Components Inside the Cabin	Aluminum	Non	
6	Elastic Components	Elastic Material	Non	
7	Connection Shafts Inside the Cabin	Structural Steel	Non	
8	Specimen Connection Block (Right)	Aluminum	Non	
9	Distribution Component Inside the Cabin	Aluminum	Non	
10	Counter Side Main Shaft	Structural Steel	Non	
11	Hollow Shaft	Structural Steel	Non	
12	Distribution Component Outside the Cabin	Aluminum	Non	
13	Force Transducer	Aluminum	Non	
14	Connection Shafts Outside the Cabin	Structural Steel	Non	
15	Connection Components Outside the Cabin	Aluminum	Non	
16	Linear Stage Connection Component	Aluminum	Non	
17	Counter Side Bracket	Structural Steel	Non	

Table 7. Design Iteration 2 for Model 0

Index	Component Name	Material	Modification	Modification Description
1	Linear Bearings Support	Structural Steel	Non	
2	Linear Bearings	Structural Steel	Non	
3	Actuator Side Main Shaft	Structural Steel	Non	
4	Specimen Connection Block (Left)	Aluminum	Yes	Structural steel is used instead of aluminum
5	Connection Components Inside the Cabin	Aluminum	Yes	Structural steel is used instead of aluminum
6	Elastic Components	Elastic Material	Non	
7	Connection Shafts Inside the Cabin	Structural Steel	Non	
8	Specimen Connection Block (Right)	Aluminum	Yes	Structural steel is used instead of aluminum
9	Distribution Component Inside the Cabin	Aluminum	Yes	Structural steel is used instead of aluminum
10	Counter Side Main Shaft	Structural Steel	Non	
11	Hollow Shaft	Structural Steel	Non	
12	Distribution Component Outside the Cabin	Aluminum	Yes	Structural steel is used instead of aluminum
13	Force Transducer	Aluminum	Yes	Structural steel is used instead of aluminum
14	Connection Shafts Outside the Cabin	Structural Steel	Non	
15	Connection Components Outside the Cabin	Aluminum	Yes	Structural steel is used instead of aluminum
16	Linear Stage Connection Component	Aluminum	Yes	Structural steel is used instead of aluminum
17	Counter Side Bracket	Structural Steel	Non	

Table 8. Design Iteration 3 for Model 0

Index	Component Name	Material	Modification	Modification Description
1	Linear Bearings Support	Structural Steel	Yes	Aluminum is used instead of steel
2	Linear Bearings	Structural Steel	Yes	Aluminum is used instead of steel
3	Actuator Side Main Shaft	Structural Steel	Yes	Aluminum is used instead of steel
4	Specimen Connection Block (Left)	Aluminum	Non	
5	Connection Components Inside the Cabin	Aluminum	Non	
6	Elastic Components	Elastic Material	Non	
7	Connection Shafts Inside the Cabin	Structural Steel	Yes	Aluminum is used instead of steel
8	Specimen Connection Block (Right)	Aluminum	Non	
9	Distribution Component Inside the Cabin	Aluminum	Non	
10	Counter Side Main Shaft	Structural Steel	Yes	Aluminum is used instead of steel
11	Hollow Shaft	Structural Steel	Yes	Aluminum is used instead of steel
12	Distribution Component Outside the Cabin	Aluminum	Non	
13	Force Transducer	Aluminum	Non	
14	Connection Shafts Outside the Cabin	Structural Steel	Yes	Aluminum is used instead of steel
15	Connection Components Outside the Cabin	Aluminum	Non	
16	Linear Stage Connection Component	Aluminum	Non	
17	Counter Side Bracket	Structural Steel	Yes	Aluminum is used instead of steel

Table 9. Design Iteration 4 for Model 0

Index	Component Name	Material	Modificiation	Modification Description
1	Linear Bearings Support	Structural Steel	Non	
2	Linear Bearings	Structural Steel	Non	
3	Actuator Side Main Shaft	Structural Steel	Non	
4	Specimen Connection Block (Left)	Aluminum	Non	
5	Connection Components Inside the	Aluminum	Non	
6	Elastic Components	Elastic Material	Non	
7	Connection Shafts Inside the Cabin	Structural Steel	Yes	Aluminum is used instead of steel
8	Specimen Connection Block (Right)	Aluminum	Non	
9	Distribution Component Inside the	Aluminum	Non	
10	Counter Side Main	Structural Steel	Non	
11	Hollow Shaft	Structural Steel	Non	
12	Distribution Component Outside	Aluminum	Non	
13	Force Transducer	Aluminum	Non	
14	Connection Shafts Outside the Cabin	Structural Steel	Non	
15	Connection Components Outside	Aluminum	Non	
16	Linear Stage Connection Comp.	Aluminum	Non	
17	Counter Side Bracket	Structural Steel	Non	

Table 10. Design Iteration 5 for Model 0

Index	Component Name	Material	Modification	Modification Description
1	Linear Bearings Support	Structural Steel	Non	
2	Linear Bearings	Structural Steel	Non	
3	Actuator Side Main Shaft	Structural Steel	Non	
4	Specimen Connection Block (Left)	Aluminum	Non	
5	Connection Components Inside the Cabin	Aluminum	Non	
6	Elastic Components	Elastic Material	Non	
7	Connection Shafts Inside the Cabin	Structural Steel	Non	
8	Specimen Connection Block (Right)	Aluminum	Non	
9	Distribution Component Inside the Cabin	Aluminum	Non	
10	Counter Side Main Shaft	Structural Steel	Non	
11	Hollow Shaft	Structural Steel	Non	
12	Distribution Component Outside the Cabin	Aluminum	Yes	Structural steel is used instead of aluminum
13	Force Transducer	Aluminum	Non	
14	Connection Shafts Outside the Cabin	Structural Steel	Non	
15	Connection Components Outside the Cabin	Aluminum	Non	
16	Linear Stage Connection Component	Aluminum	Non	
17	Counter Side Bracket	Structural Steel	Non	

Table 11. Design Iteration 6 for Model 0

Index	Component Name	Material	Modification	Modification Description
1	Linear Bearings Support	Structural Steel	Non	
2	Linear Bearings	Structural Steel	Non	
3	Actuator Side Main Shaft	Structural Steel	Non	
4	Specimen Connection Block (Left)	Aluminum	Non	
5	Connection Components Inside the Cabin	Aluminum	Non	
6	Elastic Components	Elastic Material	Non	
7	Connection Shafts Inside the Cabin	Structural Steel	Non	
8	Specimen Connection Block (Right)	Aluminum	Non	
9	Distribution Component Inside the Cabin	Aluminum	Yes	Thickness is reduced to 10 mm
10	Counter Side Main Shaft	Structural Steel	Non	
11	Hollow Shaft	Structural Steel	Non	
12	Distribution Component Outside the Cabin	Aluminum	Non	
13	Force Transducer	Aluminum	Non	
14	Connection Shafts Outside the Cabin	Structural Steel	Non	
15	Connection Components Outside the Cabin	Aluminum	Non	
16	Linear Stage Connection Component	Aluminum	Non	
17	Counter Side Bracket	Structural Steel	Non	

Table 12. Design Iteration 7 for Model 0

Index	Component Name	Material	Modification	Modification Description
1	Linear Bearings Support	Structural Steel	Non	
2	Linear Bearings	Structural Steel	Non	
3	Actuator Side Main Shaft	Structural Steel	Non	
4	Specimen Connection Block (Left)	Aluminum	Non	
5	Connection Components Inside the Cabin	Aluminum	Non	
6	Elastic Components	Elastic Material	Non	
7	Connection Shafts Inside the Cabin	Structural Steel	Non	
8	Specimen Connection Block (Right)	Aluminum	Non	
9	Distribution Component Inside the Cabin	Aluminum	Non	
10	Counter Side Main Shaft	Structural Steel	Non	
11	Hollow Shaft	Structural Steel	Non	
12	Distribution Component Outside the Cabin	Aluminum	Yes	Thickness is reduced to 10 mm
13	Force Transducer	Aluminum	Non	
14	Connection Shafts Outside the Cabin	Structural Steel	Non	
15	Connection Components Outside the Cabin	Aluminum	Non	
16	Linear Stage Connection Component	Aluminum	Non	
17	Counter Side Bracket	Structural Steel	Non	

Table 13. Design Iteration 8 for Model 0

Index	Component Name	Material	Modification	Modification Description
1	Linear Bearings Support	Structural Steel	Non	
2	Linear Bearings	Structural Steel	Non	
3	Actuator Side Main Shaft	Structural Steel	Non	
4	Specimen Connection Block (Left)	Aluminum	Yes	Thickness is reduced to 10 mm
5	Connection Components Inside the Cabin	Aluminum	Non	
6	Elastic Components	Elastic Material	Non	
7	Connection Shafts Inside the Cabin	Structural Steel	Non	
8	Specimen Connection Block (Right)	Aluminum	Yes	Thickness is reduced to 10 mm
9	Distribution Component Inside the Cabin	Aluminum	Non	
10	Counter Side Main Shaft	Structural Steel	Non	
11	Hollow Shaft	Structural Steel	Non	
12	Distribution Component Outside the Cabin	Aluminum	Non	
13	Force Transducer	Aluminum	Non	
14	Connection Shafts Outside the Cabin	Structural Steel	Non	
15	Connection Components Outside the Cabin	Aluminum	Non	
16	Linear Stage Connection Component	Aluminum	Non	
17	Counter Side Bracket	Structural Steel	Non	

Table 14. Design Iteration 9 for Model 0

Index	Component Name	Material	Modification	Modification Description
1	Linear Bearings Support	Structural Steel	Non	
2	Linear Bearings	Structural Steel	Non	
3	Actuator Side Main Shaft	Structural Steel	Non	
4	Specimen Connection Block (Left)	Aluminum	Yes	Thickness is reduced to 10 mm
5	Connection Components Inside the Cabin	Aluminum	Non	
6	Elastic Components	Elastic Material	Non	
7	Connection Shafts Inside the Cabin	Structural Steel	Yes	Aluminum is used instead of steel
8	Specimen Connection Block (Right)	Aluminum	Yes	Thickness is reduced to 10 mm
9	Distribution Component Inside the Cabin	Aluminum	Yes	Thickness is reduced to 10 mm
10	Counter Side Main Shaft	Structural Steel	Non	
11	Hollow Shaft	Structural Steel	Non	
12	Distribution Component Outside the Cabin	Aluminum	Non	
13	Force Transducer	Aluminum	Non	
14	Connection Shafts Outside the Cabin	Structural Steel	Non	
15	Connection Components Outside the Cabin	Aluminum	Non	
16	Linear Stage Connection Component	Aluminum	Non	
17	Counter Side Bracket	Structural Steel	Non	

Table 15. Results of Modal Analyses for Model 0 for all Design Iterations

	1.Mode	2.Mode	3.Mode	4.Mode	5.Mode
Design Iteration 0	25.99	145.95	146.95	163.46	227.23
Design Iteration 1	27.78	145.82	146.88	162.48	221.47
Design Iteration 2	20.32	100.68	100.74	132.58	185.04
Design Iteration 3	33.93	101.64	102.18	132.57	183.22
Design Iteration 4	26.78	145.56	146.87	161.75	241.48
Design Iteration 5	23.21	146.00	146.97	163.21	230.22
Design Iteration 6	25.75	145.95	146.82	158.31	217.04
Design Iteration 7	27.09	136.39	146.78	148.26	210.69
Design Iteration 8	26.42	161.35	174.7	177.89	220.28
Design Iteration 9	24.37	172.32	202	205.33	257.01

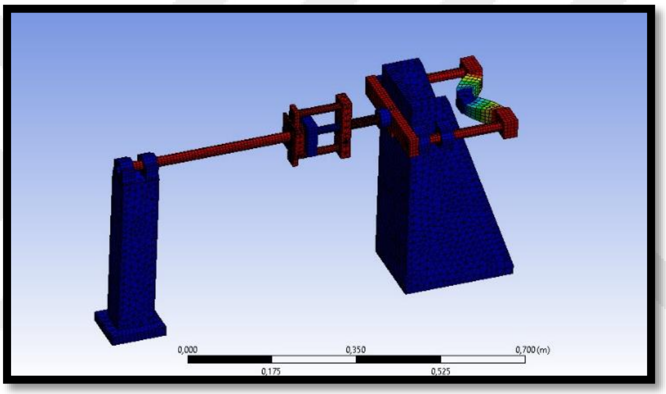

Figure 34. First Mode Shape of Model 0

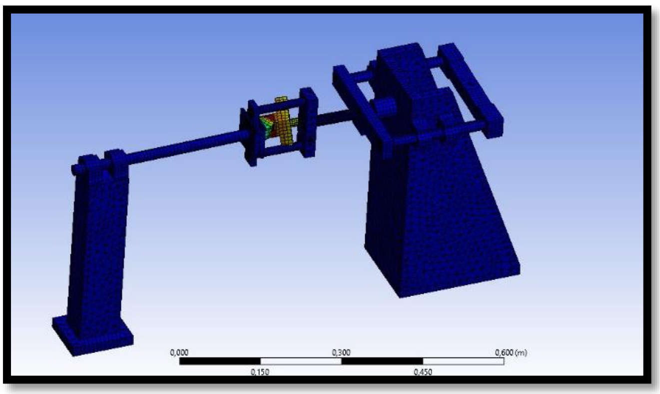

Figure 35. Second Mode Shape of Model 0

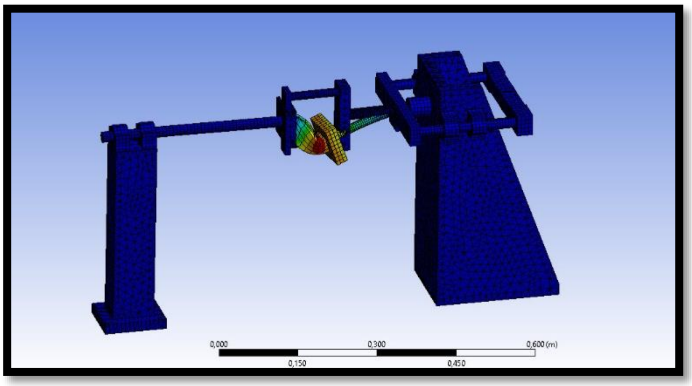

Figure 36. Third Mode Shape of Model 0

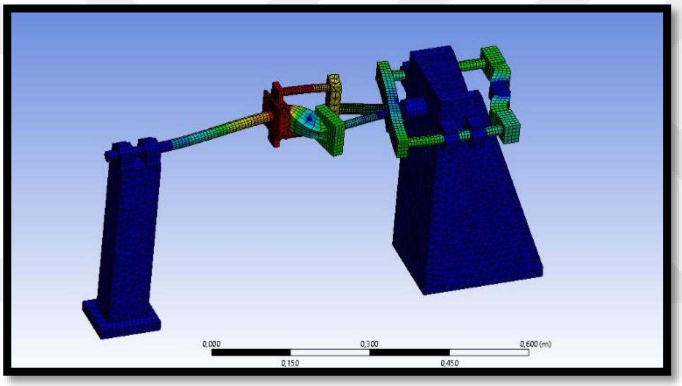

Figure 37. Fourth Mode Shape of Model 0

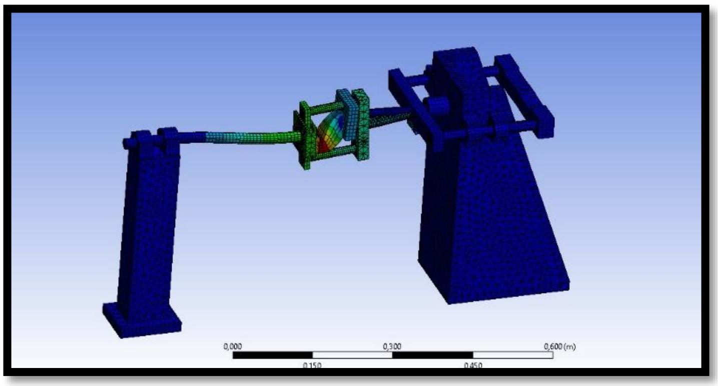

Figure 38. Fifth Mode Shape of Model 0

On the other hand, four design iterations (initial design set included) are conducted on Model 1. Each iterations are handled one by one with details in Table 16 through Table 19. Results of modal analysis for all design iterations on Model 1 are given in Table 20. Then, mode shapes, which are related to the modes given in Table 20 are presented in Fig.39 through Fig.43.

Table 16. Design Iteration 0 (Initial Design Set) for Model 1

Index	Component Name	Material	Modification	Modification Description
1	Linear Bearings Support	Structural Steel	Non	
2	Linear Bearings	Structural Steel	Non	
3	Actuator Side Main Shaft	Structural Steel	Non	
4	Specimen Connection Block (Left)	Aluminum	Non	
5	Connection Components Inside the Cabin	Aluminum	Non	
6	Elastic Components	Elastic Material	Non	
7	Connection Shafts Inside the Cabin	Structural Steel	Non	
8	Specimen Connection Block (Right)	Aluminum	Non	
9	Distribution Component Inside the Cabin	Aluminum	Non	
10	Counter Side Main Shaft	Structural Steel	Non	
11	Hollow Shaft	Structural Steel	Non	
12	Distribution Component Outside the Cabin	Aluminum	Non	
13	Force Transducer	Aluminum	Non	
14	Connection Shafts Outside the Cabin	Structural Steel	Non	
15	Connection Components Outside the Cabin	Aluminum	Non	
16	Linear Stage Connection Component	Aluminum	Non	
17	Counter Side Bracket	Structural Steel	Non	
18	Extra Linear Bearings	Structural Steel	Non	

Table 17. Design Iteration 1 for Model 1

Index	Component Name	Material	Modification	Modification Description
1	Linear Bearings Support	Structural Steel	Non	
2	Linear Bearings	Structural Steel	Non	
3	Actuator Side Main Shaft	Structural Steel	Non	
4	Specimen Connection Block (Left)	Aluminum	Non	
5	Connection Components Inside the Cabin	Aluminum	Non	
6	Elastic Components	Elastic Material	Non	
7	Connection Shafts Inside the Cabin	Structural Steel	Yes	Aluminum is used instead of steel
8	Specimen Connection Block (Right)	Aluminum	Non	
9	Distribution Component Inside the Cabin	Aluminum	Yes	Thickness is reduced to 10 mm
10	Counter Side Main Shaft	Structural Steel	Non	
11	Hollow Shaft	Structural Steel	Non	
12	Distribution Component Outside the Cabin	Aluminum	Non	
13	Force Transducer	Aluminum	Non	
14	Connection Shafts Outside the Cabin	Structural Steel	Non	
15	Connection Components Outside the Cabin	Aluminum	Non	
16	Linear Stage Connection Component	Aluminum	Non	
17	Counter Side Bracket	Structural Steel	Non	
18	Extra Linear Bearings	Structural Steel	Non	

Table 18. Design Iteration 2 for Model 1

Index	Component Name	Material	Modification	Modification Description
1	Linear Bearings Support	Structural Steel	Non	
2	Linear Bearings	Structural Steel	Non	
3	Actuator Side Main Shaft	Structural Steel	Non	
4	Specimen Connection Block (Left)	Aluminum	Yes	Thickness is reduced to 10 mm
5	Connection Components Inside the Cabin	Aluminum	Non	
6	Elastic Components	Elastic Material	Non	
7	Connection Shafts Inside the Cabin	Structural Steel	Non	
8	Specimen Connection Block (Right)	Aluminum	Yes	Thickness is reduced to 10 mm
9	Distribution Component Inside the Cabin	Aluminum	Non	
10	Counter Side Main Shaft	Structural Steel	Non	
11	Hollow Shaft	Structural Steel	Non	
12	Distribution Component Outside the Cabin	Aluminum	Non	
13	Force Transducer	Aluminum	Non	
14	Connection Shafts Outside the Cabin	Structural Steel	Non	
15	Connection Components Outside the Cabin	Aluminum	Non	
16	Linear Stage Connection Component	Aluminum	Non	
17	Counter Side Bracket	Structural Steel	Non	
18	Extra Linear Bearings	Structural Steel	Non	

Table 19. Design Iteration 3 for Model 1

Index	Component Name	Material	Modification	Modification Description
1	Linear Bearings Support	Structural Steel	Non	
2	Linear Bearings	Structural Steel	Non	
3	Actuator Side Main Shaft	Structural Steel	Non	
4	Specimen Connection Block (Left)	Aluminum	Yes	Thickness is reduced to 10 mm
5	Connection Components Inside the Cabin	Aluminum	Non	
6	Elastic Components	Elastic Material	Non	
7	Connection Shafts Inside the Cabin	Structural Steel	Yes	Aluminum is used instead of steel
8	Specimen Connection Block (Right)	Aluminum	Yes	Thickness is reduced to 10 mm
9	Distribution Component Inside the Cabin	Aluminum	Yes	Thickness is reduced to 10 mm
10	Counter Side Main Shaft	Structural Steel	Non	
11	Hollow Shaft	Structural Steel	Non	
12	Distribution Component Outside the Cabin	Aluminum	Non	
13	Force Transducer	Aluminum	Non	
14	Connection Shafts Outside the Cabin	Structural Steel	Non	
15	Connection Components Outside the Cabin	Aluminum	Non	
16	Linear Stage Connection Component	Aluminum	Non	
17	Counter Side Bracket	Structural Steel	Non	
18	Extra Linear Bearings	Structural Steel	Non	

Table 20. Results of Modal Analyses for Model 1 for all Design Iterations

	1.Mode	2.Mode	3.Mode	4.Mode	5.Mode
Design Iteration 0	25.78	142.89	188.89	210.99	252.65
Design Iteration 1	27.15	139.15	191.53	239.94	252.13
Design Iteration 2	26.52	171.16	217.57	254.37	260.59
Design Iteration 3	27.75	173.44	225.98	253.67	260.59

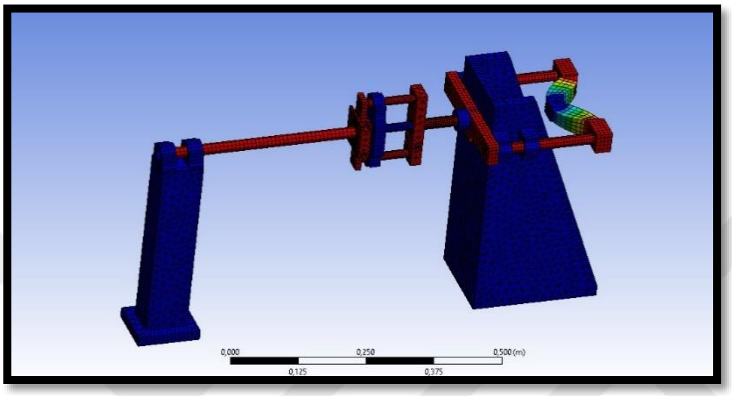

Figure 39. First Mode Shape of Model 1

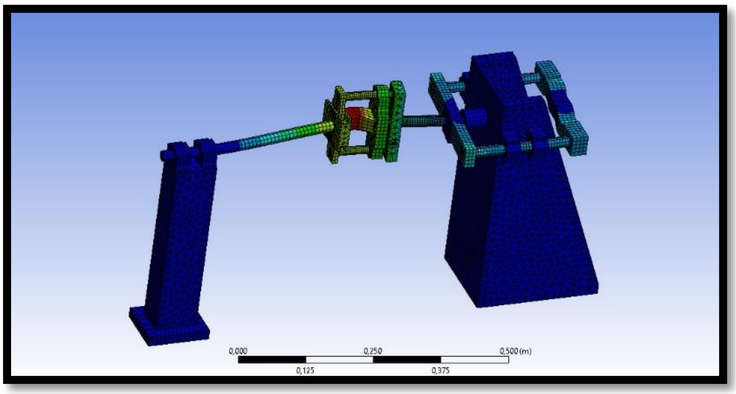

Figure 40. Second Mode Shape of Model 1

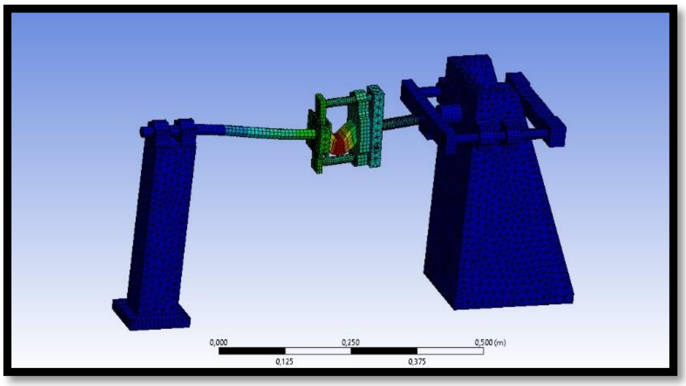

Figure 41. Third Mode Shape of Model 1

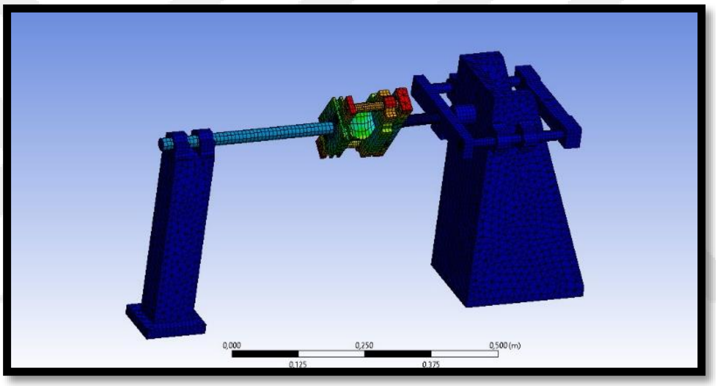

Figure 42. Fourth Mode Shape of Model 1

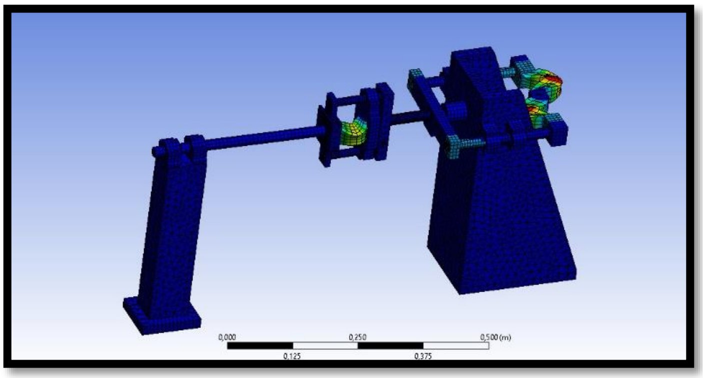

Figure 43. Fifth Mode Shape of Model 1

After the design iterations on model 0 and 1, the results of the modal analyses show that model 0 iteration 9 and model 1 iterations 2 and 3 have more favorable modal frequency (highest 2nd modal frequency) values than remaining iterations. The first mode results are about 26 Hz which is an unavoidable mode due to the motion of actuator armature and preload mechanism. For this reason, the attention is on the second mode and above mainly. Between three alternatives for the final model, design iteration 9 of Model 0 and design iteration 3 of Model 1 are very similar. The design difference between these models are the extra linear bearings which are positioned on and under the right connection block of test specimen. Because of the results of these models according to the modal analyses are very similar, design iteration 9 of Model 0 is chosen as the final design of the test setup.

After the model is selected, the dimensions and positions of the test set-up components are roughly determined. At this point, suitable linear stage and reducer are selected for the preload mechanism. CAD files of these components are downloaded from the related websites which are given in Fig.44 and Fig.45 [28-29]. These components are added to the selected model. Then, the support of the actuator side main shaft linear bearings is remodeled because this support should be connected to the actuator bracket. The new support model is prepared and added to the whole model which is given in Fig.46.

In addition, one more support is necessary for the reducer. Reducer support should be connected to the preload mechanism side main bracket. For this reason, this bracket model is modified to fulfil this purpose. Reducer support and its connection to the bracket is given in Fig.47. Linear stage connection component is also modified a little to prevent the contact between linear stage and elastic components which can be seen in Fig.47.

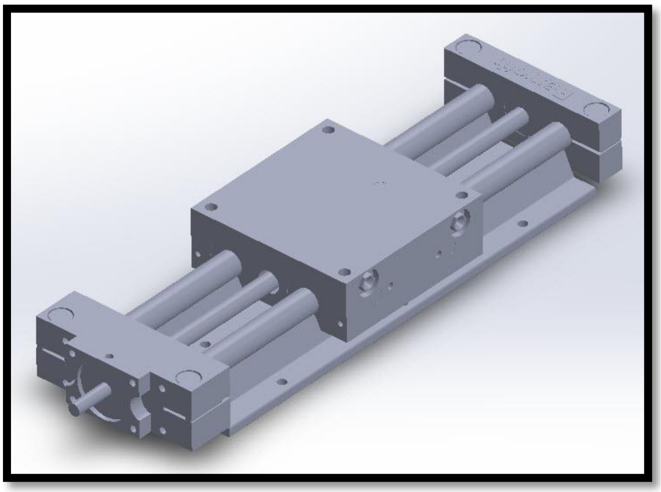

Figure 44. CAD Model of Linear Stage [28]

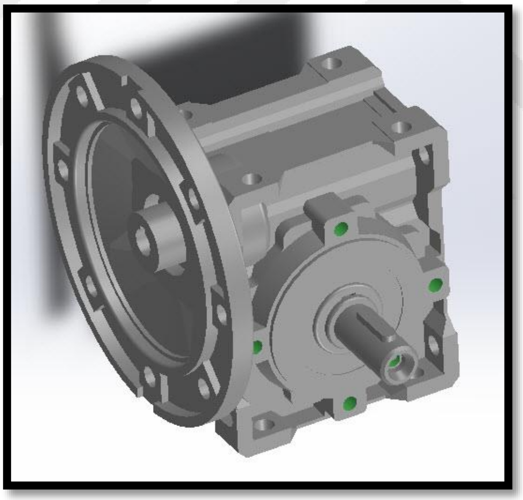

Figure 45. CAD Model of Reducer [29]

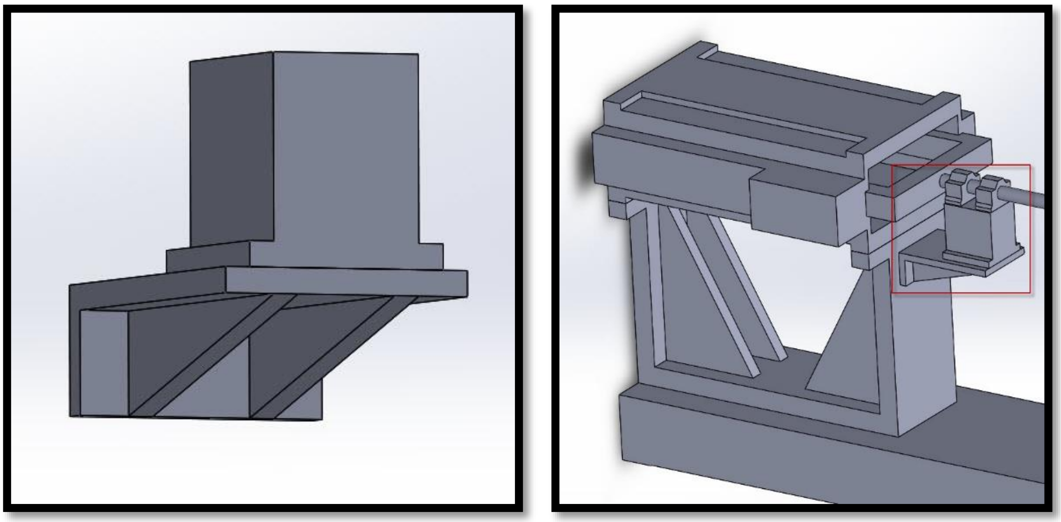

Figure 46. Solid Model of Support Extension for Actuator Side Main Shaft Linear Bearings

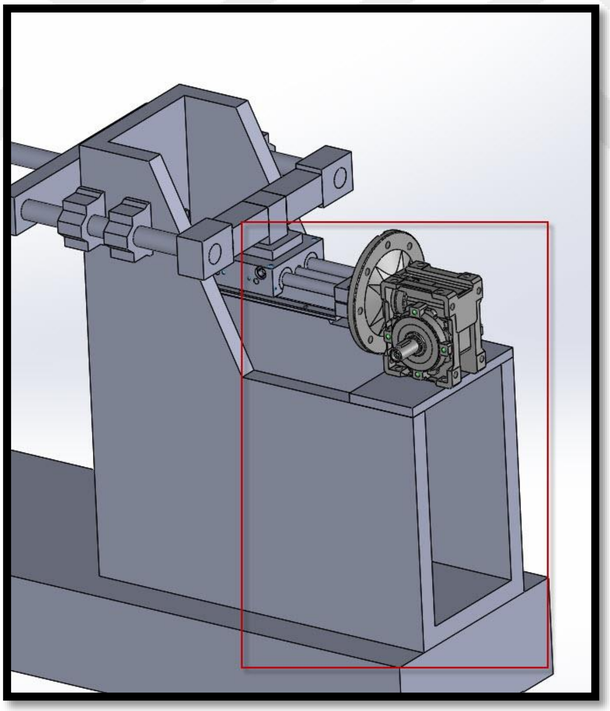

Figure 47. Modified Model of Preload Mechanism Side Bracket and Support Extension for Reducer

Finally, whole model is prepared for the remaining test set-up components. In the previous section, actuator-bracket assembly model was also prepared. Now these two models can be arranged and connected to each other (see Fig.48). The connections and exact positions of components will be determined as a final touch in detailed design. Also, some minor or less likely major changes may be done on the component's dimensions.

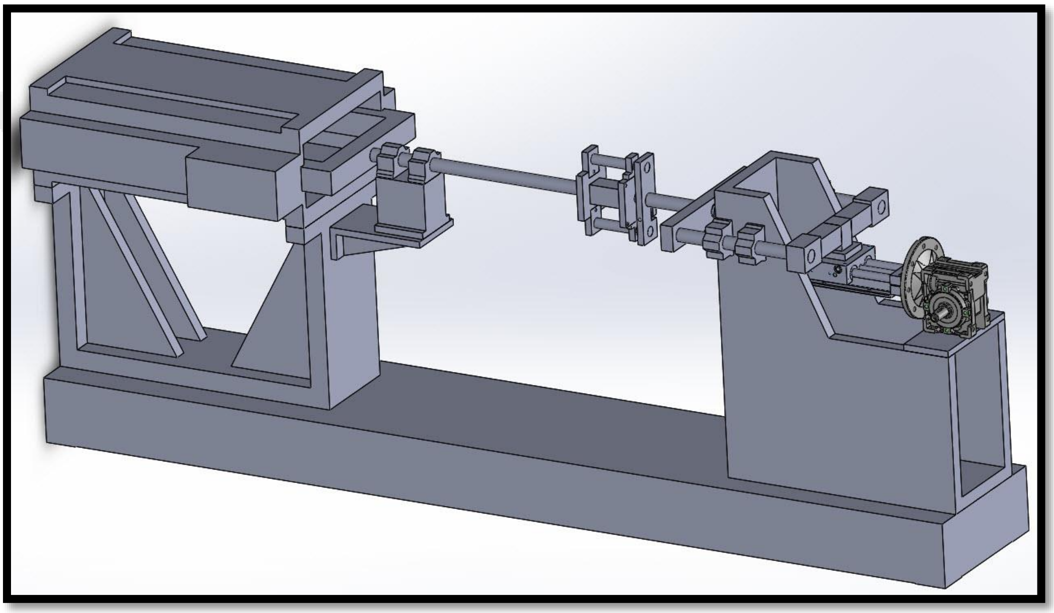

Figure 48. Final Whole Model of Test Set-Up

Modal analysis is conducted on the model given in Fig.48 to see the final modal frequency values of test set-up. The results of this modal analysis are given in Table 21. Mode shapes, which are related to the values given in Table 21, are presented in Fig.49 through Fig.53. According to the results of modal analysis, first important mode (second mode) is above the critical value of 100 Hz which is the upper limit of test frequency range. As a result, prepared final model for the test set-up is found as a suitable design.

Table 21. Results of Modal Analysis for Whole Model of Test Set-up

	1.Mode	2.Mode	3.Mode	4.Mode	5.Mode
Frequency (Hz)	14.34	132.90	173.83	186.24	203.07

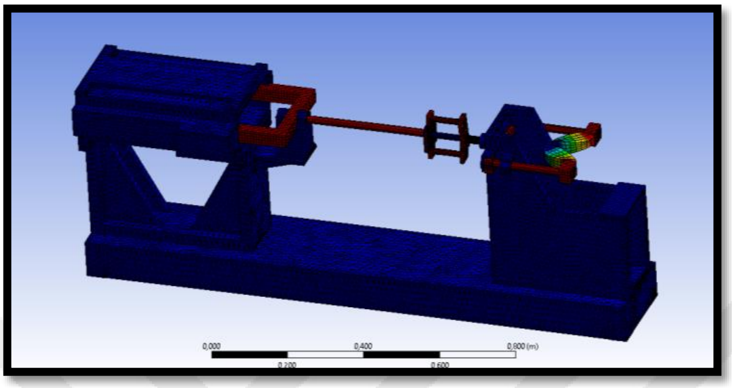

Figure 49. First Mode Shape of Whole Model of Test Set-up

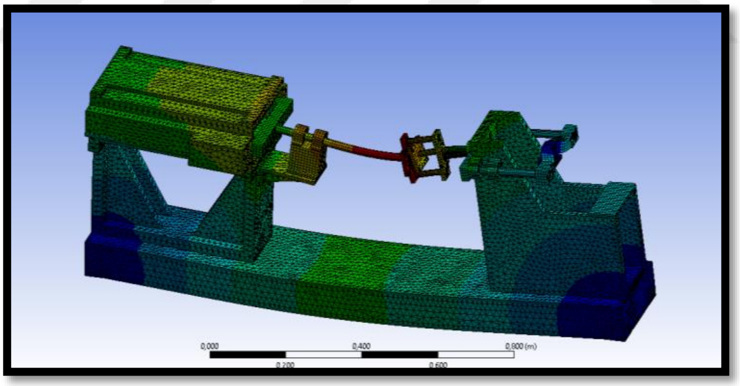

Figure 50. Second Mode Shape of Whole Model of Test Set-up

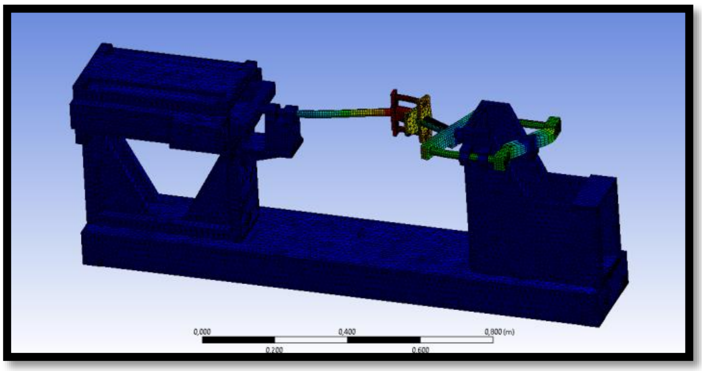

Figure 51. Third Mode Shape of Whole Model of Test Set-up

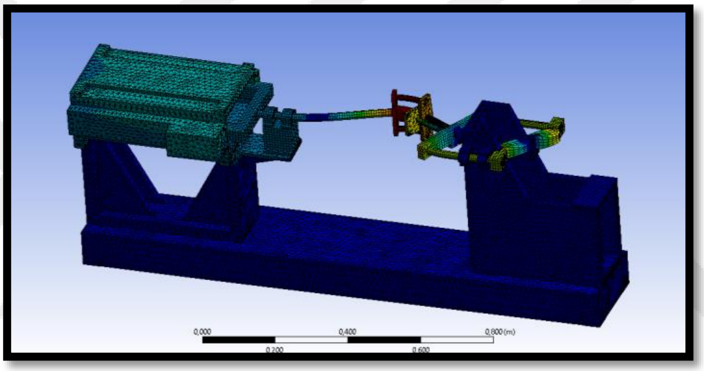

Figure 52. Fourth Mode Shape of Whole Model of Test Set-up

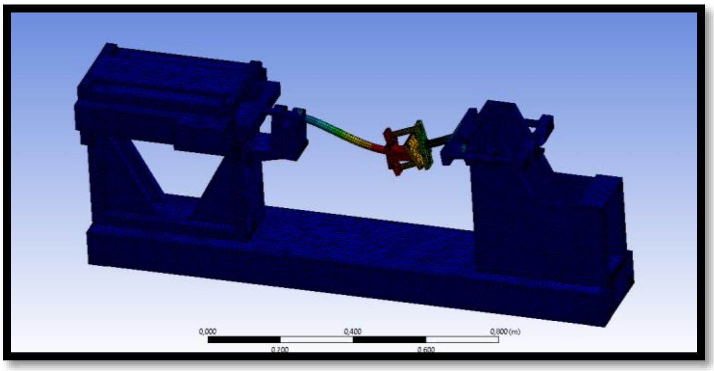

Figure 53. Fifth Mode Shape of Whole Model of Test Set-up

4.2. DETAILED DESIGN OF T-SLOT TABLE

At the end of the conceptual design stage of T-slot table, a generic design is prepared. The detailed design of the T-slot table is used this generic design as a reference. Using the T-slot standards, T-slot dimensions are selected. Then, the general dimensions which are length, width and thickness are selected according to the other components dimensions and positions. According to this selection, the length is 1500 mm, the width is 1000 mm and the thickness is 100 mm.

Then, some analyses are conducted to see the behaviours of T-slot table. The APS 400 actuator and its generic bracket is used to create realistic analyses. For the bracket which is opposite to the actuator bracket, same bracket is used. The locations of the brackets are determined according to the lifting system for the temperature chamber which is positioned at the center of T-slot table and 100 mm clearences are given between the temperature chamber and brackets. T-slot table is designed without its T-slots to simplfy the analyses. Prepared assembly is given in Fig.54.

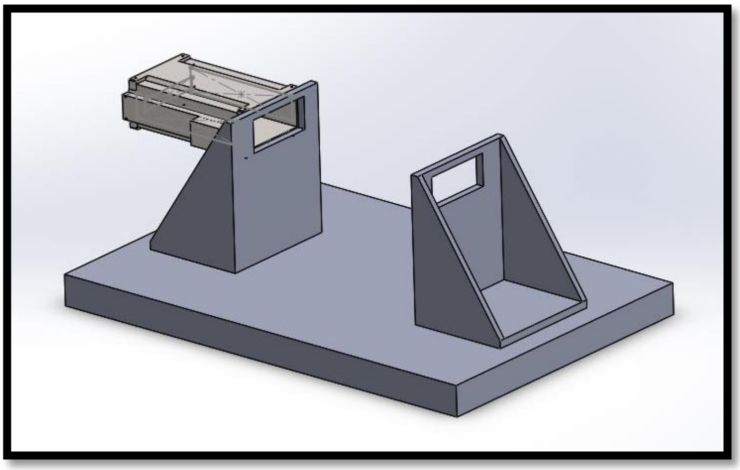

Figure 54. Prepared Assembly for Modal Analyses of T-slot Table

Firstly, modal analysis are conducted. The material properties are assigned to the components as a starting point of the analysis. Steel is defined for the brackets and T-slot table and special material is defined for the actuator. Specific material properties are defined for the actuator. A rough mesh is defined to this assembly and T-slot table is fixed from its four corners (see Fig.55). Then, modal analyses are began with first iteration.

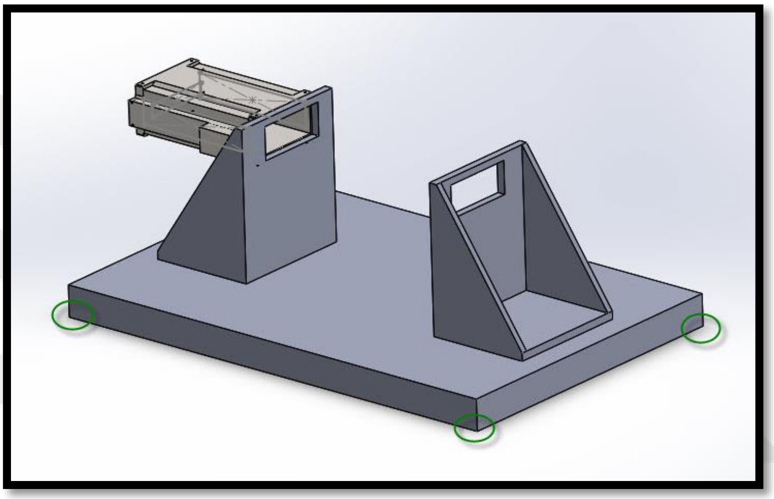

Figure 55. Fixing Locations of Prepared Assembly

During modal analysis, modal frequency values of this assembly is observed. Becaused of the test system operating frequency range is between 0-100 Hz, the modal frequency of this assembly must be higher (if possible much higher) than 100 Hz. At first iteration, first modal frequency value which is the most critical one is found as 97.58 Hz. This result is not suitable for the test system. For this reason, further design iterations are applied to this assembly to improve this result. Results of thickness iterations are given in Table 22.

Table 22. Results of Modal Analyses According to the Thickness Iterations of T-slot Table

Thickness of T-slot Table (mm)	First Modal Frequency (Hz)	Weight of T-slot Table (kg)
100	97.58	1177
150	139.12	1766
200	157.32	2355
250	168.35	2944

According to the results of thickness iterations, first modal frequency values are increased with increasing T-slot table thickness. On the other hand, weight of the T-slot table is increased as well. The critical first modal frequency value is improved through thickness iterations. However, this improvement is not satisfactory enough because it is wanted that first frequency value is about 200 Hz which is two times of operating frequency range upper limit. In addition, wieght of the T-slot table is too high to transport from the manufacturer. As a result, one another way is decided to apply for increasing first modal frequency value. This way is placing an I-beam under the T-slot table to increase stiffness of it. Dimensions of prepared I-beam is given in Fig.56. Prepared assembly for T-slot table analysis with I-beams is given in Fig.57. Firstly, two I-beams are placed under the T-slot table between short sides of it which means the length of I-beams is 1500 mm. The modal analysis is applied with 100 mm T-slot table thickness. Then, same analysis is repeated with 6 and 7 beams too. The results of the analyses with I-beam placement are given in Table 23 and Table 24. These results are also not satisfactory because the first modal frequency is only a little higher than 100 Hz and corresponding weight increment due to beams are not low enough. Then, further iterations with I-beams at different sizes are applied. Instead of 100×100×10, I-beams with dimensions 100×100×20 and 100×200×20 are prepared. These dimension are width, height and thickness of the I-beam repsectively which means height and thickness of the I-beam are changed for the iterations. At this iterations, number of I-beams is held at 7.

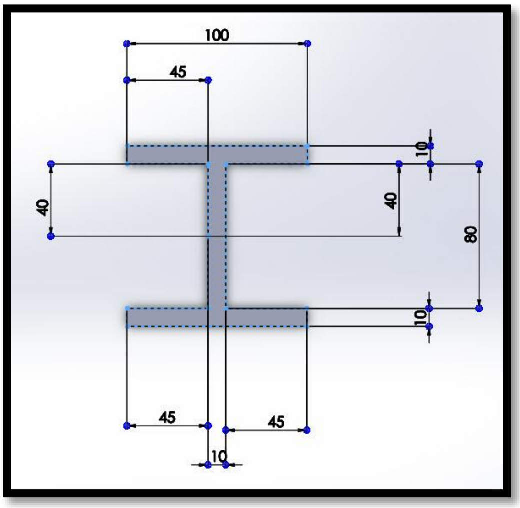

Figure 56. Dimensions of I-Beam

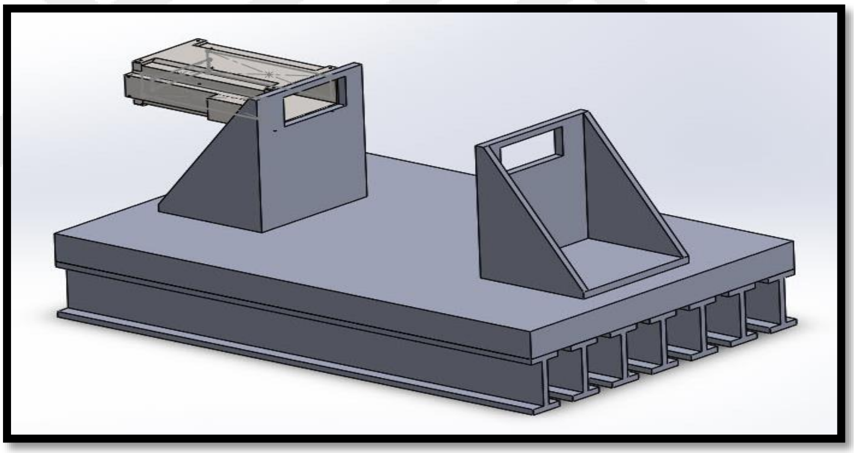

Figure 57. Prepared Assembly with I-Beams

Table 23. Results of Modal Analyses According to the Number of I-Beam

Number of I-Beam	First Modal Frequency (Hz)	Weight Increase (kg)
2	115.5	66
6	125.9	198
7	126.5	231

Table 24. Results of Modal Analyses According to the Dimensions of I-Beam

Number of I-Beam	Dimensions of I-Beam (mm)	First Modal Frequency (Hz)	Weight Increase (kg)
7	100×100×10	126.5	231
7	100×100×20	131.5	364
7	100×200×20	146.2	595

First modal frequency increase is not enough with respect to the weight increase according to the analysis results. Final design iterations for the modal analyses of T-slot table are conducted on fixing locations. Up to now, the T-slot table is fixed from its four corners. From now on, the fixing locations are changed. The changes are applied to the final design of assembly which has a first modal frequency of 146.2 Hz. At first iteration, number of fixing points is increased from 4 to 6 and these additional two points are located at the short sides midpoints of the T-slot table (see Fig.58). Then, modal analysis is conducted again. As a result of this analysis, the first modal frequency is found as 194.7 Hz which is a satisfactory result for this assembly.

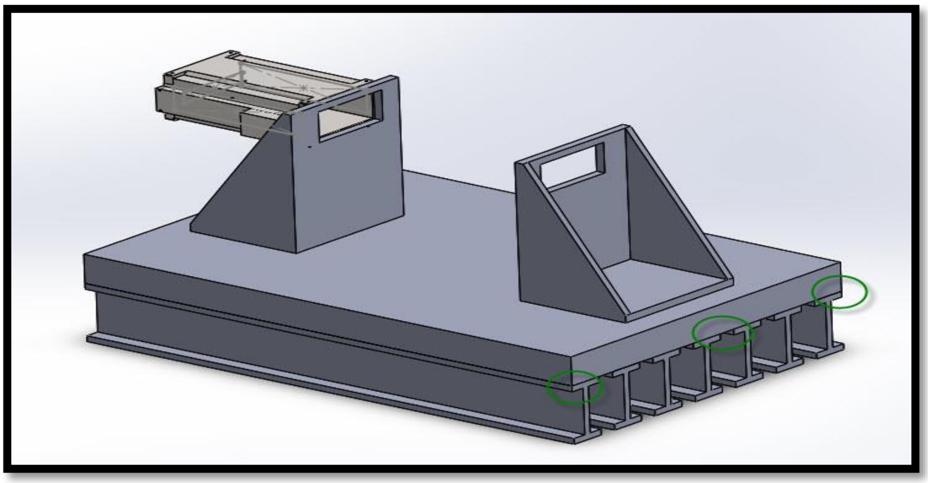

Figure 58. Prepared Assembly with Additional Midpoint Fixing

At the second and last iteration, the short sides are fixed entirely instead of 6 fixing points (see Fig.59). Modal analysis is conducted for the last time and the modal analyses of this assembly are completed. The first modal frequency according to this final analysis is 247.8 Hz which is also a satisfactory result for this assembly.

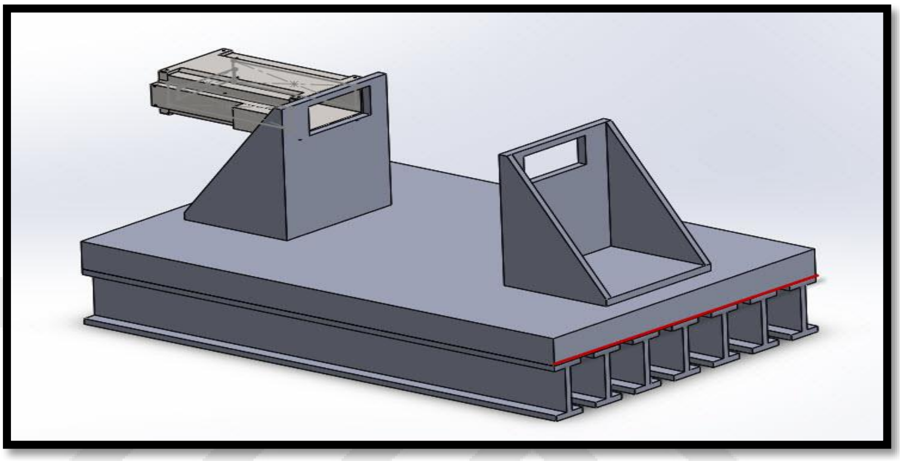

Figure 59. Prepared Assembly with Short Sides Fixing

At the end of these modal analyses stage of T-slot table assembly, it is seen that, fixing is very important to overcome resonance frequency problem. The other iterations are not satisfactory and practically applicable due to weight and resonance concerns.

After the test set-up is modeled, the necessary T-slot table dimensions are determined (see Fig.60). These dimensions are 1500 mm length and 250 mm width. The thickness of T-slot table is selected ad 100 mm for the virtua test section of the thesis. According to these dimensions, T-slot table is modeled without its T-slots for the simplicity of analyses. For the analyses, square areas are prepared at the corners of T-slot table to provide touching to the ground. In modal analyses, T-slot table is fixed from these four square areas. Final decisions about the details of T-slot table are made after the virtual tests and detailed design of test set-up are completed.

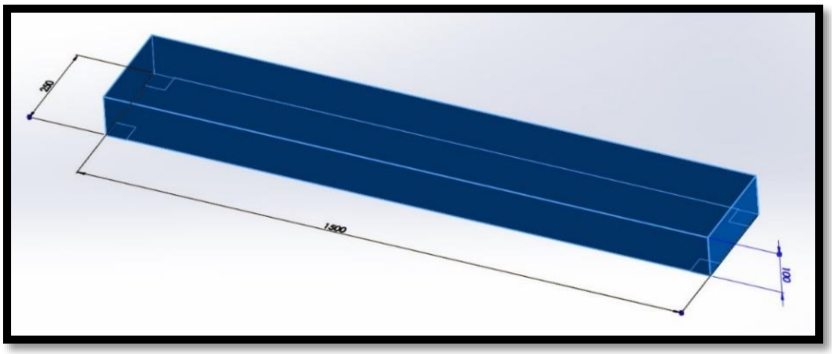

Figure 60. Dimensions of T-Slot Table

4.3. DETAILED DESIGN OF LIFTING SYSTEM

At the end of the conceptual design stage of the lifting system, a suitable design for the multipurpose usage is prepared. At the detailed design stage of the lifting system, the general dimensions with respect to the other components dimensions and locations, the stroke of the linear motion system according to the other test systems where lifting system can be used and other specific things for the design are determined. During the detailed design stage, the final conceptual design (see Fig.61) is used as a reference.

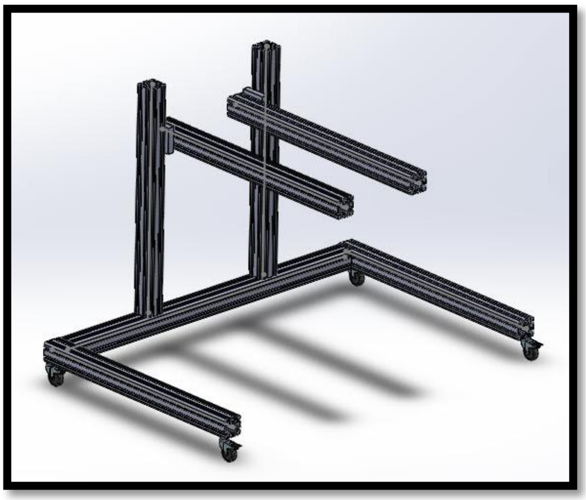

Figure 61. Final Conceptual Design of Lifting System

Four general dimensions are determined for this design. The first one is the distance between the inner sides of the lower carrier feet of the lifting system which is determined with respect to the T-slot table dimensions and location. There are also clearances between these carrier feet and T-slot table. This dimension is determined with respect to the stroke of the linear motion system and comfortable position for anyone with average height to give an input for lifting system through handle. This dimension is specified as 1250 mm. Third general dimension is the length of carrier arms of lifting system from the inner side of the lower long profile. By the way, the inner side represents the hugging side of the lifting system profiles to the T-slot table. This dimension is determined with respect to the temperature chamber dimensions. For this test system, ESPEC SU-261 model temperature chamber will probably be used during tests. However, it is planned to lift SU-262 which has a minor difference from the SU-261 and SU-662 models temperature chambers through this lifting system. For this reason, lifting system is designed to lift these three models. Third dimension is specified as 1050 mm according to the length of SU-662 which is about 1000 mm. Last general dimension of the lifting system is the distance between the lifting system carrier arms connection points. This dimension is also determined with respect to the temperature chambers. According to the feet positions of temperature chambers, this dimension is specified as 510 mm for the use of 90×90 profile as a carrier arm. This dimension can be changed according to the profile which is used as a carrier arm.

In addition to the general dimensions of the lifting system, stroke of the linear motion system is determined as well. Stroke is the difference between the minimum and the maximum distance between the lower side of the carrier arms and the ground. These minimum and maximum distances are determined with respect to the other test systems where lifting system can be used. Minimum distance is determined according to the MTS Acumen test systems. The data sheet of these test systems are given in Fig.62 [30]. The working height value which is 133 mm is used to specify this minimum distance. This distance specified as 150 mm. Maximum distance is determined according to the MTS 200 Hz elastomer test system. The data sheet of this test system is given in Fig.63 [31]. The working height value which is 922 mm is used to specify this maximum distance. This distance specified as 950 mm.

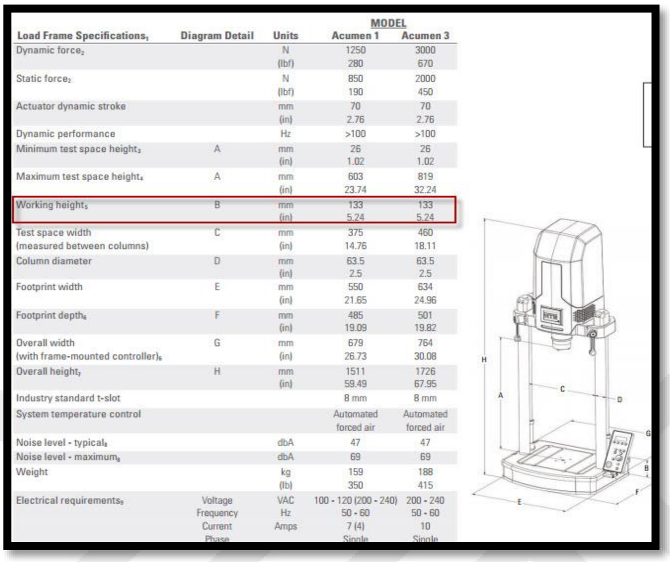

Load Frame Specifications[1]	Diagram Detail	Units	MODEL Acumen 1	MODEL Acumen 3
Dynamic force[2]		N (lbf)	1250 280	3000 670
Static force[2]		N (lbf)	850 190	2000 450
Actuator dynamic stroke		mm (in)	70 2.76	70 2.76
Dynamic performance		Hz	>100	>100
Minimum test space height[3]	A	mm (in)	26 1.02	26 1.02
Maximum test space height[4]	A	mm (in)	603 23.74	819 32.24
Working height[5]	B	mm (in)	133 5.24	133 5.24
Test space width (measured between columns)	C	mm (in)	375 14.76	460 18.11
Column diameter	D	mm (in)	63.5 2.5	63.5 2.5
Footprint width	E	mm (in)	550 21.65	634 24.96
Footprint depth[6]	F	mm (in)	485 19.09	501 19.82
Overall width (with frame-mounted controller)[6]	G	mm (in)	679 26.73	764 30.08
Overall height[7]	H	mm (in)	1511 59.49	1726 67.95
Industry standard t-slot			8 mm	8 mm
System temperature control			Automated forced air	Automated forced air
Noise level - typical[8]		dbA	47	47
Noise level - maximum[8]		dbA	69	69
Weight		kg (lb)	159 350	188 415
Electrical requirements[9]	Voltage Frequency Current Phase	VAC Hz Amps	100 - 120 (200 - 240) 50 - 60 7 (4) Single	200 - 240 50 - 60 10 Single

Figure 62. Data Sheet of MTS Acumen Test Systems [30]

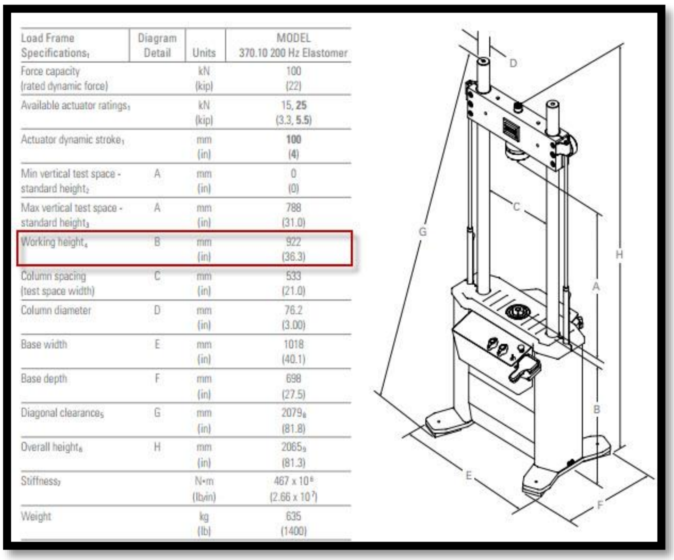

Load Frame Specifications[1]	Diagram Detail	Units	MODEL 370.10 200 Hz Elastomer
Force capacity (rated dynamic force)		kN (kip)	100 (22)
Available actuator ratings[1]		kN (kip)	15, **25** (3.3, **5.5**)
Actuator dynamic stroke[1]		mm (in)	**100** **(4)**
Min vertical test space - standard height[2]	A	mm (in)	0 (0)
Max vertical test space - standard height[3]	A	mm (in)	788 (31.0)
Working height[4]	B	mm (in)	922 (36.3)
Column spacing (test space width)	C	mm (in)	533 (21.0)
Column diameter	D	mm (in)	76.2 (3.00)
Base width	E	mm (in)	1018 (40.1)
Base depth	F	mm (in)	698 (27.5)
Diagonal clearance[5]	G	mm (in)	2079[8] (81.8)
Overall height[6]	H	mm (in)	2065[9] (81.3)
Stiffness[7]		N•m (lb/in)	467×10^{6} (2.66×10^{7})
Weight		kg (lb)	635 (1400)

Figure 63. Data Sheet of MTS 200 Hz Elastomer Test System [31]

Then, some specific things are remained to determine for the detailed design of lifting system. The first thing is the distance between the upper side of the lower carrier feet and the ground. This distance is specified as it should be as short as possible. For this reason, a certain value is not determined for this distance and to determine it is left to the manufacturer with this request. Similar application is used at the length of the lower carrier feet. This length is specified as it should be long enough to provide static balance. To determine this length is also left to the manufacturer with this request.

There is a need to connect the vertical profiles and carrier arms seperately to each other with connection profiles. To locate these connection profiles are left to manufacturer according to some restrictions about accessing temperature chamber.

One last thing is to determine the location of handle which is used to give an input to the lifting system. The location of this handle is specified as the highest point of the lifting system from the ground which is given in Fig.64.

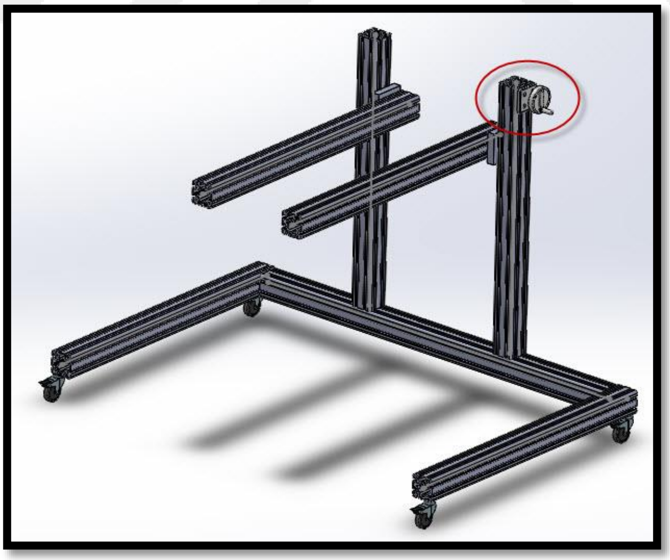

Figure 64. The Locations of Handle on Lifting System

Vertical profiles are equidistant from the sides which means they are centered. This lifting system is planned to carry 130 kg maximum weight which is the weight of ESPEC SU-662 temperature chamber. Finally, the details are determined and the detailed design of lifting system is completed. At this point, this final detailed design is offered to the manufacturer firm and some discussions are made on this design. According to the manufacturer, this design can not carry 130 kg weight without significant deflection. To overcome this problem, they are suggested a design modification. At this design, additional vertical profiles and a long profile which is located under these vertical profiles to carry them are used (see Fig.65). Also, additional linear motion system is used to carry the heavy load of temperature chamber. After some discussions on this design, it is accepted and price offer is made by the manufacturer for this design. This offer is found as reasonable.

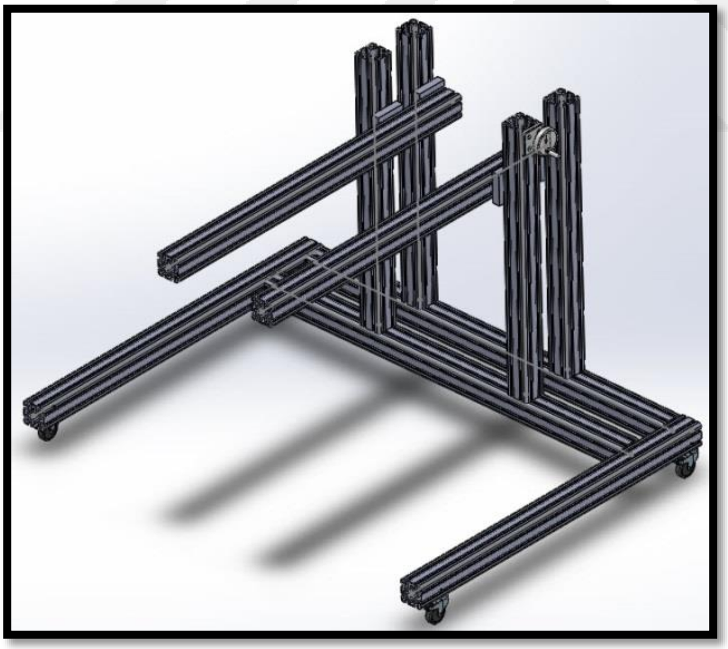

Figure 65. Final Detailed Design of Lifting System

4.4. DETAILED DESIGN OF WHOLE TEST SET-UP

Up to now, detailed design of lifting system and test set-up (roughly not finally) are completed. Also, dimensions of T-slot table are determined but final decisions about T-slot table are not made. As a result, the final design shown in Fig.66 is prepared according to the completed design workings until now.

Some minor or less likely major changes can be conducted on this model according to the virtual test results. In the short run, the detailed design of these components are planned to complete. Then, all designed components are planned to manufacture simultaneously.

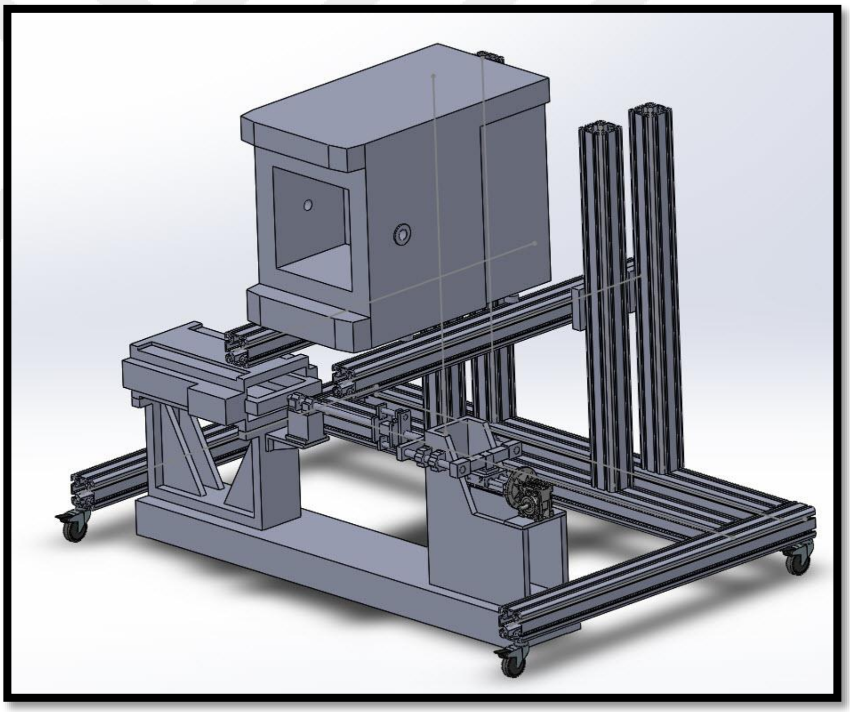

Figure 66. Final Detailed Design of Whole Test Setup

CHAPTER 5

5. VALIDATION OF TEST SYSTEM

Detailed design of all test system components is completed roughly and final model of whole setup is prepared at the end of detailed design stage. At this point, before all components are manufactured, virtual step sine tests are conducted to see the performance of test system. For this purpose, harmonic analyses are conducted on the final model without the lifting system and temperature chamber because these components are not necessary for the analyses.

Before harmonic analyses of test set-up, modal analyses are conducted to perform a convergence analysis that will enable the determination of the optimum element size. During the analysis, materials dimensions are defined as same as the ninth design iteration of model 0 (see Table 14). After that, material properties of elastomer components are defined as temperature and frequency dependent through command object in ANSYS environment (see Fig.67). These material properties are taken from previous experimental test data of a 50 ShA EPDM material specimen (see Fig.68 elastic modulus and loss factor plots). Modulus and loss factor values can be calculated for the specific temperature and frequency values using a fractional derivative mathematical model curve fitted to the measures experimental data seen in Fig.68. The results of modal analysis conducted for convergence analysis are given in Fig.69 and Fig.70 for two distinct temperatures.

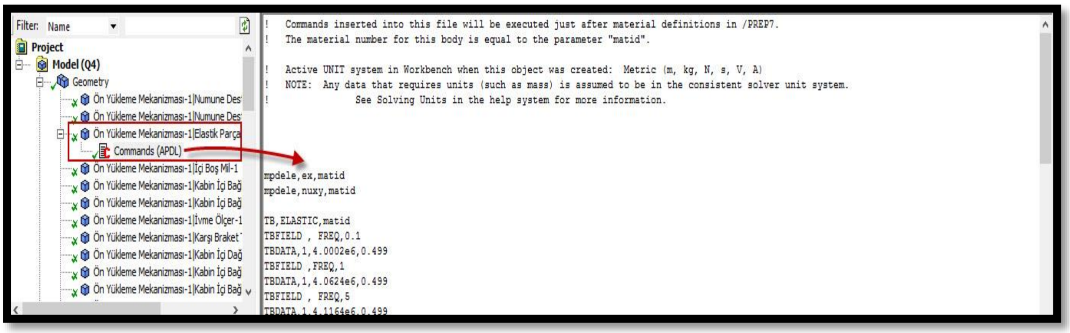

Figure 67. Command Object of ANSYS Workbench

- **EPDM 50 Shore A Çekme Numunesi 2**

K1a	7,143E-2
K1b	5,192E-7
na	1,122E-1
nb	4,694E-1
Gmin	1,894E+6
Gmid	6,122E+7
Gmax	2,727E+9
K2a	1,224E-1
K2b	2,551E-2
K3a	2,250E-1
K3b	4,082E-13
ma	4,867E-1
mb	2,571E-1
Pa	1,056E+0
Pb	1,141E+0
TA	12500
T0	10,52 (Celcius)

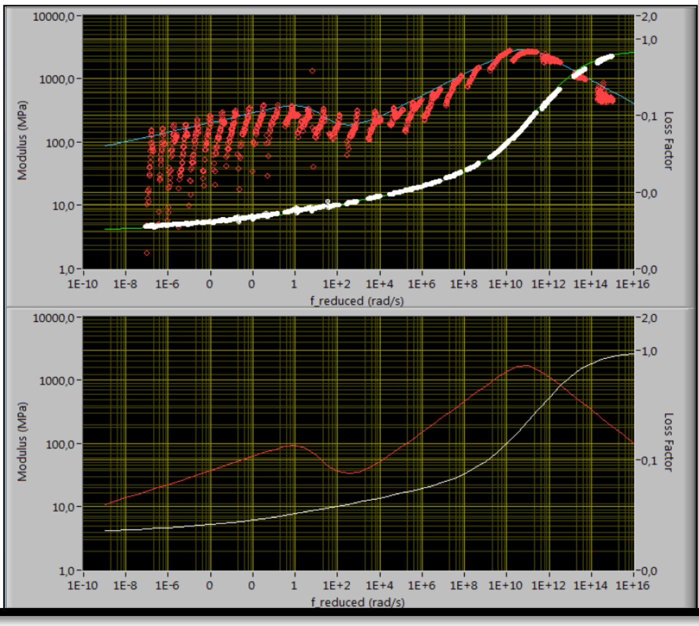

Figure 68. Data Set of 50 ShA EPDM Test Specimen

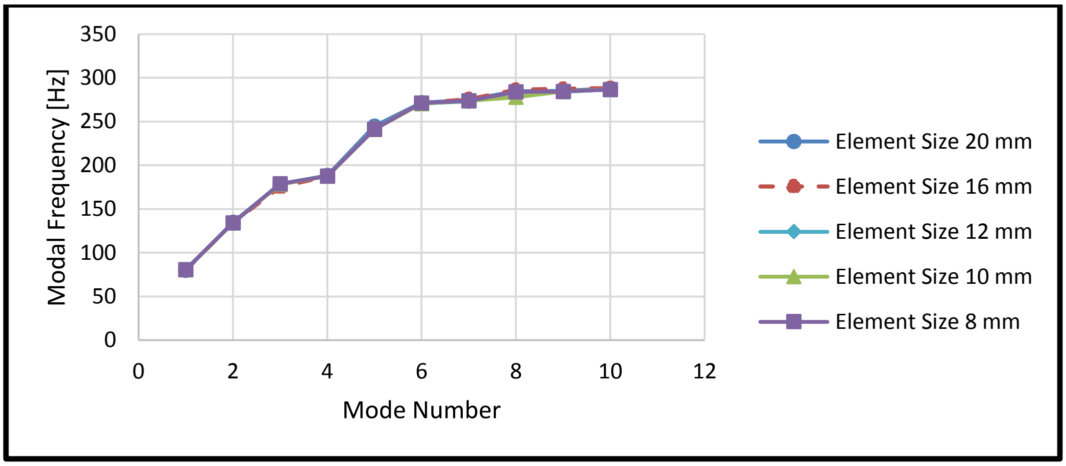

Figure 69. Convergence Analysis Based on First 10 Structural Modal Frequencies at -50 ºC.

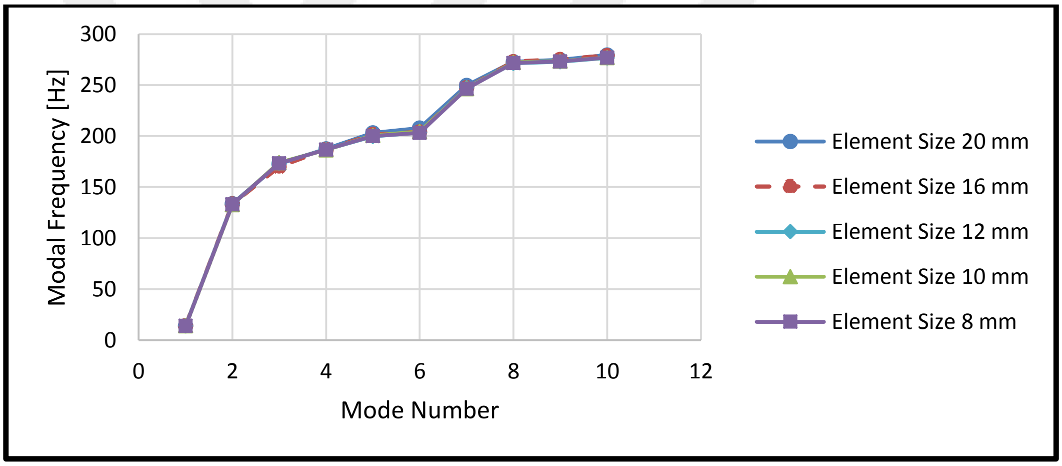

Figure 70. Convergence Analysis Based on First 10 Structural Modal Frequencies at +50 ºC

According to the convergence method analyses, the modal frequency values are almost same for each element sizes. For this reason, most reasonable value is selected as element size for the harmonic analyses which is 9 mm. In addition, some mesh data are defined as coarse to shorten the solution time of the analyses. Then, harmonic analyses are conducted to the test set-up.

To conduct virtual tests to use in our validation efforts, a harmonic dynamic force is applied from the armature of the actuator as 1000 N to represent an actual harmonic sweep sine test with constant force amplitude (see Fig.71). In addition, due to the permanent magnets employed by APS 400 actuator, the armature coil of actuator remains in magnetic field. Because of this magnetic field, a counter force is produced. This counter force is equal to the applied dynamic force from the actuator armature but in opposite direction (see Fig.71). After the forces of actuator is defined, set-up is fixed from necessary locations to provide real conditions nearly. Fixed locations are given in Fig.72. In addition, necessary contact definitions are made to provide real conditions as well. Mesh is defined as mentioned before. Full method is chosen for the analyses to see and collect damping information for the set-up.

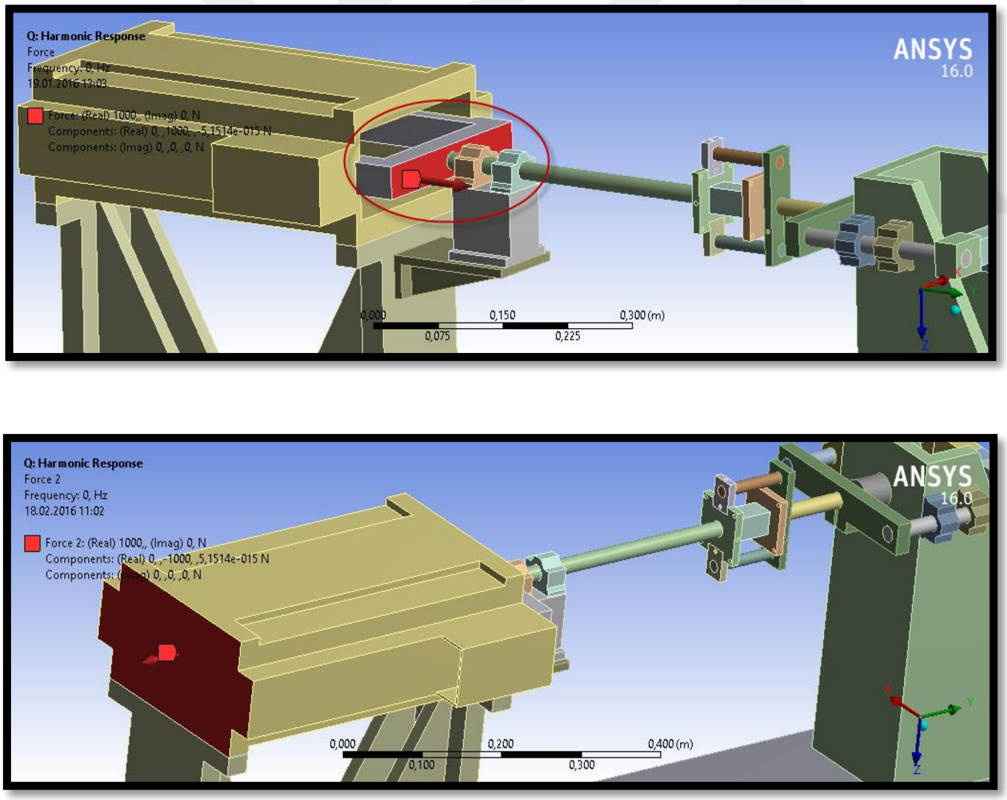

Figure 71. Location and Direction of Applied Forces

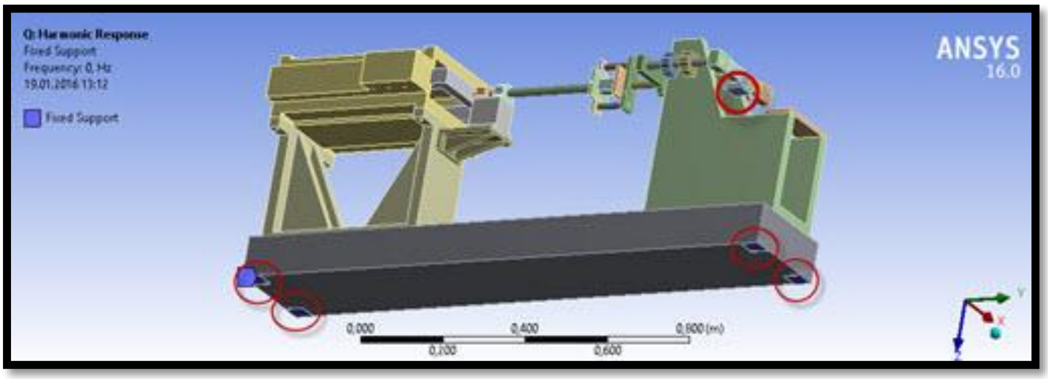

Figure 72. Fixed Locations of Test Set-up

Finally, to obtain the deformations and transmitted force data solution tool is used for appropriate definitions. Deformations are defined through frequency response object because both real and imaginary values are necessary for further calculations. On the other hand, transmitted force is defined through force reaction object. All these definitions are made for y direction according to the model because force is applied for this direction (see the axes in Fig.72). The locations of these definitions are given in Fig.73. Deformations are defined through face selections of test specimen connection blocks and transmitted force is defined through contact surface of force transducer and preload mechanism side main bracket.

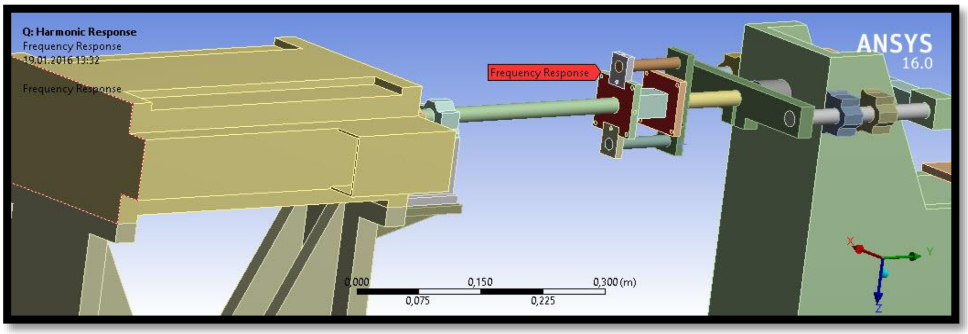

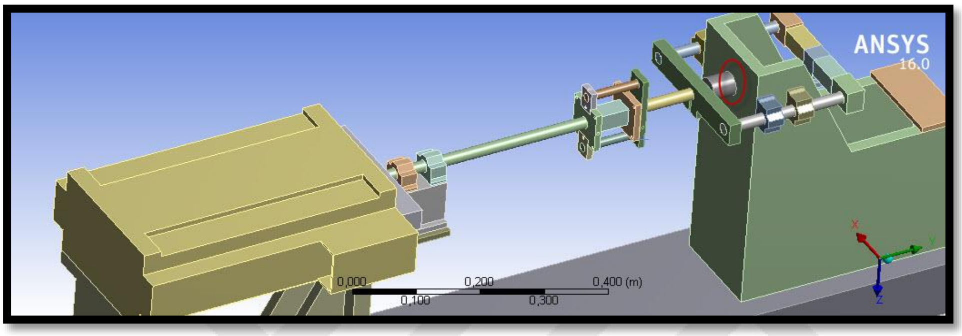

Figure 73. Locations of Deformations and Transmitted Force on Test Set-up

Then, frequency range of the harmonic analysis is specified through analysis settings object which is selected as 0-200 Hz. Five temperatures and eight frequency data points are selected for the whole model test simulations.

Finally, harmonic analyses are conducted and deformations and transmitted force data of the setup are collected. These results are used to calculate the complex modulus and loss factor data of test specimen via the following equations:

$$\Delta Y_{specimen}(f,T) = (Y_1(f,T) - Y_2(f,T) \quad (1)$$

$$k^*(f,T) = \frac{F_{transmitted}(f,T)}{\Delta Y_{specimen}(f,T)} = k(f,T) \times (1 + i\eta(f,T)) \quad (2)$$

$$E^*(f,T) = k^*(f,T) \times \frac{L_{specimen}}{A_{specimen}} \quad (3)$$

At these formulas, Y_1 and Y_2 values represent the harmonic amplitudes of deformations of test specimen left (actuator side) and right (preload mechanism side) connection blocks in y direction respectively, f represents frequency in Hz, T represents temperature in Celcius, k^* represents complex stiffness, k represents real part of complex stiffness, η represents loss factor, $F_{transmitted}$ represents transmitted force, E^* represents complex young modulus, $L_{specimen}$ represents length of test specimen and finally $A_{specimen}$ represents cross-sectional area of test specimen. Using these formulas, complex modulus and loss factor values can be calculated which are frequency and temperature dependent. These are the dynamic properties of test specimen. To validate the test setup, the material complex modulus obtained using the results of the harmonic analysis (virtual step sine tests) and the material properties calculated from the mathematical model for the complex modulus of the elastomer specimen are compared through graphs. Validation of the test system is done by obtaining a good agreement between complex modulus obtained using the results of the harmonic analysis (virtual tests) and the real material properties calculated from the mathematical model for the complex modulus of the elastomer specimen.

5.1. Virtual Step Sine Tests: Harmonic Analysis on the Test Set-up

The analysis procedure is explained at the previous section. Some details and the results of the analyses are handled at this section. There are three elastomer components in test set-up. For this reason, temperature and frequency dependent material properties are defined for all these three elastomer components through command objects. In actual tests, test specimen will be inside the temperature chamber. On the other hand, the other two elastomer components (of the preload mechanism) will be outside the temperature chamber (see Fig.74). Because of that, the elastomer material properties of test specimen are defined at -50 ^{o}C, -20 ^{o}C, +20 ^{o}C, +50 ^{o}C and +100 ^{o}C respectively but the material properties of other two elastomer components are defined at 20 ^{o}C (room temperature) because these temperatures are selected for the simulated virtual tests to provide temperature chamber conditions in five separate analysis.

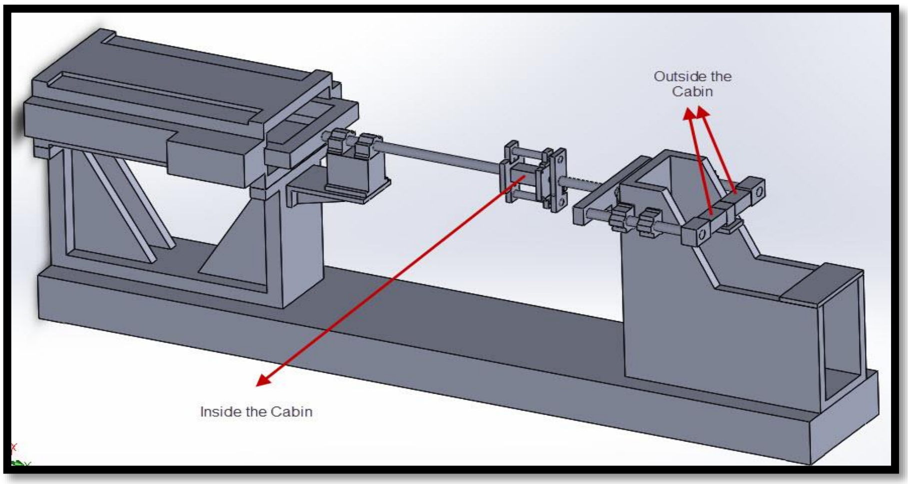

Figure 74. Locations of Elastomer Components

On the other hand, eight frequency data points are selected for the simulations. These data points are 0.1, 1, 10, 20, 50, 100, 150 and 200 Hz. Then, analyses are conducted at five different temperatures with these frequency data points.

The results of analysis at -50 ^{o}C, -20 ^{o}C, +20 ^{o}C, +50 ^{o}C and +100 ^{o}C are given in Fig.75 through Fig.84 respectively as comparison of elastic tensile modulus and loss factor values from mathematical model (material model) and the calculated data from virtual step sine tests. In addition, percent error in elastic tensile modulus and loss factor of these comparisons are given in Table 25 through Table 29. In error calculations elastic modulus and loss factor are made assuming results from mathematical model are correct and results virtual step sine tests simulate an actual experiment.

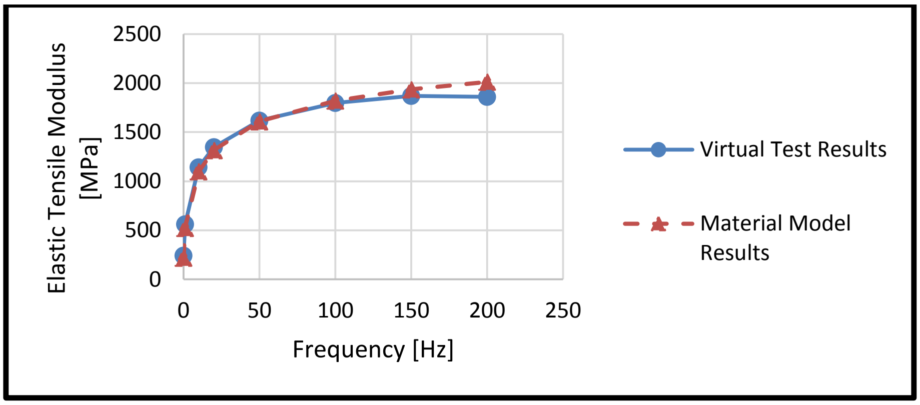

Figure 75. Comparison of Elastic Tensile Modulus Data of Material Model and Virtual Test at -50 °C

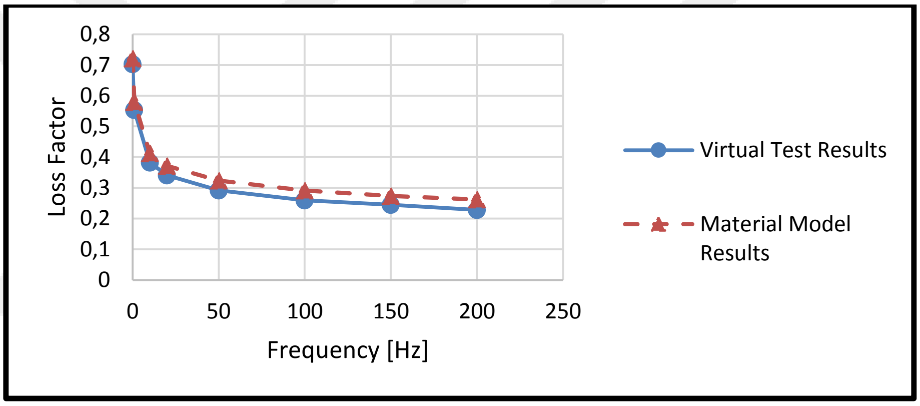

Figure 76. Comparison of Loss Factor Data of Material Model and Virtual Test at -50 °C

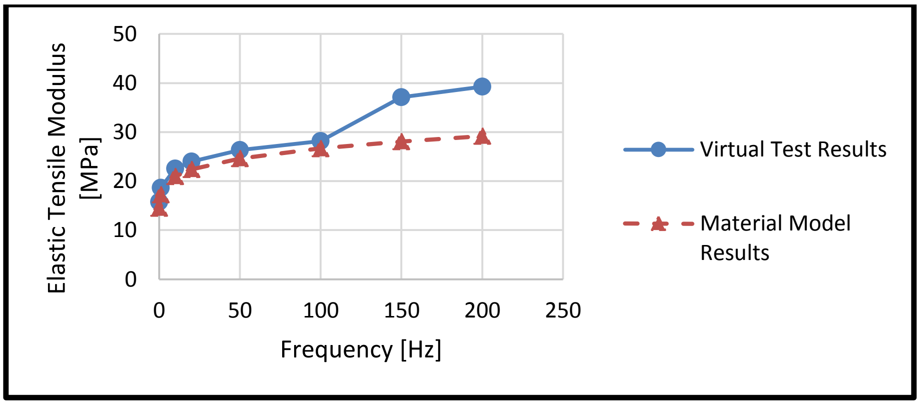

Figure 77. Comparison of Elastic Tensile Modulus Data of Material Model and Virtual Test at -20 °C

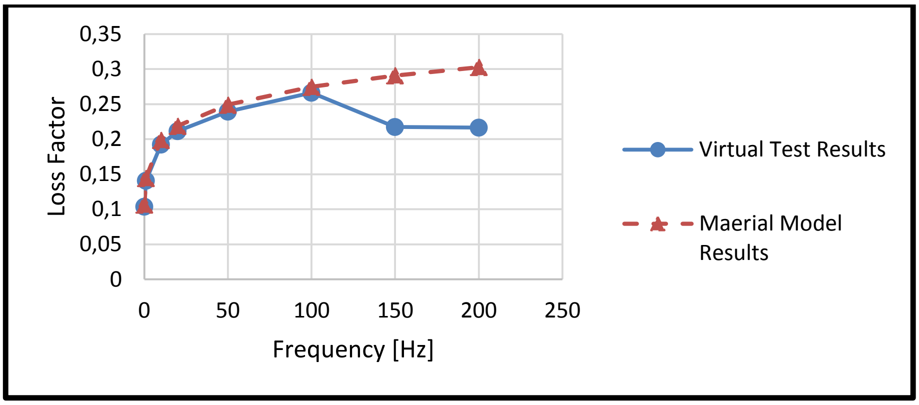

Figure 78. Comparison of Loss Factor Data of Material Model and Virtual Test at -20 ºC

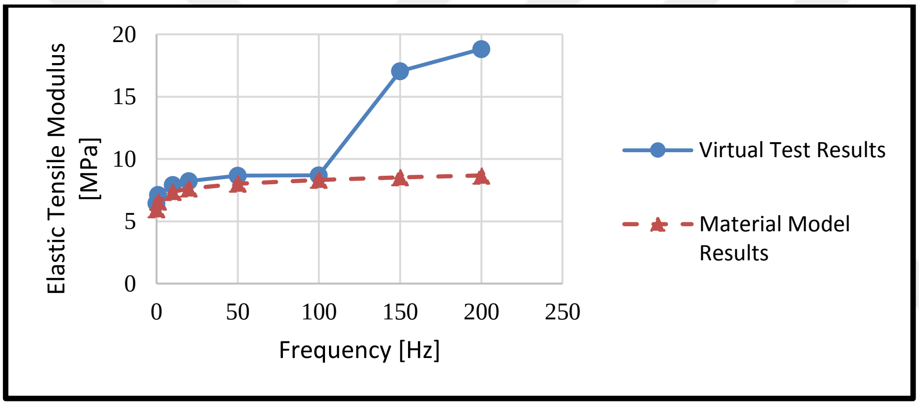

Figure 79. Comparison of Elastic Tensile Modulus Data of Material Model and Virtual Test at +20 ºC

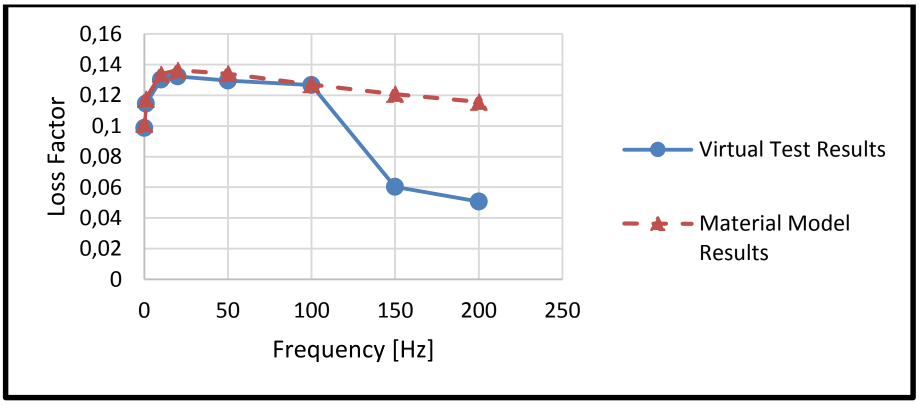

Figure 80. Comparison of Loss Factor Data of Material Model and Virtual Test at +20 ºC

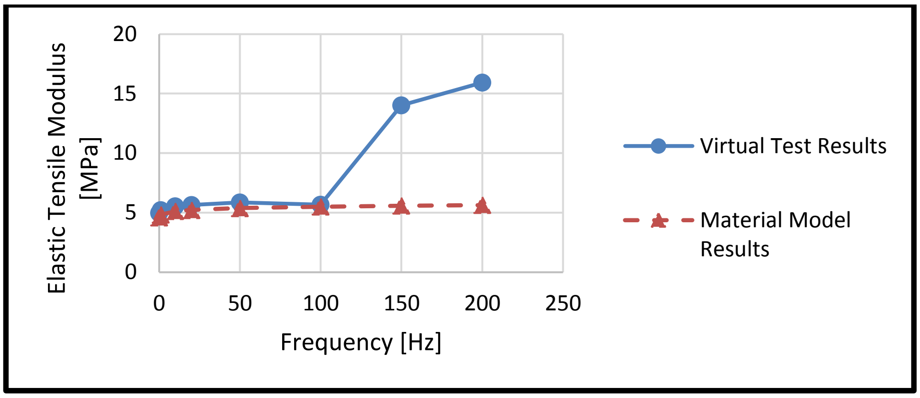

Figure 81. Comparison of Elastic Tensile Modulus Data of Material Model and Virtual Test at +50 ºC

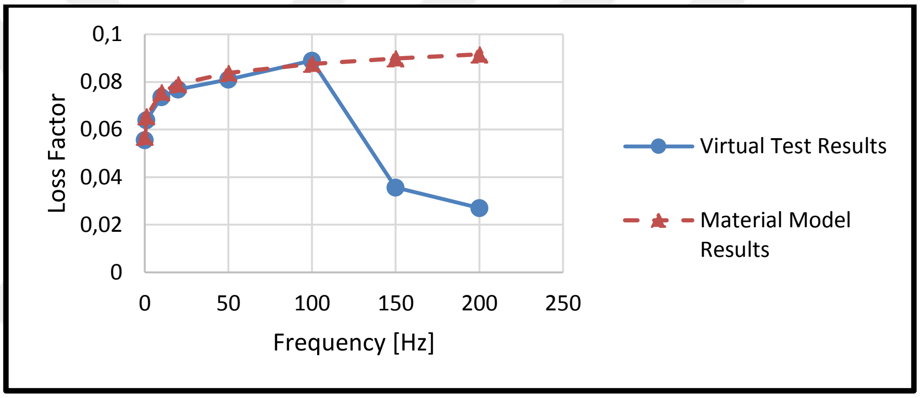

Figure 82. Comparison of Loss Factor Data of Material Model and Virtual Test at +50 ºC

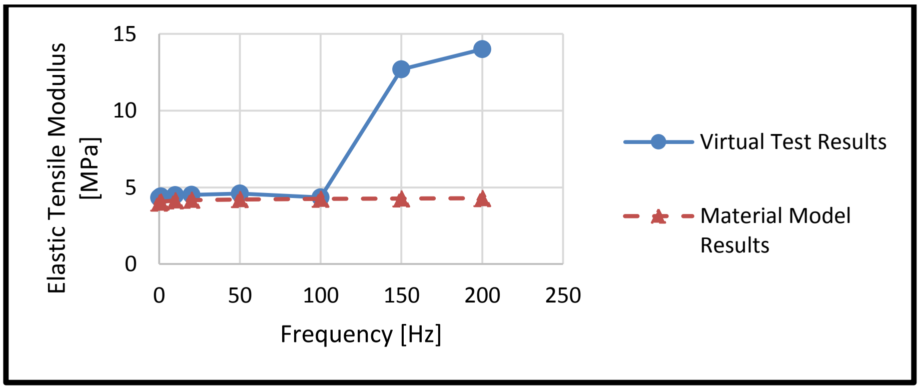

Figure 83. Comparison of Elastic Tensile Modulus Data of Material Model and Virtual Test at +100 ºC

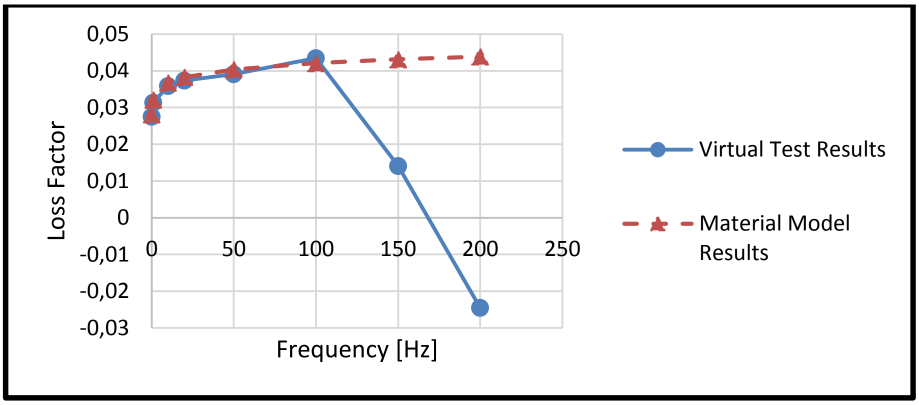

Figure 84. Comparison of Loss Factor Data of Material Model and Virtual Test at +100 ºC

Table 25. Percent Error in Elastic Tensile Modulus and Loss Factor Data of Virtual Test at -50 ºC

Frequency (Hz)	% Error in Elastic Tensile Modulus	% Error in Loss Factor
0,1	9,78	2,61
1	7,67	4,52
10	3,82	7,47
20	2,44	8,49
50	0,53	9,85
100	1,28	11,11
150	3,33	10,71
200	7,59	12,90

Table 26. Percent Error in Elastic Tensile Modulus and Loss Factor Data of Virtual Test at -20 ºC

Frequency (Hz)	% Error in Elastic Tensile Modulus	% Error in Loss Factor
0,1	8,34	2,32
1	7,91	2,62
10	7,40	3,13
20	7,23	3,40
50	7,04	3,85
100	5,51	3,09
150	32,09	25,26
200	34,44	28,52

Table 27. Percent Error in Elastic Tensile Modulus and Loss Factor Data of Virtual Test at +20 ºC

Frequency (Hz)	% Error in Elastic Tensile Modulus	% Error in Loss Factor
0,1	8,31	2,30
1	8,07	2,54
10	7,81	2,78
20	7,79	2,92
50	8,06	3,44
100	4,28	0,27
150	99,84	50,08
200	117,10	56,25

Table 28. Percent Error in Elastic Tensile Modulus and Loss Factor Data of Virtual Test at +50 ºC

Frequency (Hz)	% Error in Elastic Tensile Modulus	% Error in Loss Factor
0,1	8,30	2,30
1	8,17	2,42
10	8,07	2,59
20	8,14	2,71
50	8,72	3,35
100	3,26	1,55
150	151,26	60,39
200	182,60	70,50

Table 29. Percent Error in Elastic Tensile Modulus and Loss Factor Data of Virtual Test at +100 ºC

Frequency (Hz)	% Error in Elastic Tensile Modulus	% Error in Loss Factor
0,1	8,29	2,27
1	8,25	2,34
10	8,25	2,49
20	8,41	2,44
50	9,25	3,33
100	2,34	3,15
150	197,45	67,29
200	227,08	155,92

5.2. Investigation of Edge Effect (Poisson’s Effect) on the Accuracy of Virtual Step Sine Test Results

Edge effect causes difference between the experimental complex stiffness and modulus data of test specimen and its real material properties because the equations that are used to calculate the complex stiffness and modulus are assumed that test specimen is deformed at ideal basic tensile and shear modes. However, to provide this condition is not possible in practice. The difference is occurred between the ideal and practical conditions results because of the definitions of boundary conditions.

Some analyses are conducted to see the difference between the results for ideal and practical conditions for the designed test set-up for this thesis. For this purpose, very simple model which consists of a test specimen and a connection block is prepared (see Fig.85). Analyses about edge effect are handled as practical and ideal cases which are defined as Case 1 and Case 2 respectively.

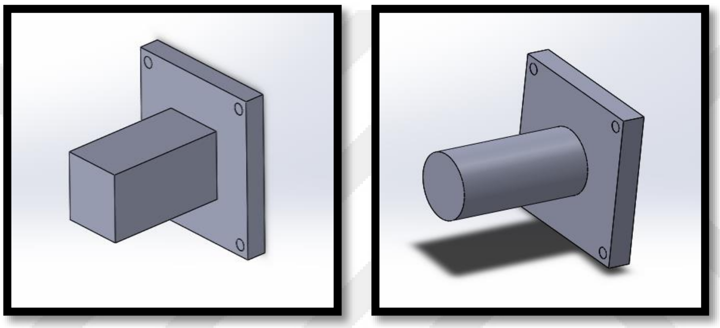

Figure 85. Prepared Model for Edge Effect Investigation with Different Test Specimens

5.2.1. CASE 1: VIRTUAL STEP SINE TEST WITH EDGE EFFECT

This case is the virtual test case (practical case) in which edge effects are taken into account. Analysis definitions for the rectangular prism test specimen are prepared to provide practical case conditions.

Force is defined as 1000 N like previous analyses on whole test set-up. Force definition is given in Fig.86.

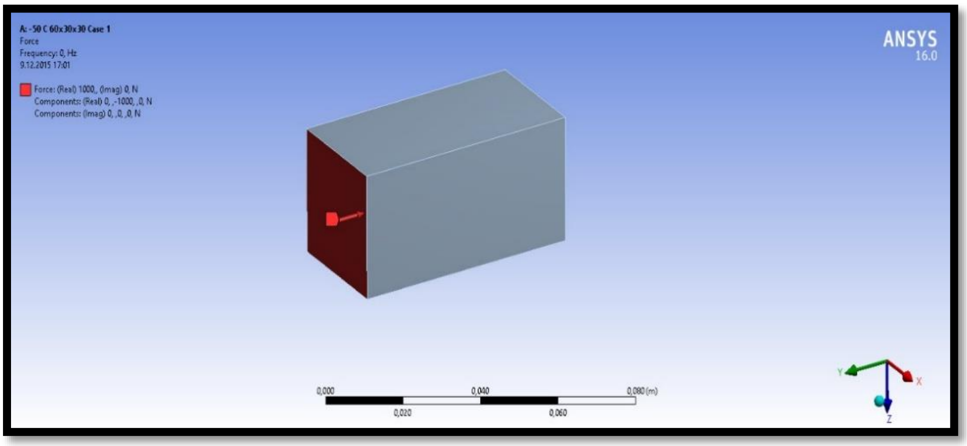

Figure 86. Location and Direction of Applied Force for Case 1

Two separate boundary conditions are defined for the Case 1 analyses. For the first boundary condition which is given in Fig.87, motion of the selected surface for all directions (x, y and z) is prevented. On the other hand, for the second boundary condition which is given in Fig.88, motion of the selected surface is prevented for x and z directions but motion in y direction (direction of applied force) is defined as free.

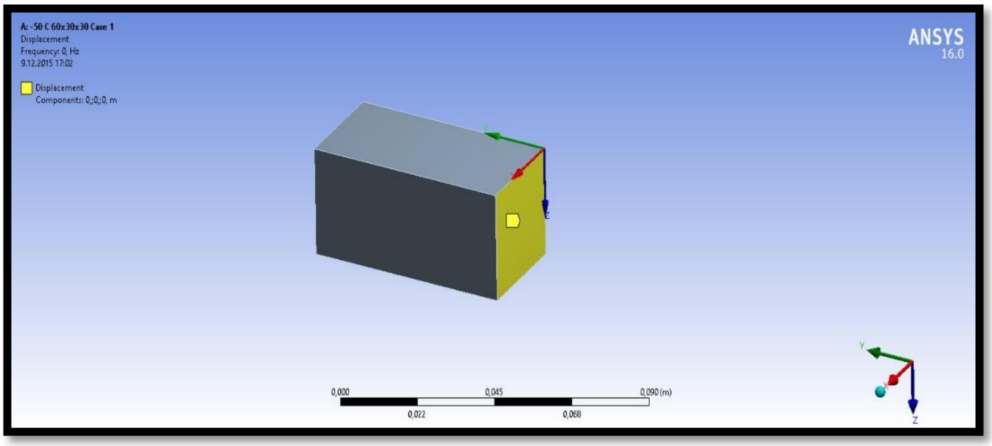

Figure 87. Location of First Boundary Condition for Case 1

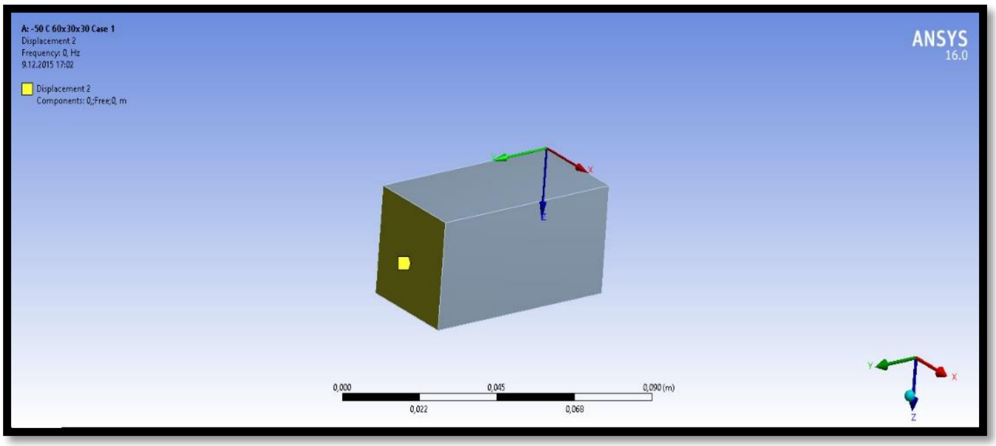

Figure 88. Location of Second Boundary Condition for Case 1

Material properties of test specimen is defined like previous analyses. For the analyses, five different temperatures (-50 ^{o}C, -20 ^{o}C, +20 ^{o}C, +50 ^{o}C and +100 ^{o}C) and eight different data points (0.1, 1, 10, 20, 50, 100, 150, 200 Hz) are selected for the frequency dependent results. Full method is used during the harmonic analyses to provide exact damping effect. The outputs of the analyses are defined as frequency dependent deformations and transmitted force.

Frequency dependent deformation values of the surface where force is applied are gathered through this definition which is given in Fig.89. Real and imaginary deformation values are obtained through this definition at the same direction with force.

Transmitted force is taken from the contact between the test specimen and fixed block. Location and direction of transmitted force is given in Fig.90.

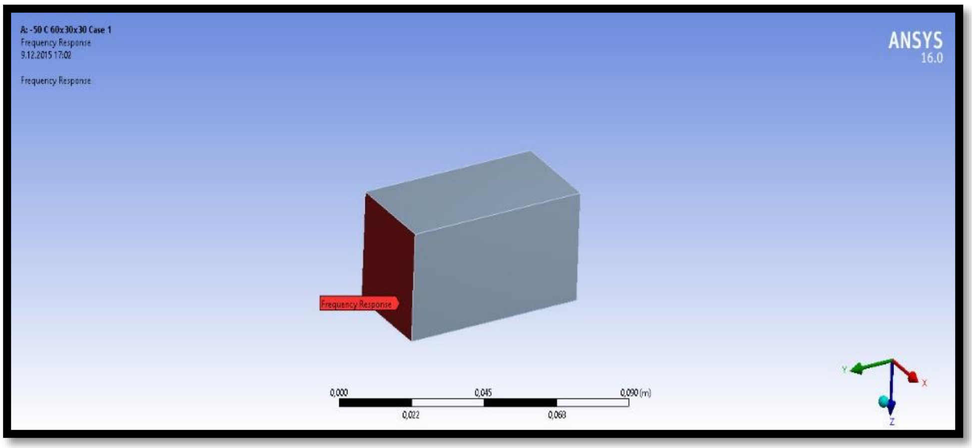

Figure 89. Selected Surface for Frequency Response of Deformation Data

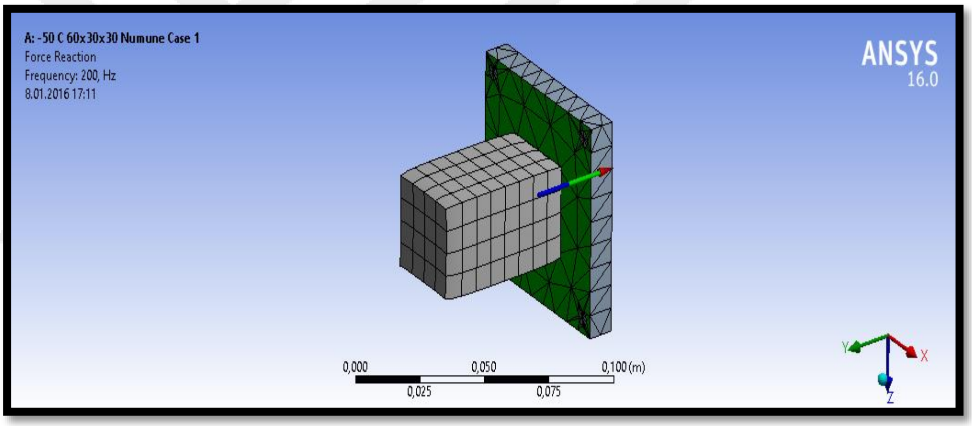

Figure 90. Selected Surface for Transmitted Force Data

5.2.2. Case 2: Ideal Virtual Step Sine Test with No Edge Effect

This case is the ideal case in which edge effects are not taken into account. Analysis definitions for the rectangular prism test specimen are prepared to provide ideal case conditions.

Only difference between Case 1 and Case 2 is the definitions of boundary conditions. For this reason, other definitions are accepted as the same for both cases. One boundary condition is defined for Case 2. For this boundary condition which is given in Fig.91, motion of the selected surface is prevented for y direction but motion in other directions (x and z) is defined as free, i.e. edge effect is eliminated.

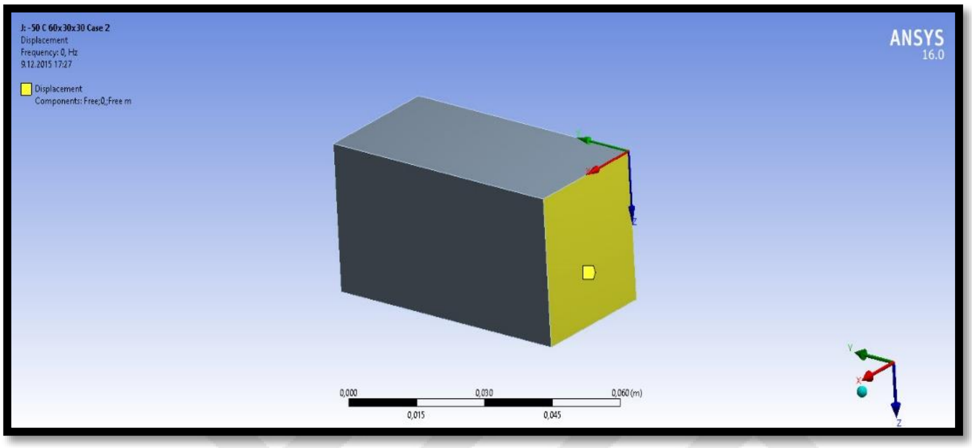

Figure 91. Location of Boundary Condition for Case 2

The results of Case 1 and Case 2 analyses are processed in Excel files with using the necessary formulations which are given in previous sections. Relevant graphs (elastic tensile modulus and loss factor) for both virtual test and material model (mathematical model) results are drawn. Also, the error calculations are made. All analyses are conducted for both 60x30x30 mm rectangular prism and cylinder test specimens.

5.2.3. VIRTUAL STEP SINE TESTS: HARMONIC ANALYSES OF RECTANGULAR PRISM TEST SPECIMEN

Analyses are conducted on rectangular test specimen for both Case 1 and Case 2 at five different temperatures (-50 °C, -20 °C, +20 °C, +50 °C and +100 °C) with eight different data points (0.1, 1, 10, 20, 50, 100, 150, 200 Hz). In addition, same analyses are conducted on weightless specimen as well to see the inertial effects. The results of analyses are given in Fig.92 through Fig.111 respectively as comparison of real (material model results) and experimental (virtual test results) data. In addition, error information of these comparisons are given in Table 30 through Table 39. For the weightless specimen analyses, only error information are presented and no more graphs are prepared.

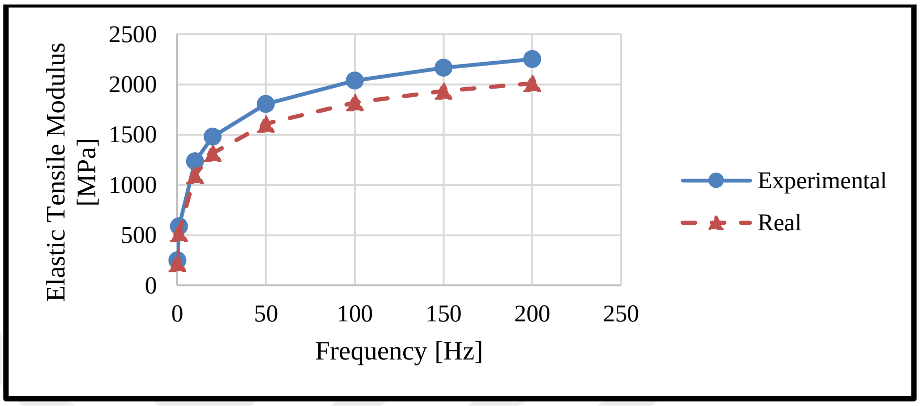

Figure 92. Comparison of Elastic Tensile Modulus Data at -50 ºC for Case 1

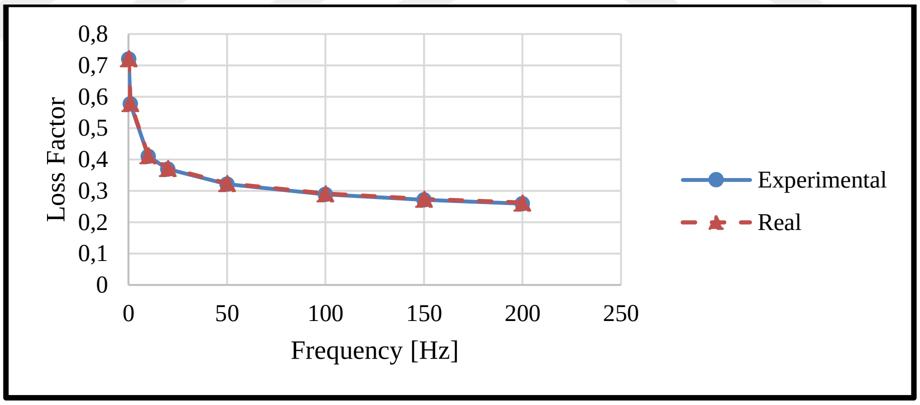

Figure 93. Comparison of Loss Factor Data at -50 ºC for Case 1

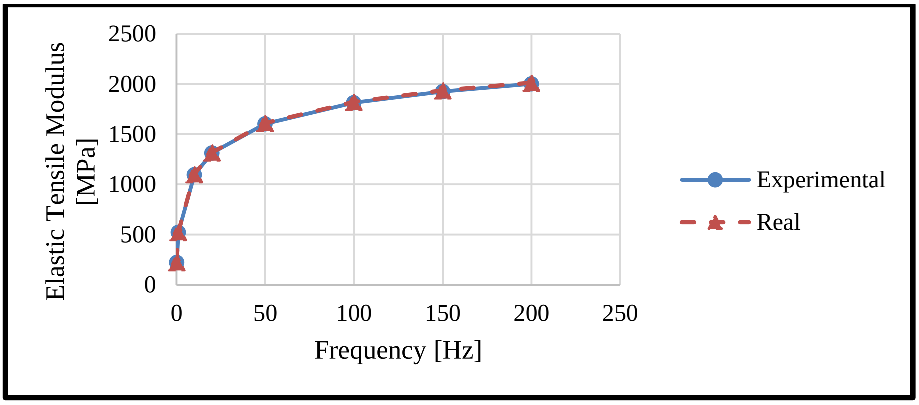

Figure 94. Comparison of Elastic Tensile Modulus Data at -50 ºC for Case 2

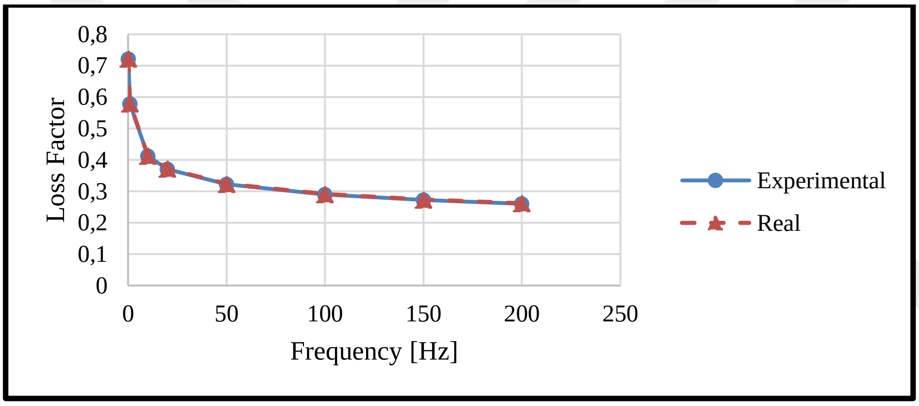

Figure 95. Comparison of Loss Factor Data at -50 ºC for Case 2

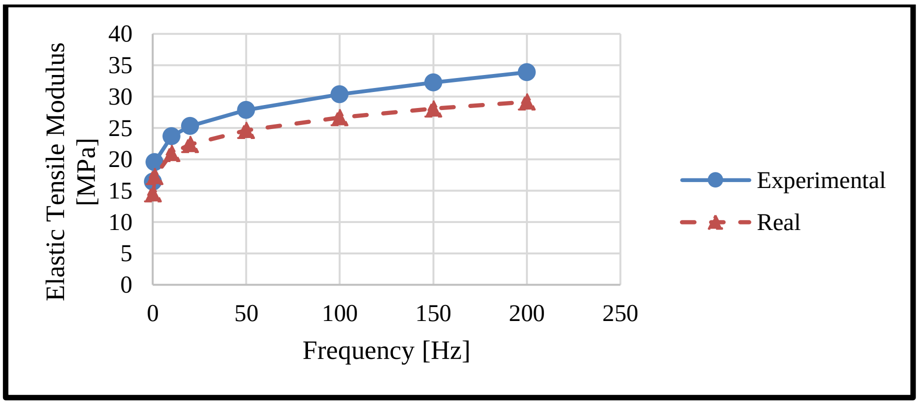

Figure 96. Comparison of Elastic Tensile Modulus Data at -20 ºC for Case 1

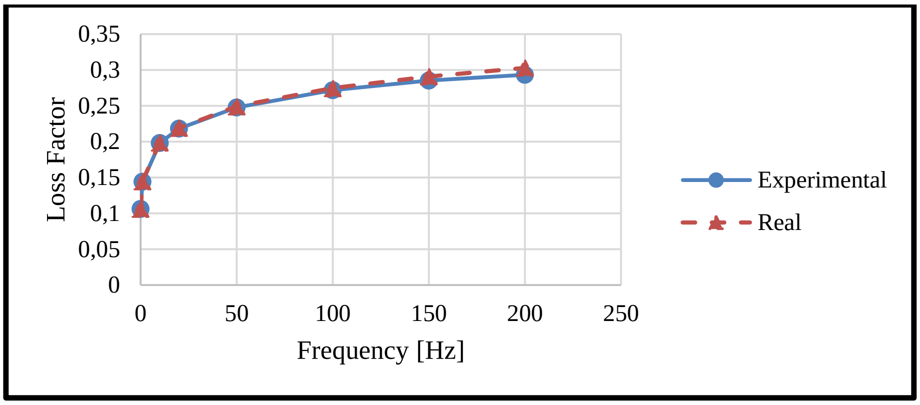

Figure 97. Comparison of Loss Factor Data at -20 ºC for Case 1

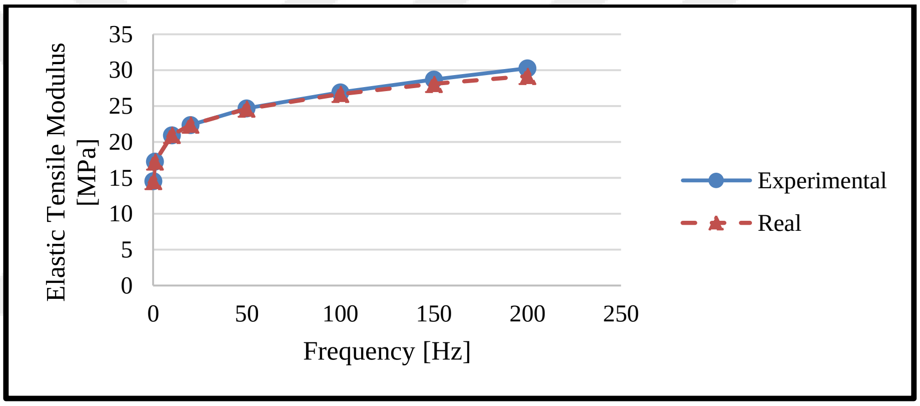

Figure 98. Comparison of Elastic Tensile Modulus Data at -20 ºC for Case 2

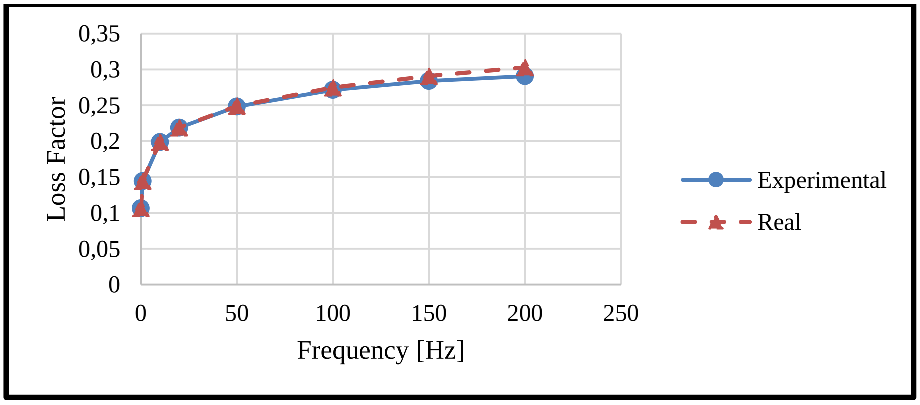

Figure 99. Comparison of Loss Factor Data at -20 ºC for Case 2

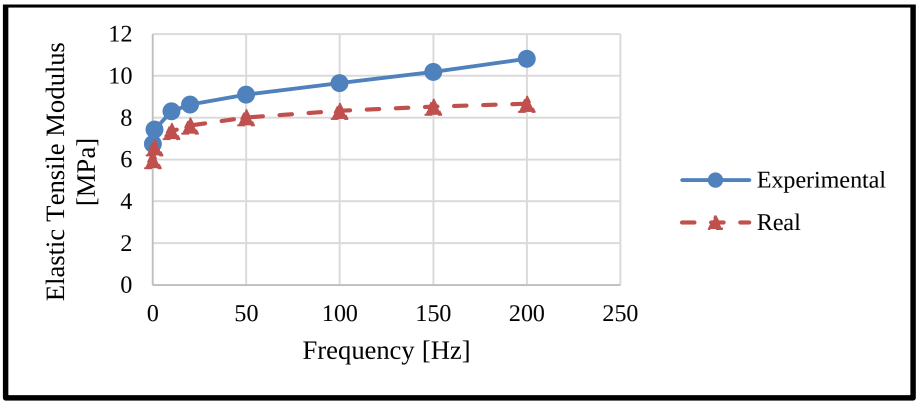

Figure 100. Comparison of Elastic Tensile Modulus Data at +20 ºC for Case 1

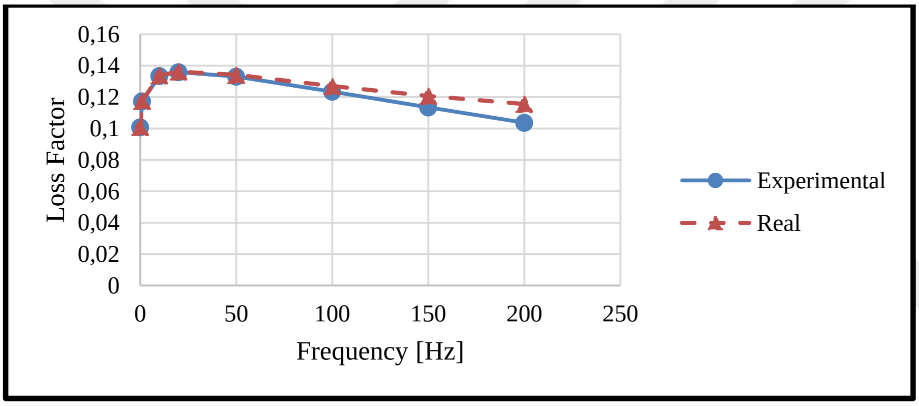

Figure 101. Comparison of Loss Factor Data at +20 ºC for Case 1

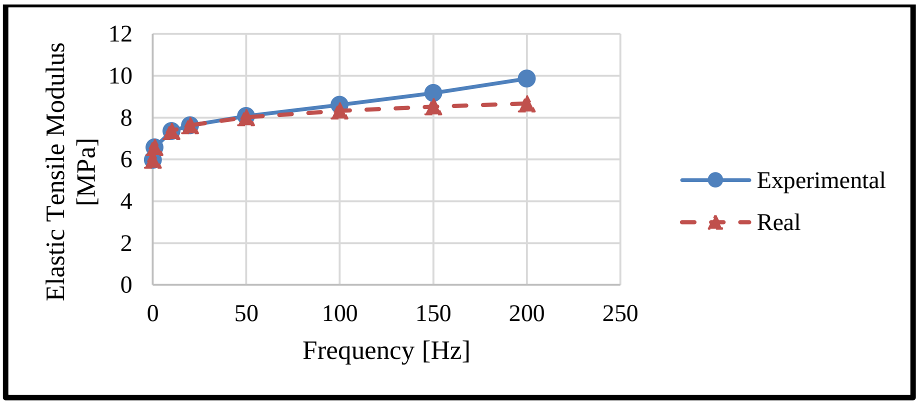

Figure 102. Comparison of Elastic Tensile Modulus Data at +20 ºC for Case 2

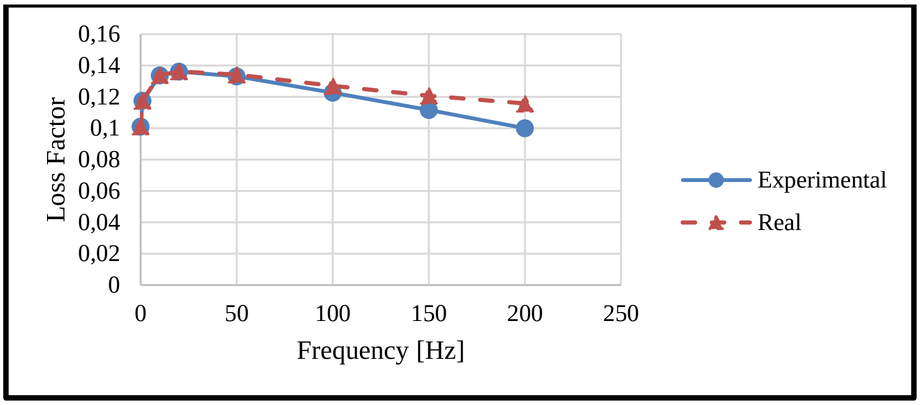

Figure 103. Comparison of Loss Factor Data at +20 ºC for Case 2

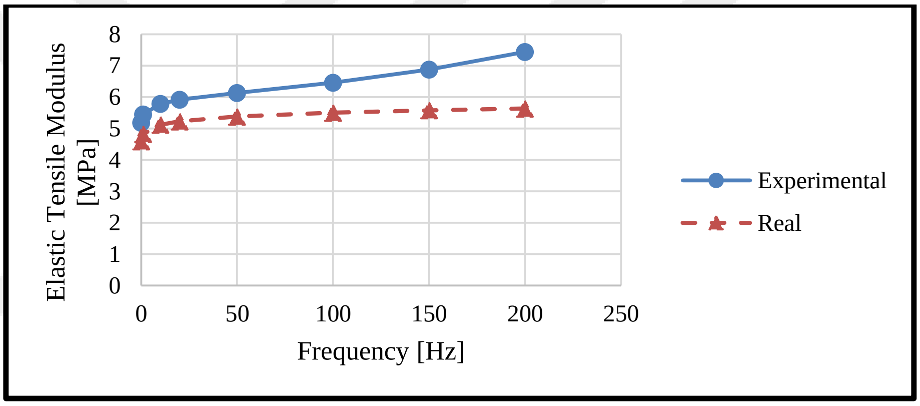

Figure 104. Comparison of Elastic Tensile Modulus Data at +50 ºC for Case 1

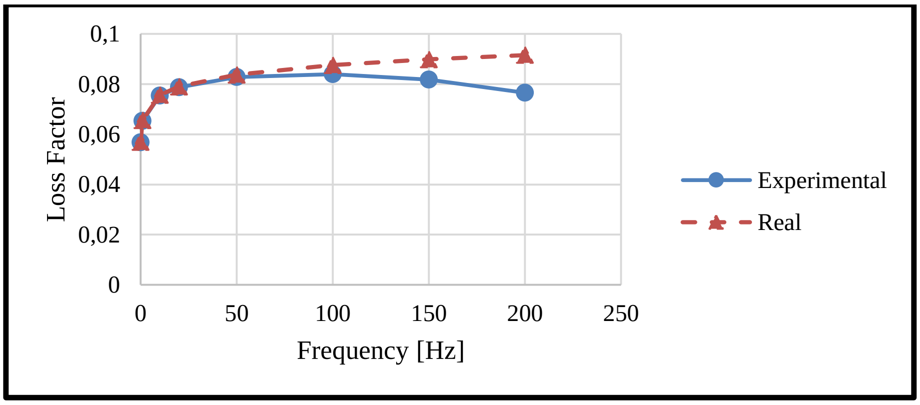

Figure 105. Comparison of Loss Factor Data at +50 ºC for Case 1

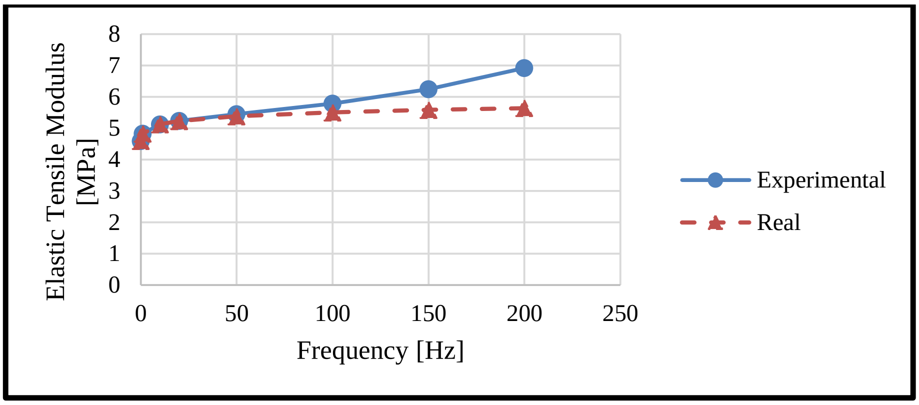

Figure 106. Comparison of Elastic Tensile Modulus Data at +50 ºC for Case 2

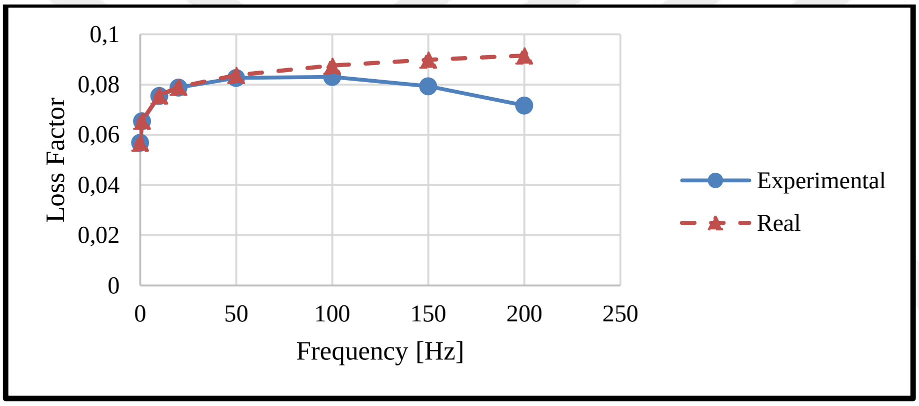

Figure 107. Comparison of Loss Factor Data at +50 ºC for Case 2

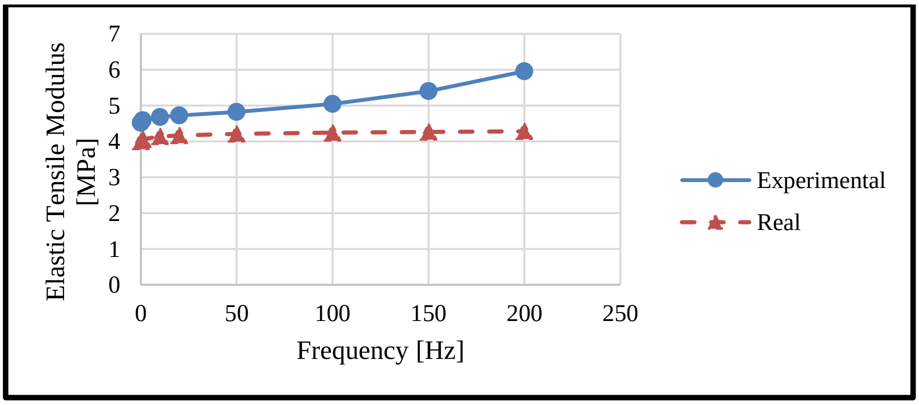

Figure 108. Comparison of Elastic Tensile Modulus Data at +100 ºC for Case 1

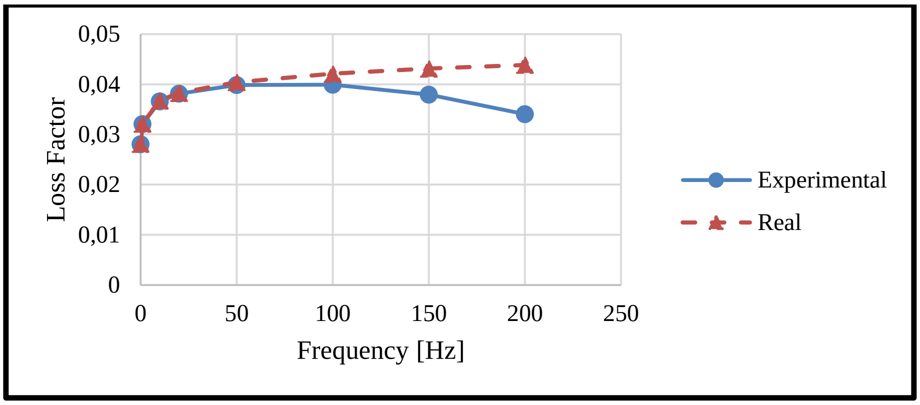

Figure 109. Comparison of Loss Factor Data at +100 °C for Case 1

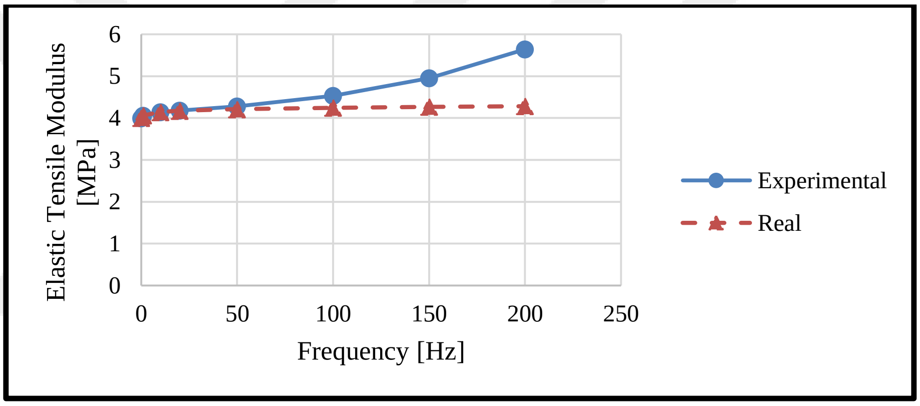

Figure 110. Comparison of Elastic Tensile Modulus Data at +100 °C for Case 2

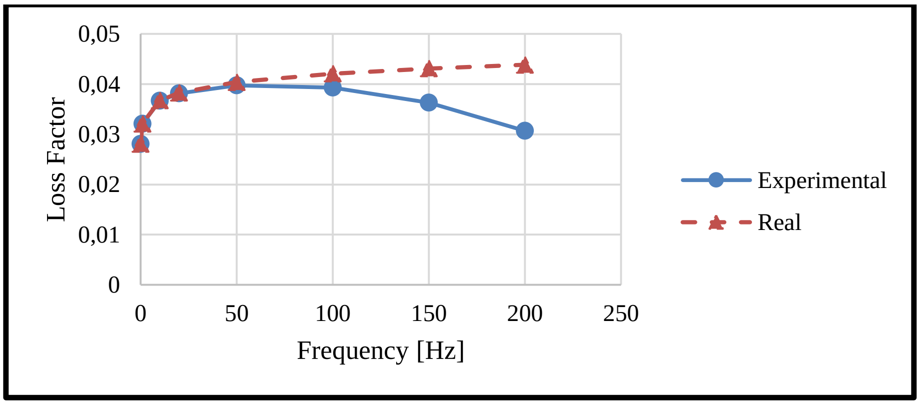

Figure 111. Comparison of Loss Factor Data at +100 °C for Case 2

Table 30. Percent Error in Elastic Tensile Modulus and Loss Factor Data at -50 ºC for Case 1

Frequency (Hz)	% Error in Elastic Tensile Modulus	% Error in Loss Factor	% Error in Elastic Tensile Modulus for Weightless Specimen	% Error in Loss Factor for Weightless Specimen
0,1	13,13	0,27	13,13	0,27
1	12,89	0,46	12,89	0,46
10	12,46	0,74	12,47	0,74
20	12,32	0,82	12,32	0,83
50	12,13	0,95	12,13	0,95
100	12,00	1,03	11,99	1,02
150	11,95	1,10	11,92	1,08
200	11,92	1,13	11,87	1,09

Table 31. Percent Error in Elastic Tensile Modulus and Loss Factor Data at -50 ºC for Case 2

Frequency (Hz)	% Error in Elastic Tensile Modulus	% Error in Loss Factor	% Error in Elastic Tensile Modulus for Weightless Specimen	% Error in Loss Factor for Weightless Specimen
0,1	0,01	0,10	0,01	0,10
1	0,10	0,19	0,10	0,19
10	0,26	0,36	0,26	0,36
20	0,32	0,42	0,32	0,41
50	0,40	0,50	0,40	0,50
100	0,46	0,56	0,47	0,55
150	0,47	0,63	0,50	0,60
200	0,47	0,66	0,53	0,60

Table 32. Percent Error in Elastic Tensile Modulus and Loss Factor Data at -20 ºC for Case 1

Frequency (Hz)	% Error in Elastic Tensile Modulus	% Error in Loss Factor	% Error in Elastic Tensile Modulus for Weightless Specimen	% Error in Loss Factor for Weightless Specimen
0,1	13,02	0,21	13,02	0,21
1	12,98	0,18	12,98	0,18
10	12,95	0,24	12,94	0,23
20	12,96	0,32	12,92	0,29
50	13,14	0,52	12,90	0,30
100	13,77	1,08	12,88	0,30
150	14,79	2,10	12,86	0,32
200	16,18	3,25	12,85	0,34

Table 33. Percent Error in Elastic Tensile Modulus and Loss Factor Data at -20 ^{o}C for Case 2

Frequency (Hz)	% Error in Elastic Tensile Modulus	% Error in Loss Factor	% Error in Elastic Tensile Modulus for Weightless Specimen	% Error in Loss Factor for Weightless Specimen
0,1	0,06	0,09	0,06	0,09
1	0,07	0,04	0,07	0,04
10	0,07	0,09	0,09	0,07
20	0,04	0,17	0,09	0,12
50	0,18	0,40	0,10	0,13
100	0,92	1,13	0,11	0,11
150	2,11	2,33	0,11	0,13
200	3,72	3,93	0,11	0,14

Table 34. Percent Error in Elastic Tensile Modulus and Loss Factor Data at +20 ^{o}C for Case 1

Frequency (Hz)	% Error in Elastic Tensile Modulus	% Error in Loss Factor	% Error in Elastic Tensile Modulus for Weightless Specimen	% Error in Loss Factor for Weightless Specimen
0,1	13,02	0,18	13,02	0,18
1	13,00	0,24	13,00	0,24
10	13,00	0,26	12,97	0,24
20	13,09	0,30	12,96	0,19
50	13,69	0,85	12,95	0,20
100	15,85	2,77	12,94	0,23
150	19,48	5,96	12,93	0,26
200	24,78	10,44	12,93	0,22

Table 35. Percent Error in Elastic Tensile Modulus and Loss Factor Data at +20 ^{o}C for Case 2

Frequency (Hz)	% Error in Elastic Tensile Modulus	% Error in Loss Factor	% Error in Elastic Tensile Modulus for Weightless Specimen	% Error in Loss Factor for Weightless Specimen
0,1	0,06	0,05	0,06	0,05
1	0,07	0,11	0,07	0,10
10	0,04	0,13	0,08	0,09
20	0,06	0,19	0,08	0,06
50	0,78	0,91	0,08	0,05
100	3,27	3,40	0,09	0,07
150	7,52	7,59	0,09	0,11
200	13,83	13,58	0,09	0,07

Table 36. Percent Error in Elastic Tensile Modulus and Loss Factor Data at +50 ºC for Case 1

Frequency (Hz)	% Error in Elastic Tensile Modulus	% Error in Loss Factor	% Error in Elastic Tensile Modulus for Weightless Specimen	% Error in Loss Factor for Weightless Specimen
0,1	13,02	0,20	13,02	0,20
1	13,00	0,24	13,01	0,24
10	13,04	0,30	13,00	0,25
20	13,17	0,39	12,99	0,23
50	14,09	1,13	12,98	0,15
100	17,42	4,06	12,97	0,17
150	23,22	9,05	12,97	0,18
200	32,02	16,41	12,97	0,16

Table 37. Percent Error in Elastic Tensile Modulus and Loss Factor Data at +50 ºC for Case 2

Frequency (Hz)	% Error in Elastic Tensile Modulus	% Error in Loss Factor	% Error in Elastic Tensile Modulus for Weightless Specimen	% Error in Loss Factor for Weightless Specimen
0,1	0,06	0,08	0,06	0,08
1	0,06	0,11	0,06	0,11
10	0,01	0,18	0,07	0,12
20	0,14	0,30	0,07	0,09
50	1,20	1,30	0,08	0,03
100	5,07	5,12	0,07	0,02
150	11,93	11,74	0,08	0,04
200	22,64	21,73	0,07	0,03

Table 38. Percent Error in Elastic Tensile Modulus and Loss Factor Data at +100 ºC for Case 1

Frequency (Hz)	% Error in Elastic Tensile Modulus	% Error in Loss Factor	% Error in Elastic Tensile Modulus for Weightless Specimen	% Error in Loss Factor for Weightless Specimen
0,1	13,02	0,21	13,02	0,21
1	13,01	0,25	13,01	0,25
10	13,07	0,36	13,01	0,31
20	13,23	0,31	13,01	0,11
50	14,42	1,42	13,00	0,17
100	18,81	5,22	13,00	0,15
150	26,70	11,98	13,00	0,20
200	39,17	22,36	13,00	0,30

Table 39. Percent Error in Elastic Tensile Modulus and Loss Factor Data at +100 °C for Case 2

Frequency (Hz)	% Error in Elastic Tensile Modulus	% Error in Loss Factor	% Error in Elastic Tensile Modulus for Weightless Specimen	% Error in Loss Factor for Weightless Specimen
0,1	0,06	0,08	0,06	0,08
1	0,06	0,12	0,06	0,12
10	0,01	0,24	0,07	0,18
20	0,20	0,24	0,07	0,02
50	1,58	1,67	0,06	0,04
100	6,68	6,67	0,07	0,02
150	16,09	15,72	0,07	0,08
200	31,60	29,98	0,06	0,17

5.2.4. Virtual Step Sine Tests: Harmonic Analyses of Cylinder Test Specimen

Analyses are conducted on cylinder test specimen for both Case 1 and Case 2 at four different temperatures (-50 °C, -20 °C, +20 °C, +50 °C) with eight different data points (0.1, 1, 10, 20, 50, 100, 150, 200 Hz) to see the effect of specimen geometry on the results. Both cylinder and rectangular prism test specimen have 60x30x30 dimensions but cylinder specimen has smaller cross-sectional area because of its geometry. The results of analyses are given in Fig.112 through Fig.127 respectively as comparison of real (material model results) and experimental (virtual test results) data. In addition, error information of these comparisons are given in Table 40 through Table 47.

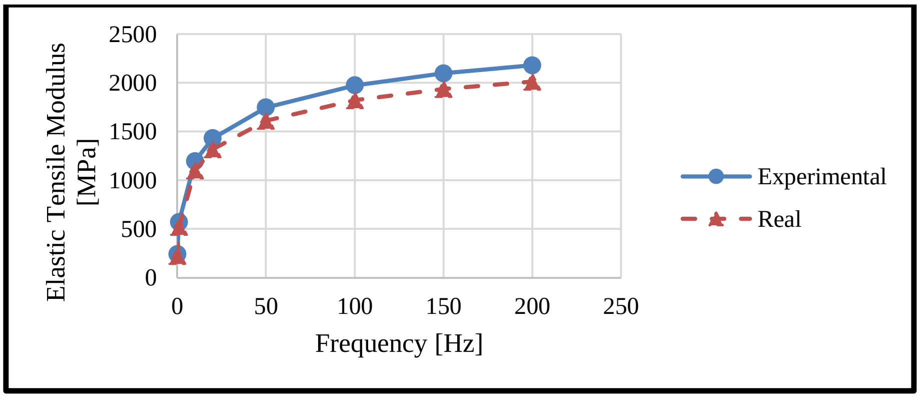

Figure 112. Comparison of Elastic Tensile Modulus Data at -50 °C for Case 1

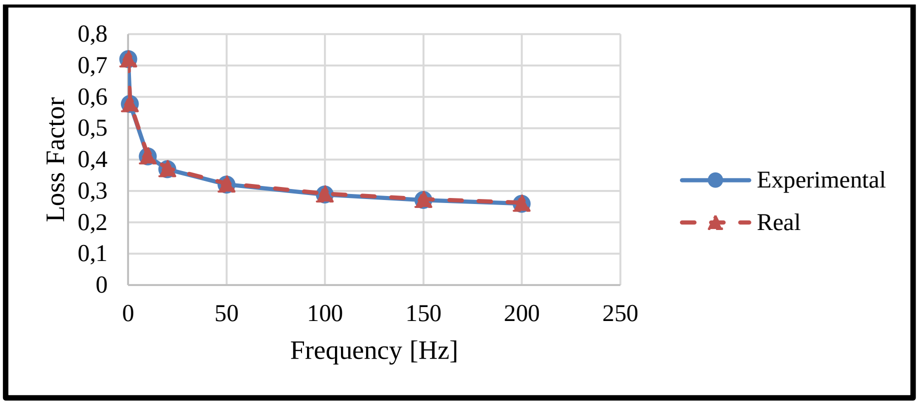

Figure 113. Comparison of Loss Factor Data at -50 ºC for Case 1

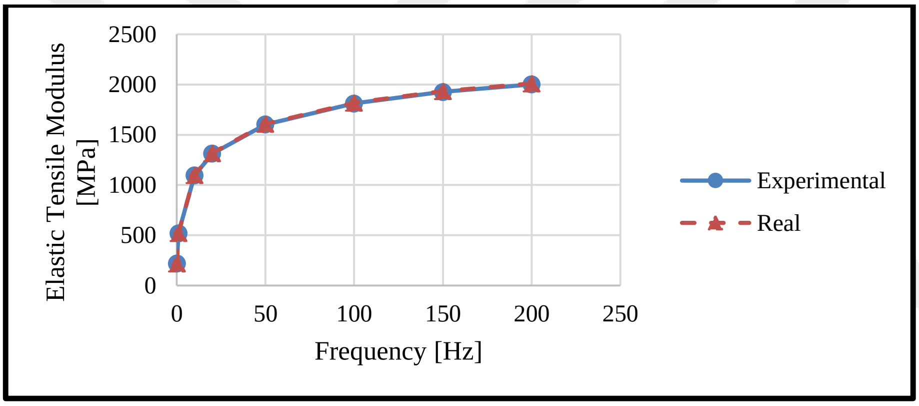

Figure 114. Comparison of Elastic Tensile Modulus Data at -50 ºC for Case 2

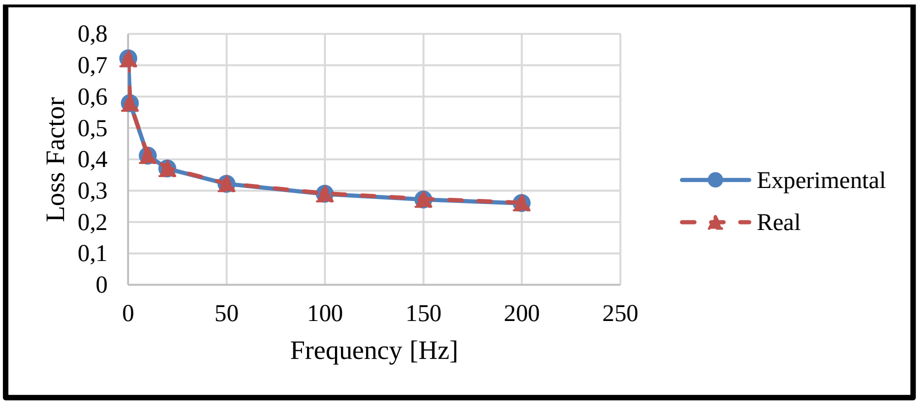

Figure 115. Comparison of Loss Factor Data at -50 ºC for Case 2

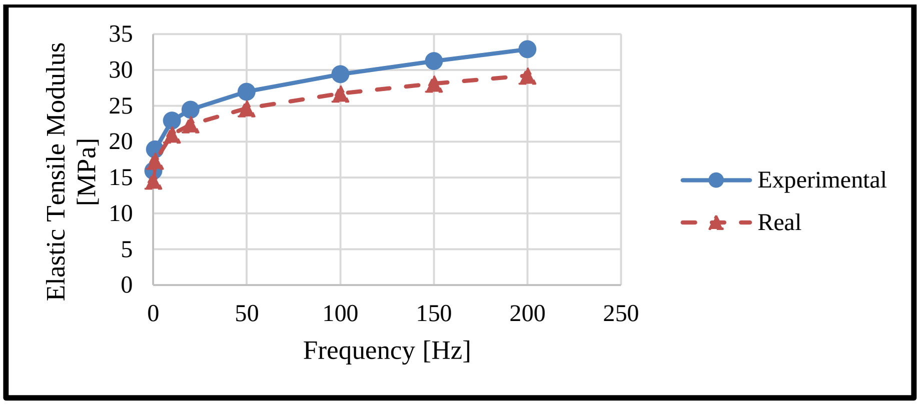

Figure 116. Comparison of Elastic Tensile Modulus Data at -20 ºC for Case 1

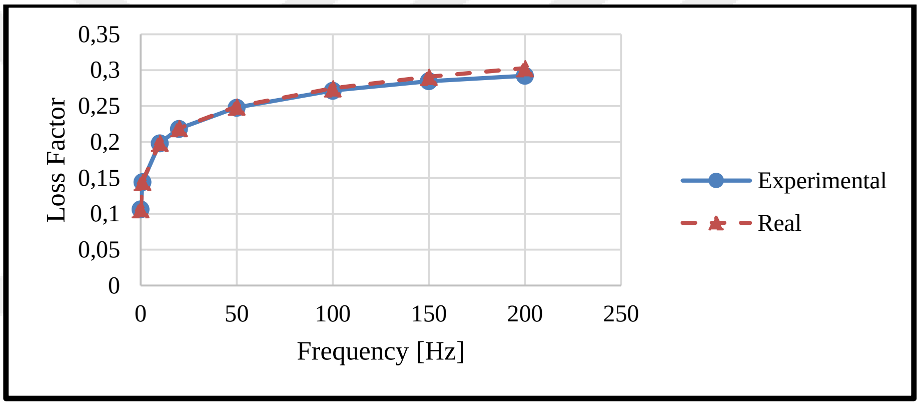

Figure 117. Comparison of Loss Factor Data at -20 ºC for Case 1

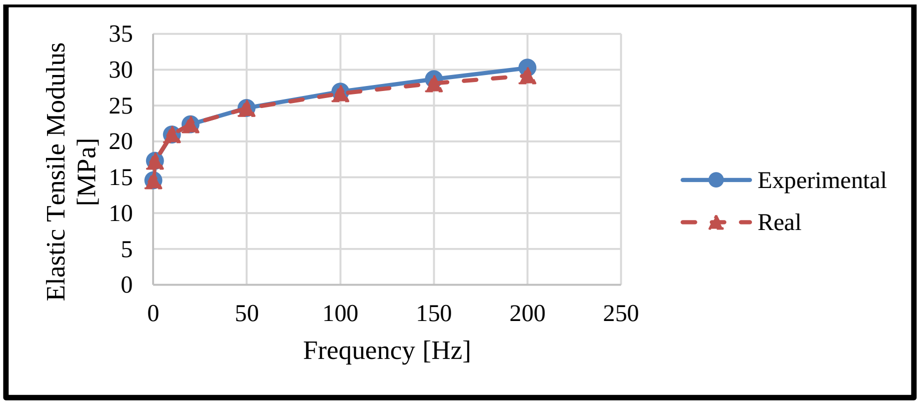

Figure 118. Comparison of Elastic Tensile Modulus Data at -20 ºC for Case 2

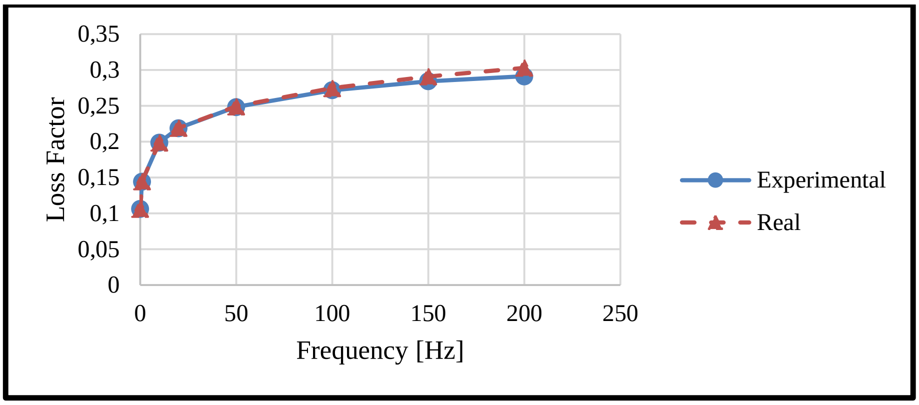

Figure 119. Comparison of Loss Factor Data at -20 ºC for Case 2

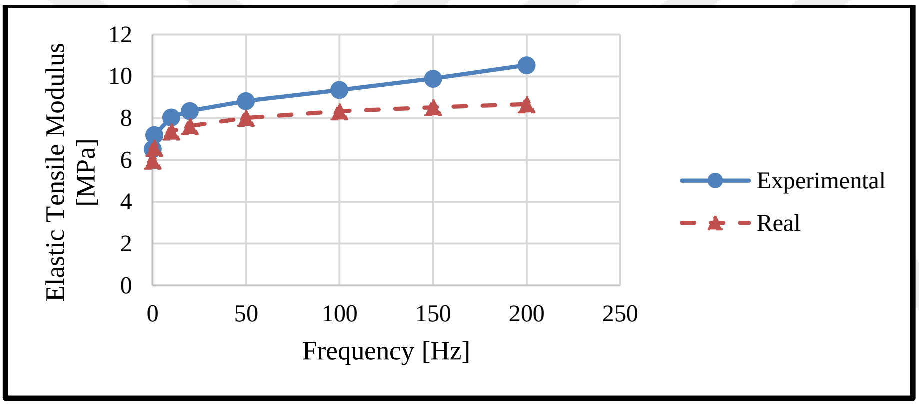

Figure 120. Comparison of Elastic Tensile Modulus Data at +20 ºC for Case 1

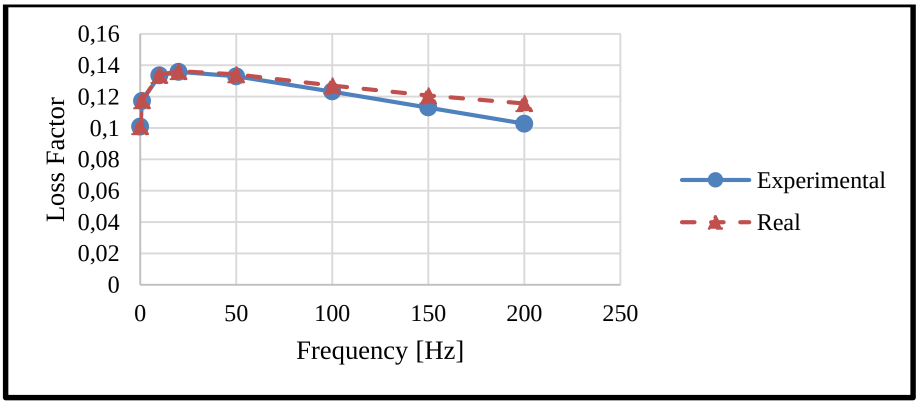

Figure 121. Comparison of Loss Factor Data at +20 ºC for Case 1

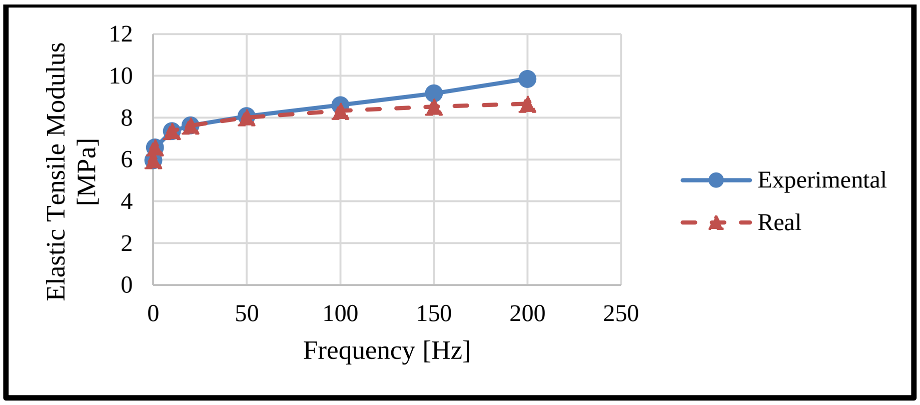

Figure 122. Comparison of Elastic Tensile Modulus Data at +20 ºC for Case 2

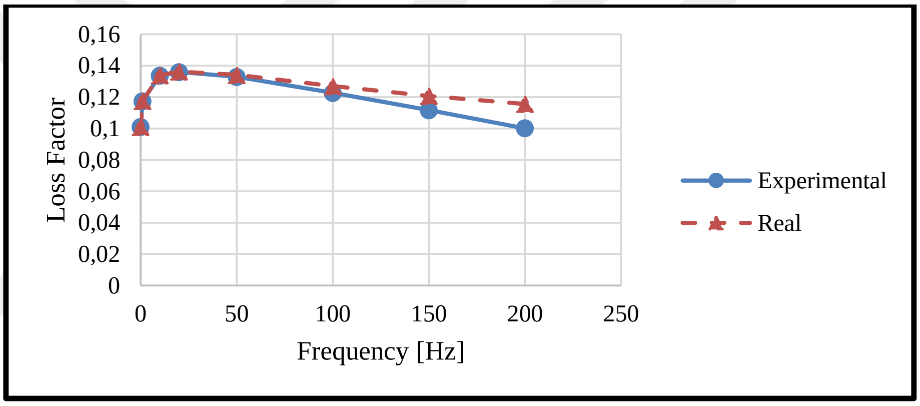

Figure 123. Comparison of Loss Factor Data at +20 ºC for Case 2

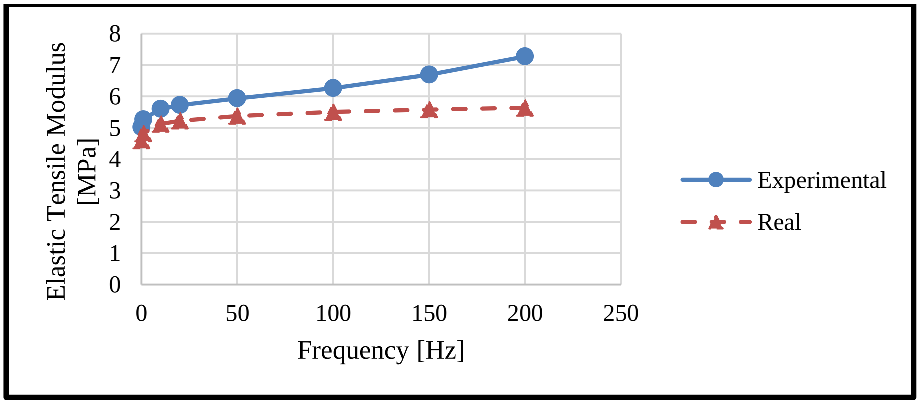

Figure 124. Comparison of Elastic Tensile Modulus Data at +50 ºC for Case 1

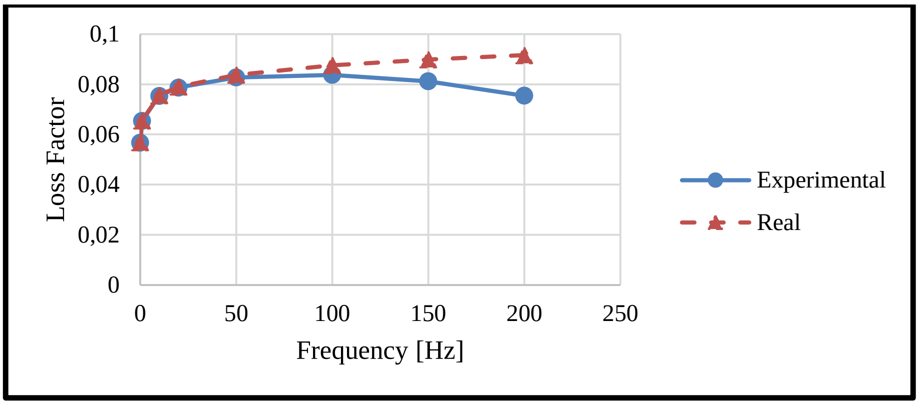

Figure 125. Comparison of Loss Factor Data at +50 ºC for Case 1

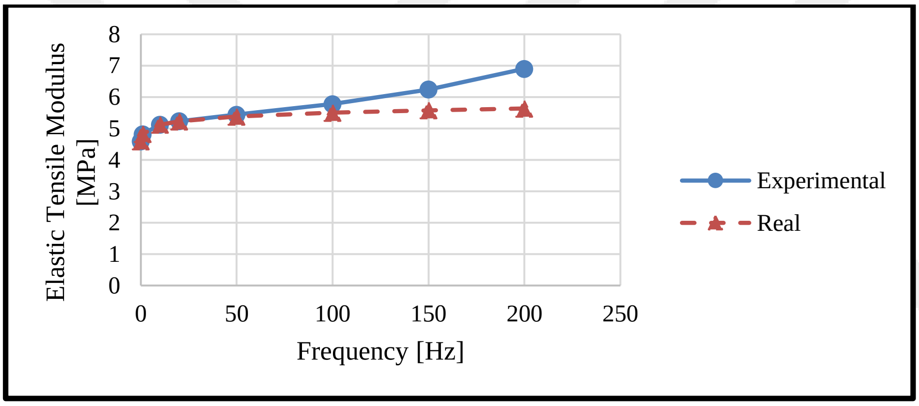

Figure 126. Comparison of Elastic Tensile Modulus Data at +50 ºC for Case 2

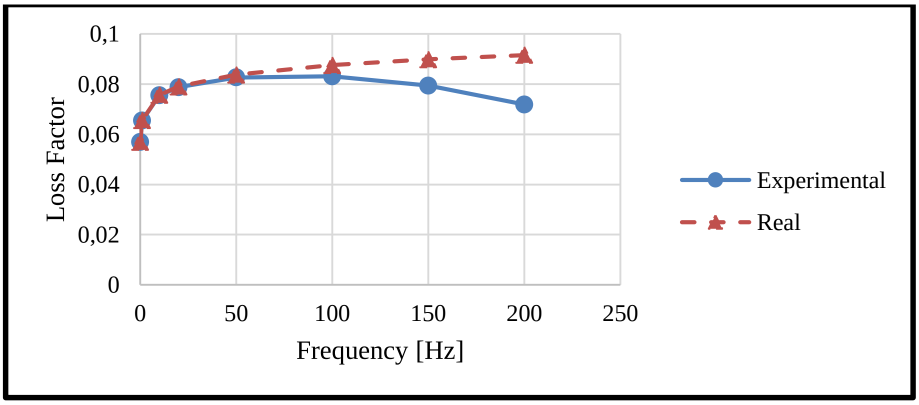

Figure 127. Comparison of Loss Factor Data at +50 ºC for Case 2

Table 40. Percent Error in Elastic Tensile Modulus and Loss Factor Data at -50 ºC for Case 1

Frequency (Hz)	% Error in Elastic Tensile Modulus	% Error in Loss Factor
0,1	9,44	0,29
1	9,19	0,46
10	8,80	0,68
20	8,67	0,75
50	8,51	0,85
100	8,40	0,93
150	8,36	0,99
200	8,34	1,02

Table 41. Percent Error in Elastic Tensile Modulus and Loss Factor Data at -50 ºC for Case 2

Frequency (Hz)	% Error in Elastic Tensile Modulus	% Error in Loss Factor
0,1	0,02	0,10
1	0,10	0,19
10	0,27	0,36
20	0,33	0,42
50	0,41	0,50
100	0,47	0,57
150	0,48	0,63
200	0,48	0,66

Table 42. Percent Error in Elastic Tensile Modulus and Loss Factor Data at -20 ºC for Case 1

Frequency (Hz)	% Error in Elastic Tensile Modulus	% Error in Loss Factor
0,1	9,33	0,22
1	9,29	0,19
10	9,27	0,25
20	9,27	0,34
50	9,45	0,54
100	10,11	1,14
150	11,17	2,13
200	12,61	3,44

Table 43. Percent Error in Elastic Tensile Modulus and Loss Factor Data at -20 ºC for Case 2

Frequency (Hz)	% Error in Elastic Tensile Modulus	% Error in Loss Factor
0,1	0,07	0,09
1	0,08	0,04
10	0,08	0,09
20	0,05	0,17
50	0,17	0,40
100	0,91	1,13
150	2,09	2,32
200	3,70	3,91

Table 44. Percent Error in Elastic Tensile Modulus and Loss Factor Data at +20 ºC for Case 1

Frequency (Hz)	% Error in Elastic Tensile Modulus	% Error in Loss Factor
0,1	9,33	0,19
1	9,30	0,25
10	9,32	0,27
20	9,40	0,33
50	10,03	0,91
100	12,26	2,95
150	16,02	6,37
200	21,54	11,15

Table 45. Percent Error in Elastic Tensile Modulus and Loss Factor Data at +20 ºC for Case 2

Frequency (Hz)	% Error in Elastic Tensile Modulus	% Error in Loss Factor
0,1	0,07	0,06
1	0,08	0,11
10	0,05	0,13
20	0,06	0,19
50	0,77	0,91
100	3,24	3,38
150	7,47	7,53
200	13,72	13,46

Table 46. Percent Error in Elastic Tensile Modulus and Loss Factor Data at +50 ºC for Case 1

Frequency (Hz)	% Error in Elastic Tensile Modulus	% Error in Loss Factor
0,1	9,33	0,21
1	9,32	0,25
10	9,35	0,31
20	9,49	0,41
50	10,44	1,21
100	13,89	4,33
150	19,92	9,67
200	29,10	17,57

Table 47. Percent Error in Elastic Tensile Modulus and Loss Factor Data at +50 ºC for Case 2

Frequency (Hz)	% Error in Elastic Tensile Modulus	% Error in Loss Factor
0,1	0,07	0,08
1	0,07	0,11
10	0,02	0,18
20	0,13	0,30
50	1,19	1,29
100	5,04	5,08
150	11,83	11,65
200	22,42	21,47

5.3. Virtual Step Sine Tests under Offset Loading and Disturbances

Applying offset loading instead of centered loading or applying disturbance forces provide that model is excited at different modes like bending mode. Through this way, the results of the test set-up under these conditions are observed.

5.3.1. Virtual Step Sine Tests under Offset Loading

To apply offset loading to the set-up, the position and height of actuator and its bracket are changed. Through this way, the position of actuator side main shaft is changed as well. During these analyses, 1, 5 and 10 mm offsets are applied to the model in two direction at the same time. Centered and offset loadings are given in Fig.128.

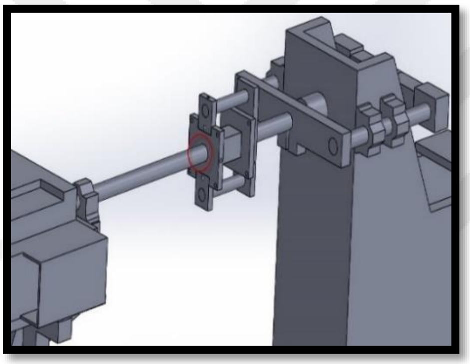

(a)

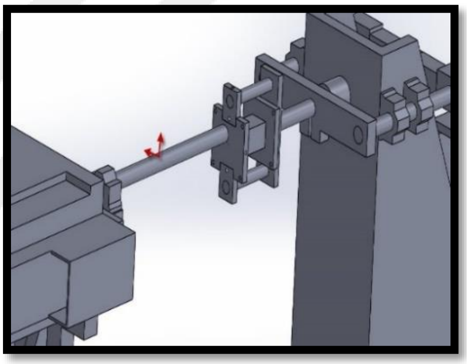

(b)

Figure 128. Types of Loading (a) Centered Loading (b) Offset Loading

The remaining parts of the analyses are the same as the previous analyses. Analyses are conducted at five temperatures (-50 ^oC, -20 ^oC, +20 ^oC, +50 ^oC and +100 ^oC) for eight frequency data points (0.1, 1, 10, 20, 50, 100, 150 and 200 Hz). Same analysis procedure is used with the previous analyses. The results of lowest (-50 ^oC) and highest (+100 ^oC) temperatures analyses are given in Fig. 129 through Fig.136 respectively as comparison of material model results and virtual test results and error information of them.

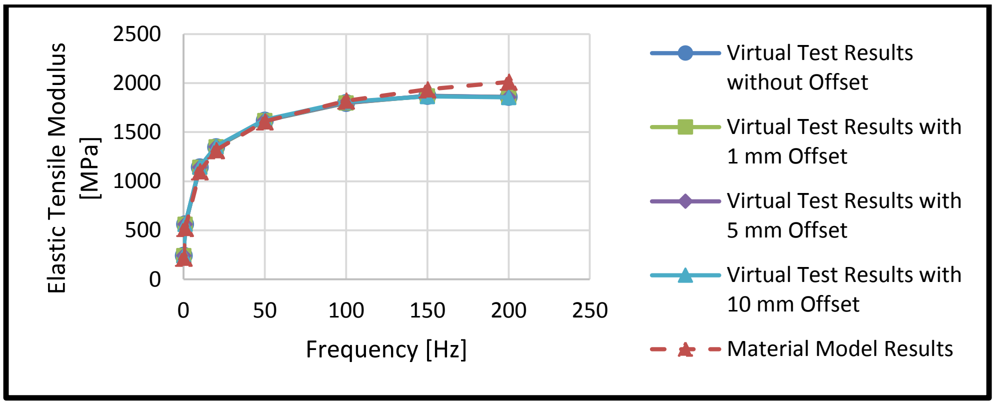

Figure 129. Comparison of Elastic Tensile Modulus Data at -50 ºC

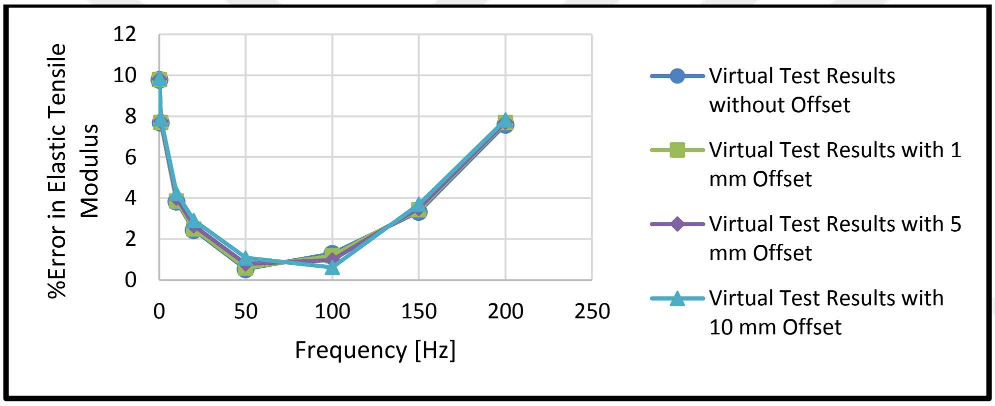

Figure 130. Comparison of Percent Error in Elastic Tensile Modulus at -50 ºC

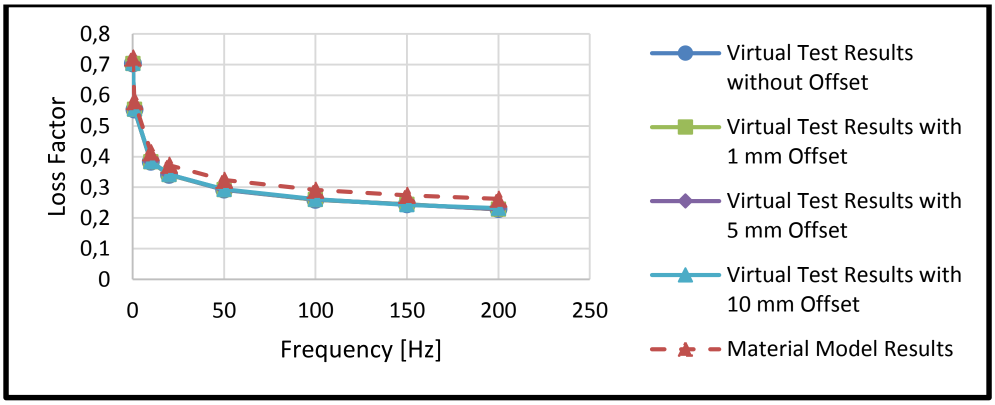

Figure 131. Comparison of Loss Factor Data at -50 ºC

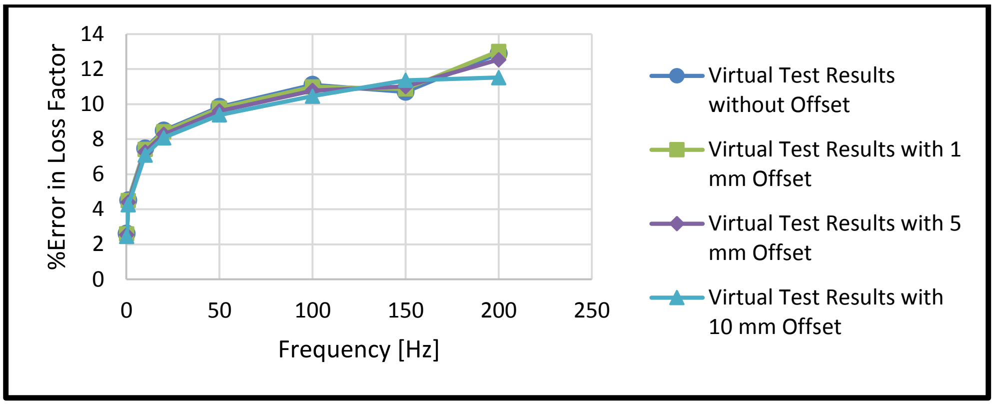

Figure 132. Comparison of Percent Error in Loss Factor Data at -50 °C

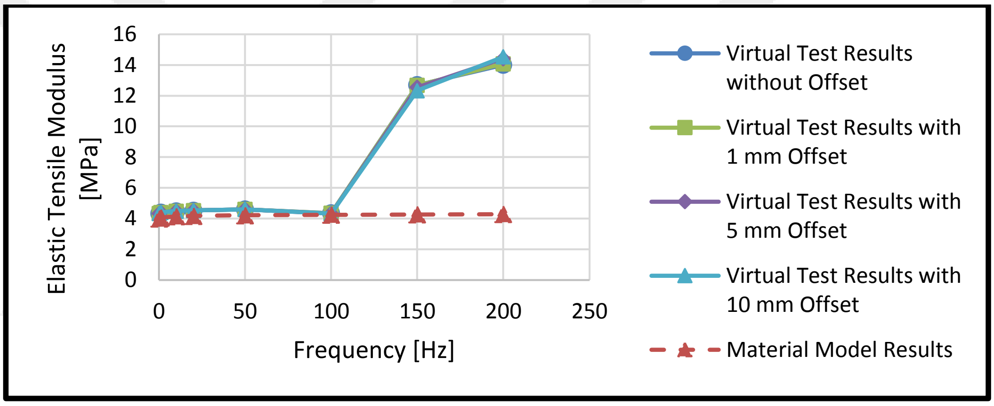

Figure 133. Comparison of Elastic Tensile Modulus Data at +100 °C

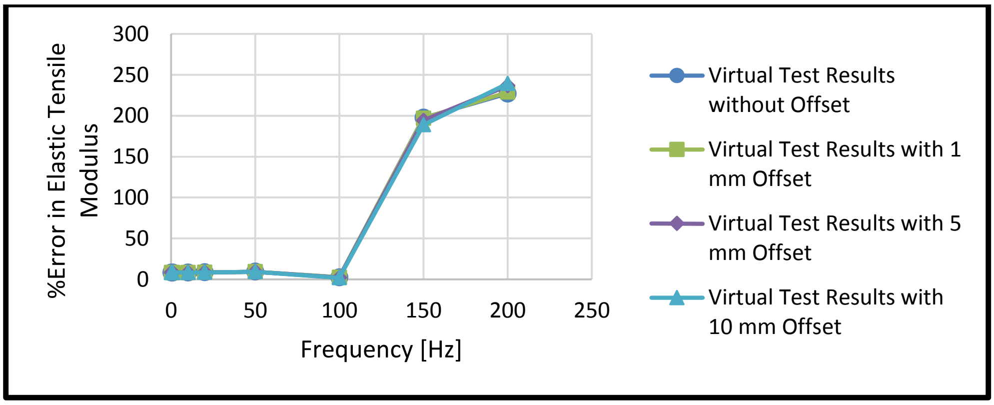

Figure 134. Comparison of Percent Error in Elastic Tensile Modulus Data +100 °C

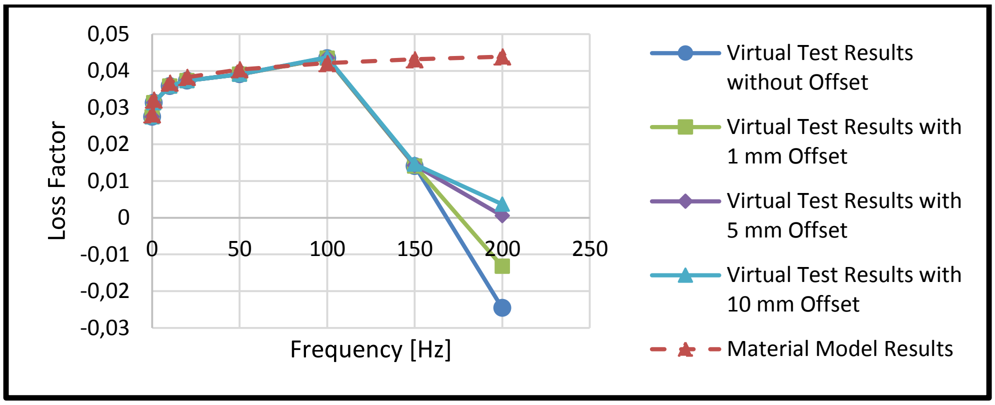

Figure 135. Comparison of Loss Factor Data at +100 ºC

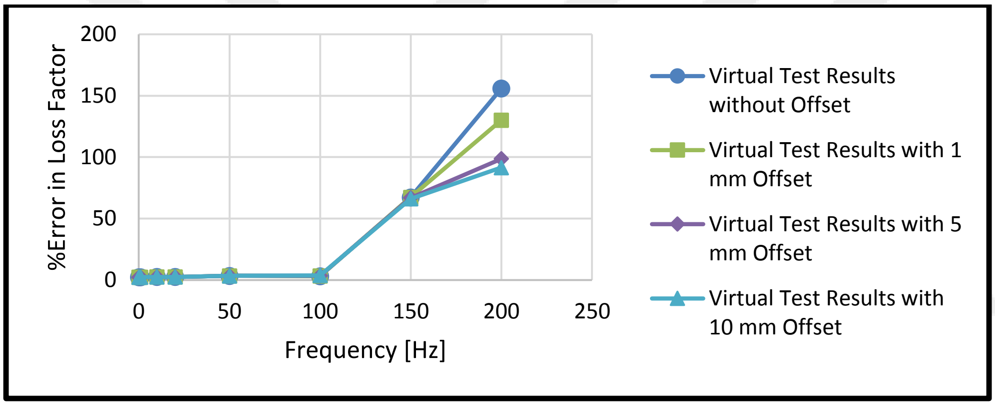

Figure 136. Comparison of Percent Error in Loss Factor Data at +100 ºC

5.3.2. Virtual Step Sine Tests under Disturbance

To apply disturbances to the set-up, forces are applied to the model from the upper and left sides of left test specimen connection block. As disturbances, %1 (10 N) and %10 (100 N) of main loading (1000 N) which is applied from the actuator are conducted (see Fig.137).

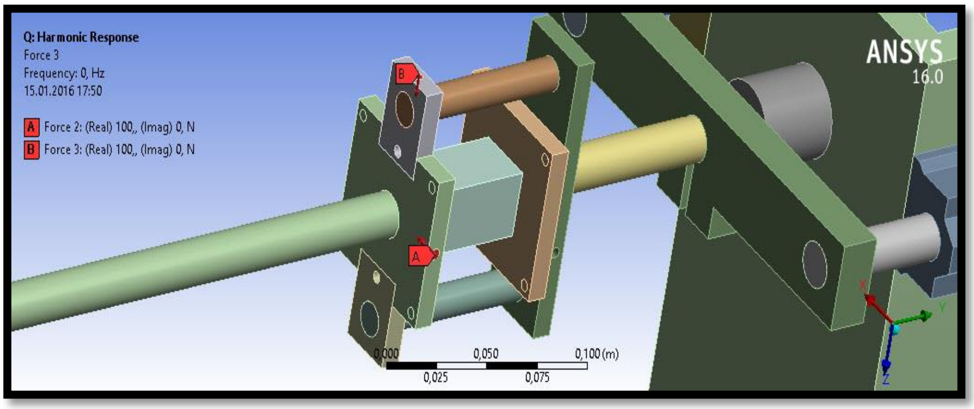

Figure 137. Locations and Directions of Disturbance Forces

Analyses are conducted at only +100 ^{o}C for eight frequency data points (0.1, 1, 10, 20, 50, 100, 150 and 200 Hz). The results are given in Fig.138 through Fig.141 respectively as comparison of material model results and virtual test results and error information of them.

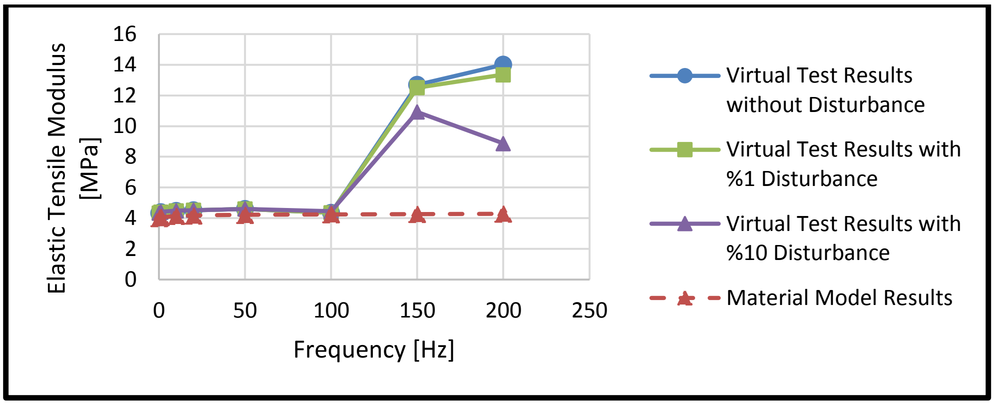

Figure 138. Comparison of Elastic Tensile Modulus Data at +100 ^{o}C

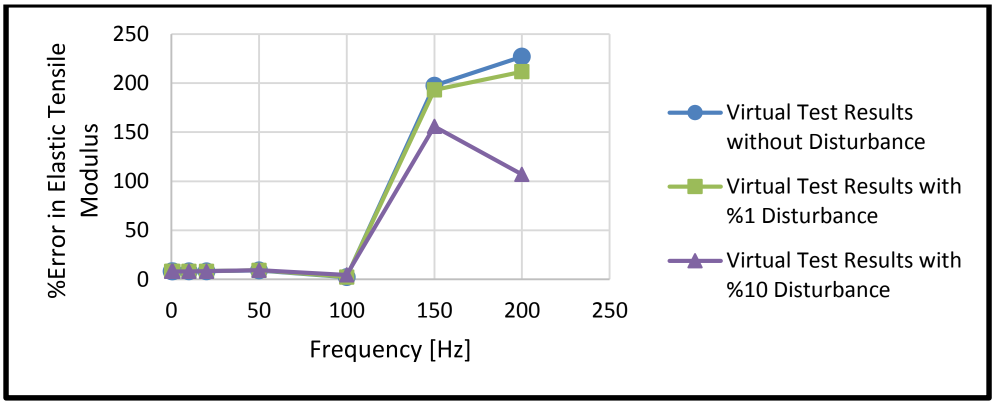

Figure 139. Comparison of Percent Error in Elastic Tensile Modulus Data at +100 ºC

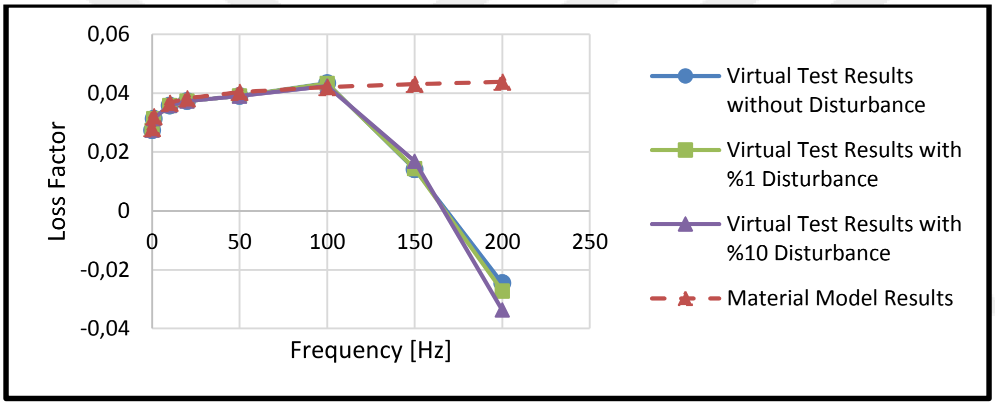

Figure 140. Comparison of Loss Factor Data at +100 ºC

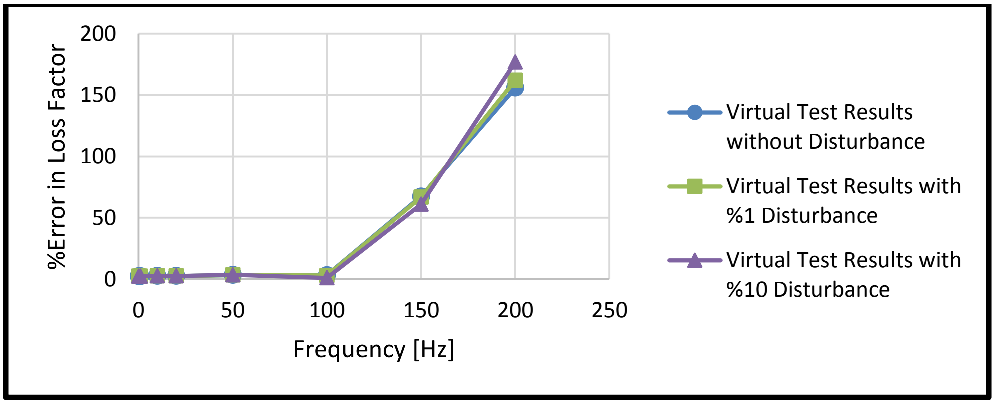

Figure 141. Comparison of Percent Error in Loss Factor Data at +100 ºC

5.4. DISCUSSIONS ON VIRTUAL STEP SINE TEST RESULTS

During the virtual tests, various harmonic analyses are conducted to identify the behaviours of test set-up under different conditions. According to the predetermined test set-up specifications, operating frequency will be between 0-100 Hz and tests will be conducted at both low and high temperatures. Virtual tests are conducted at five different temperatures (-50 ^oC, -20 ^oC, +20 ^oC, +50 ^oC and +100 ^oC) to provide realistic conditions about temperature. In addition, eight frequency data points (0.1, 1, 10, 20, 50, 100, 150, 200 Hz) are used for the tests. Thus, operating frequency range (0-100 Hz) is handled with six data points and above this range is handled with two data points. Through this way, either effective operating frequency range or problematic frequency regions of test set-up are determined.

At first, whole test set-up is analysed for five temperatures through eight frequency data points. The results of these analyses are processed in Excel files through necessary calculations. In the end, elastic tensile modulus and loss factor of test specimen are gathered and presented as graphs with real material properties of test specimen. In addition, the percent error for both elastic tensile modulus and loss factor data according to the material model and virtual test results are also gathered and presented as tables. According to the graphs and tables, significant errors exist for both elastic tensile modulus and loss factor data which are about % 8-9 and % 2-3 respectively at 0.1 Hz for all temperatures. These errors are changed with frequency and temperature. To identify the reasons of changes in errors, modal analyses are conducted on whole test set-up at five temperatures (see the results in Table 48).

Table 48. Results of Modal Analysis of Whole Test Set-up for Different Temperatures

	1.Mode (Hz)	**2.Mode (Hz)**	**3.Mode (Hz)**	**4.Mode (Hz)**	**5.Mode (Hz)**
-50 ^oC	80.71	133.95	178.51	187.31	239.89
-20 ^oC	22.84	132.92	175.60	186.56	220.87
+20 ^oC	15.66	132.88	174.40	186.35	207.21
+50 ^oC	14.17	132.87	173.71	186.22	200.65
+100 ^oC	13.48	132.87	173.13	186.09	195.99

Main reason of changes in error is the internal resistance of test specimen. At low temperatures, test specimen is stiff and its internal resistance is high. On the other hand, test specimen is getting softer with increasing temperature and its internal resistance is getting low. For this reason, errors are increased at high temperatures. Effect of internal resistance is observed at weightless specimen analyses clearly. For the weightless specimen, there is almost no difference in error at low and high temperatures. Also, drastical changes in errors are observed about resonance frequency (see Table 48) of test set-up.

On the other hand, there is a need to identify the reasons of the existing errors at 0.1 Hz (about 0 Hz) for both elastic tensile modulus and loss factor. For this purpose, edge effect phenomenon is investigated. Both elastic tensile modulus and loss factor (especially elastic tensile modulus) is affected from edge effect factor. Test set-up is reduced to the test specimen and one of its connection block to identify the edge effect factor. Two cases are prepared for these further analyses, one of them represents the ideal condition and the other one represents the analysis condition. During these analyses, cylinder test specimen with similar measurements as rectangular prism specimen is also analysed to see the effect of test specimen geometry. The results of these analyses show that edge effect is the main factor of the initial errors. For the ideal condition, the initial errors are reduced to % 0-1 for both elastic tensile modulus and loss factor. However, ideal conditions are not practically applicable. For this reason, initial errors for the whole model analyses are not avoidable. In addition, it can be seen from the analyses that specimen geometry is also important for the test results. Cylinder specimen, which has smaller cross-sectional area, has better results than rectangular prism specimen.

After the identifications of errors according to the analyses, some further analyses are conducted on the test setup to see the behaviour under offset loadings and disturbances. According to the results of these analyses, drastical changes in errors are observed mainly above 100 Hz.

5.5. CONCLUSION OF VIRTUAL STEP SINE TESTS

After significant number of analyses, many useful informations are gathered about the test set-up. According to the results of tests, it should be necessary to define correction factor to cancel initial errors which are unavoidable because of the test conditions. On the other hand, test specimen geometry is found as important after some iterations on it. Another important thing is to determine suitable frequency range for the test set-up according to the virtual test results. Significant differences between the material model and virtual test results of both elastic modulus and loss factor are observed above 100 Hz mainly after 150 Hz at almost all analyses. There are also differences up to 100 Hz but these differences are relatively negligible according to the differences above 100 Hz.

As a result, suitable frequency range for the test set-up is determined. Designed test set-up can be used in its predetermined frequency range which is 0-100 Hz without hesitation.

CHAPTER 6

6. CONCLUSION

In this thesis, mainly design efforts are spent to create test set-up which is used to determine the dynamic mechanical properties of viscoelastic materials and elastic mechanical components. Design stage is divided into two; conceptual design and detailed design. Before design stage, literature survey is conducted about the standard test methods, components which are planned to design and manufacture and previous studies. Direct method, which is used to measure dynamic stiffness transfer function of some specific materials through measuring vibrations on the input side and blocking output forces, is selected to use in this thesis test system. Literature survey is provided fundamental information about these subjects.

After literature survey, conceptual design and detailed design of design stage are handled respectively. At conceptual design, design efforts are spent on test set-up, T-slot table and lifting system. Conceptual design of test set-up, T-slot table and lifting system are completed via literature survey information and some discussions on the designs and the details of the design efforts about are explained in previous chapters of this thesis. The results of the conceptual design are used in detailed design as references.

At detailed design, the dimensions and specifications of the test set-up components are determined through some analyses, brainstorming sessions and discussions with the manufacturers. Detailed design of the lifting system which will be used for temperature chamber is completed and price offer is taken from the manufacturer for the manufacturing. Despite of significant level of effort is spent on detailed designs of T-slot table and test set-up, detailed designs of these components are not fully completed especially for T-slot table. Some final decisions must be made about these designs.

At the end of detailed design stage, the final model of test set-up is attached to the roughly prepared T-slot table and some virtual tests are conducted on this model to validate the performance of test system. There are some differences between the material model and virtual test results of dynamic material properties of test specimen according to the virtual tests which are conducted through harmonic analyses. Some additional analyses are conducted on test set-up to identify the reasons of errors with respect to the edge effect. Also, test set-up is analyzed under offset loadings and disturbances. The reasons of errors and the behavior of test set-up under different conditions are identified through the results of these further analyses. According to the results of virtual tests, performance validation of test set-up is complete. However, some further improvements might be necessary later.

As a future work for this thesis work, final decisions will be made about the test set-up and T-slot table to complete detailed design of these components. If necessary, some improvements could be made on test set-up. Finally, all designed components during this thesis work will be manufactured and the test system will be assembled.

BIBLIOGRAPHY

[1] NASHIF, A.D., JONES, D.I.G. and HENDERSON, J.P., Vibration Damping, Wiley Interscience, New York, 1985

[2] JONES, D.I.G., Handbook of Viscoelastic Vibration Damping, John Wiley & Sons Ltd., 2001

[3] HARRIS, C.M. and PIERSON, A.G. (Eds.), Harris' Shock and Vibration Handbook, McGraw-Hill, 2002

[4] OZGEN, G.O., Design and development of a complex shear modulus measurement setup for viscoelastic materials, SAE 2005 Transactions Journal of Passenger Cars – Mechanical Systems (2006) 2638-2647S

[5] ISO 10846-2 2008 Acoustic and vibration - Laboratory measurement of vibro-acoustic transfer properties of resilient elements – Part 2: Direct method for determination of the dynamic stiffness of resilient supports for translatory motion

[6] ISO 10846-3 2002 Acoustic and vibration - Laboratory measurement of vibro-acoustic transfer properties of resilient elements – Part 3: Indirect method for determination of the dynamic stiffness of resilient supports for translatory motion

[7] ISO 10846-5 2008 Acoustic and vibration - Laboratory measurement of vibro-acoustic transfer properties of resilient elements – Part 5: Driving point method for determination of the low-frequency transfer stiffness of resilient supports for translatory motion

[8] ISO 18437-4 2008 Mechanical vibration and shock - Characterization of the dynamic mechanical properties of visco-elastic materials – Part 4: Dynamic stiffness method

[9] ISO 6721-4 2008 Plastics - Determination of dynamic mechanical properties – Part 4: Tensile vibration — Non-resonance method

[10] ISO 6721-6 1996 Plastics - Determination of dynamic mechanical properties – Part 6: Shear vibration — Non-resonance method

[11] ASTM D 4065-06 Standard Practice for Plactics: Dynamic Mechanical Properties: Determination and Report of Procedures

[12] ASTM D 5992-96 Standard Guide for Dynamic Testing of Vulcanized Rubber and Rubberlike Materials Using Vibratory Methods

[13] http://www.testresources.net/test-machines/160-family, [last accessed on 19/08/2015]

[14] http://www.testresources.net/test-machines/560-family, [last accessed on 19/08/2015]

[15] http://www.itbona.com/ITBONA/STOLLE/T-slot_Tables_on_support_frames.asp, [last accessed on 19/08/2015]

[16] http://mdmetric.com/tech/DIN650extract.htm, [last accessed on 19/08/2015]

[17] http://otakekouki.trustpass.alibaba.com/product/120097386-103191578/T_slot_Surface_Plate.html, [last accessed on 19/08/2015]

[18] http://www.davincimuhendislik.com/90X90h.htm, [last accessed on 19/08/2015]

[19] http://www.davincimuhendislik.com/90x180spotmodul.htm, [last accessed on 19/08/2015]

[20] http://www.davincimuhendislik.com/1520raylineerzeksenlimodul.htm, [last accessed on 19/08/2015]

[21] http://www.minitecframing.com/Products/MiniTec_Products.html, [last accessed on 19/02/2016]

[22] http://www.mts.com/en/products/producttype/test-systems/load-frames-uniaxial/servohydraulic/elastomer/index.htm, [last accessed on 19/08/2015]

[23] http://www.instron.com/tr-tr/products/testing-systems/dynamic-and-fatigue-systems/servohydraulic-fatigue/8801-floor-model, [last accessed on 19/08/2015]

[24] CANAN UZ, Design of a Test Setup for the Characterization of Vibraiton İsolators, Master Science Thesis, Department of Mechanical Engineering, Middle East Technical University, 2013

[25] FULYA EROL, Development of a Test System for Viscoelastic Material Characterization, Master Science Thesis, Department of Mechanical Engineering, Middle East Technical University, 2014

[26] Unpublished SAN-TEZ Project Final Report, Elastomer Titreşim Takozu Tasarımı, 2014

[27] http://www.adams-tech.net/vibration-system/ball-bearing-exciters/, [last accessed on 20/02/2016]

[28] http://www.boschrexroth.com/en/xc/products/product-groups/linear-motion-technology/linear-motion-systems/linear-motion-slides/index, [last accessed on 18/02/2016]

[29] http://www.tramec.it/en-us/products.aspx?idC=61688&LN=en-US

[30] https://www.mts.com/ucm/groups/public/documents/library/mts_006623.pdf, [last accessed on 19/08/2015]

[31] http://www.mts.com/ucm/groups/public/documents/library/dev_003810.pdf, [last accessed on 19/08/2015]